

**A Thesis Submitted for the Degree of PhD at the University of Warwick**

**Permanent WRAP URL:**

<http://wrap.warwick.ac.uk/136676>

**Copyright and reuse:**

This thesis is made available online and is protected by original copyright.

Please scroll down to view the document itself.

Please refer to the repository record for this item for information to help you to cite it.

Our policy information is available from the repository home page.

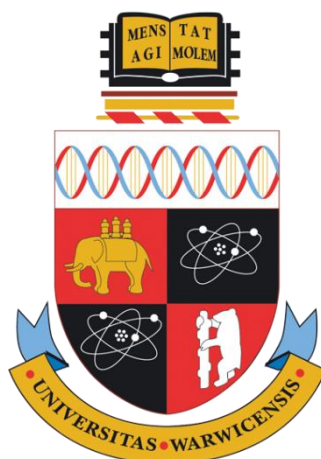
For more information, please contact the WRAP Team at: [wrap@warwick.ac.uk](mailto:wrap@warwick.ac.uk)

# **Novel Devices for Sampling and Analysis of Volatiles**

**Rachel Alice Hand**

**A thesis submitted in partial fulfilment of the  
requirements for the degree of**

**Doctor of Philosophy in Chemistry**



**Department of Chemistry**

**University of Warwick**

**March 2019**

# Table of Contents

<b>Table of Contents</b> .....	<b>i</b>
<b>Acknowledgements</b> .....	<b>vi</b>
<b>Declaration</b> .....	<b>viii</b>
<b>List of Figures</b> .....	<b>ix</b>
<b>List of Schemes</b> .....	<b>xvi</b>
<b>List of Tables</b> .....	<b>xvii</b>
<b>Table of Abbreviations</b> .....	<b>xviii</b>
<b>Abstract</b> .....	<b>xxi</b>
<b>1. Introduction</b> .....	<b>1</b>
1.1 Literature and Unilever’s Current Methods .....	2
1.2 Collection Media.....	3
1.2.1 Hydrogels .....	6
1.3 Analytical Method Development .....	15
1.3.1 Chromatography .....	16
1.4 References .....	27
<b>2. Chromatography</b> .....	<b>32</b>
2.1 Gas Chromatography.....	32
2.1.1 Column .....	35
2.1.2 Heating Method .....	38
2.1.3 Solvent.....	41
2.1.4 Quantification including Calibration .....	42
2.2 Esterification.....	49
2.2.1 Fatty Acid Methyl Esters (FAMES) .....	50
2.3 High Performance Liquid Chromatography (HPLC).....	52
2.4 Conclusion .....	53

2.5	References .....	54
<b>3.</b>	<b>Hydrogel Synthesis.....</b>	<b>55</b>
3.1	Gel Proton NMR Method Development.....	55
3.2	Curing Efficiency .....	57
3.2.1	Gravimetry .....	57
3.2.2	Proton NMR analysis.....	59
3.2.3	Infrared Spectroscopy .....	60
3.2.4	TGA.....	62
3.3	Initiator Concentration .....	63
3.4	UV Sources.....	64
3.4.1	Crazing.....	64
3.5	Crosslinker Concentration study .....	67
3.5.1	Swelling Kinetics.....	68
3.5.2	Dynamic Mechanical Analysis .....	71
3.5.3	Tensile testing .....	72
3.6	Other Monomers.....	73
3.6.1	Hydroxyethyl acrylate .....	73
3.6.2	Hydroxyethyl methacrylate.....	76
3.7	Double Networks.....	79
3.7.1	Physical-Covalent DNs.....	80
3.7.2	Covalent-Covalent DNs .....	84
3.8	Conclusions.....	89
3.9	References .....	90
<b>4.</b>	<b>Optimising Swelling, Storage and Recovery .....</b>	<b>91</b>
4.1	Current Unilever Methods .....	91
4.1.1	Gravimetry .....	92

4.2	Model Sweat Uptake Kinetics.....	92
4.3	Swelling monitored by Contact angle .....	94
4.4	Solvent Extraction.....	97
4.4.1	Recovery Optimisation – simple solvent extraction .....	97
4.5	Soxhlet .....	100
4.6	Supercritical Fluid Extraction.....	104
4.6.1	Optimisation of conditions.....	105
4.7	Stability Studies .....	106
4.7.1	One month Room Temperature Incubation .....	106
4.8	Conclusion .....	108
4.9	References .....	109
<b>5.</b>	<b>Real Sampling, bacteria and qualitative screening .....</b>	<b>110</b>
5.1	Bacterial Assay.....	110
5.2	Unilever Study .....	112
5.3	Real Sampling .....	115
5.4	Additives .....	117
5.4.1	Indicators.....	117
5.4.2	Fragrance.....	129
5.5	Conclusion .....	130
5.6	References .....	131
<b>6.</b>	<b>Conclusions &amp; Future Work.....</b>	<b>132</b>
<b>7.</b>	<b>Experimental Techniques.....</b>	<b>136</b>
7.1	Materials.....	136
7.1.1	Model Sweat Solution .....	136
7.1.2	Polymerisation .....	138
7.1.3	Indicators.....	139

7.1.4	Fragrances .....	140
7.1.5	Solvents .....	140
7.2	Model Sweat Solution .....	140
7.3	Hydrogel Synthesis .....	140
7.3.1	Standard Procedure .....	140
7.3.2	Initiator Concentration.....	141
7.3.3	Crosslinker Concentration.....	142
7.3.4	Use of indicators .....	142
7.3.5	Addition of Fragrances .....	143
7.3.6	UV source .....	143
7.3.7	Thermal Polymerisations .....	144
7.3.8	Double Network Synthesis.....	144
7.4	Hydrogel Absorption .....	145
7.4.1	Swelling Kinetics.....	146
7.5	Recovery Procedure .....	146
7.5.1	Standard Process.....	146
7.5.2	Solvent extraction optimisation.....	146
7.5.3	Soxhlet Extraction .....	147
7.5.4	Supercritical Fluid Extraction .....	147
7.5.5	One month storage stability study.....	148
7.6	Analytical Techniques.....	148
7.6.1	Gas Chromatography .....	148
7.6.2	High Performance Liquid Chromatography .....	150
7.6.3	Absorption monitoring by contact angle. ....	150
7.6.4	Proton NMR Studies.....	150
7.6.5	UV-Vis Spectroscopy .....	151

7.6.6	Fluorescence Spectroscopy.....	152
7.6.7	pH readings .....	152
7.6.8	Fourier-Transform Infrared Spectroscopy (FTIR).....	152
7.6.9	Thermogravimetric Analysis (TGA) .....	152
7.6.10	Dynamic Mechanical Analysis (DMA).....	152
7.6.11	Mechanical Testing .....	152
7.6.12	Laser Scanning Confocal Microscopy.....	153
7.7	Bacterial assay .....	153
7.8	<i>In Situ</i> Sampling .....	154
7.9	References.....	155
	<b>Publication of Research in this Thesis .....</b>	<b>156</b>

## Acknowledgements

Firstly, I would like to thank Dave for the opportunity to complete my PhD within his group. Dave's support throughout has been a perfect balance of encouragement and leaving me to get on with stuff whilst somewhat relying on my organisational skills.

Secondly, to (honorary Professor) Ezat Khoshdel and Sue Bates for the project that still baffles most, has made me department infamous, and I have absolutely loved owning, thank you for this and for your support of all my research and many invites to work at Port Sunlight. Also to Steph and Michalana and everyone else at Port Sunlight for being so warm, welcoming and helpful throughout my PhD.

Also, to Steven Cenci and Prof. Ray Marriott for providing access to the supercritical fluid extraction rig.

To 'Team Unilever' members past and present; Gavin, Pawel, Tammie, Spyros and Holly, please continue to revolutionise sweat analysis.

Next to all my Chemistry friends at Warwick; the original C210 members; Jenny (and Tom), Sam, Patrick, plus third floor additions Ross, Connah and Paul. Also, the Broomfield regulars Guillaume, George, Marie, Tom, Joji, Andy K, Satu and Chris as well as everyone else we have adopted along the way; the cider has kept me sane.

Thank you also to Tara Schiller, for always being happy to share your materials knowledge / general life wisdom / time. Keep being awesome as you would say!

To my fellow 'Warwick Lifers' Chris and Julia; the three of us that refused to leave at the end of our MChems.

Thank you also to the Polymer RTP, the Mass Spec facility (Lijang Song) and the NMR facility (Ivan Prokes) for providing maintenance, access and wisdom on many of the instruments I have been lucky to include in this thesis.

Also to Dan, as both a colleague and boss (Polymer RTP) and my favourite bean who may have had something to do with me wanting to stay and do a PhD in the first place, thanks for looking after me / cooking me tea / keeping me sane throughout this process, even if you did try to kill me.



Finally to my sister, Emily, for having a 'have sleeping bag will travel' attitude in the undergrad halls days to these days using our house as a free hotel, you are welcome any time to keep proving I am not the most Northern-sounding person my friends know and obviously, my parents, for all the lifts up and down the country and support through the many years of education, one day I will get a proper job.

## Declaration

Experimental work contained within this thesis is original research carried out by the author, unless otherwise stated, in the Department of Chemistry at the University of Warwick between October 2015 and March 2019 and at Unilever Port Sunlight in May 2017. No material contained herein has been submitted for any other degree, or at any other institution.

Work conducted by other authors are outlined below and labelled throughout the corresponding text.

- Supercritical Fluid Extraction and analysis (Chapter 4) was carried out by Steven Cenci (Suprex).
- GC-MS analysis of human samples (Chapter 5) was carried out by Stephanie Blissett (Unilever).
- Bacterial Assay (Chapter 5) was carried out by Diana Cox (Unilever, Colworth).

Signed: \_\_\_\_\_

Rachel Alice Hand

Date: \_\_\_\_\_

## List of Figures

<b>Figure 1-1:</b> Formation of malodour by axillary bacteria adapted from James <i>et al.</i> <sup>5</sup>	2
<b>Figure 1-2:</b> Representation of the PharmChek <sup>®</sup> patch reproduced from Kintz <i>et al.</i> <sup>21</sup>	5
<b>Figure 1-3:</b> Results by year from the search term 'hydrogels' on pubmed. <sup>31</sup>	7
<b>Figure 1-4:</b> Structure of AMPS monomer.	8
<b>Figure 1-5:</b> Structure of HEMA monomer.	8
<b>Figure 1-6:</b> Structure of Irgacure 1173.	12
<b>Figure 1-7:</b> Comparison of the mechanical strength of various polymeric materials taken from Gong. <sup>66</sup>	13
<b>Figure 1-8:</b> Left diagram of the phases of carbon dioxide by temperature / pressure. Right schematic of supercritical fluid extraction apparatus.	20
<b>Figure 1-9:</b> A GC-Olfactometer.	21
<b>Figure 2-1:</b> Overlaid SIM and TIC chromatograms.	34
<b>Figure 2-2:</b> Highlighting the ability to differentiate between <i>i</i> -C <sub>5</sub> and <i>n</i> -C <sub>5</sub> by using SIM mode.	35
<b>Figure 2-3:</b> Illustration of the different types of column available for gas chromatography; packed (left), WCOT (middle) and PLOT (right). <sup>6</sup>	35
<b>Figure 2-4:</b> Comparison of the effect of column material and length on the separation of analytes by comparing chromatograms from a non-polar 15 m length column (Rxi1MS) and a polar 30 m length column (Stabilwax) both on the GC-FID using the Fleming oven heating method.	38
<b>Figure 2-5:</b> GC-FID chromatogram of the attempt to separate the 12 malodour compounds using the original, fast method.	39
<b>Figure 2-6:</b> Comparison of the heating profiles employed in the different GC-FID methods.	39
<b>Figure 2-7:</b> Chromatogram illustrating improved separation using the slower heating rate method.	40
<b>Figure 2-8:</b> TIC chromatograms for the two different column oven heating methods tested, where the black line uses the same method as successfully used on the longer, polar column on the GC-FID (left). Corresponding heating profiles (matching colours)	

where the Fleming method (GC-FID standard) heats from 60 to 200 °C at 8 °C min<sup>-1</sup> whereas the new method is from 35 to 100 °C at 2 °C min<sup>-1</sup> (right). All other conditions remained the same. ....40

**Figure 2-9:** Overlaid chromatograms illustrating that changing the eluent did not affect the chromatography. ....42

**Figure 2-10:** Calibration curves of the 5 separated VFAs. ....45

**Figure 2-11:** Overlaid chromatogram of the serial dilution highlighting the VFAs of interest. ....45

**Figure 2-12:** Chromatogram of lowest concentration determinable peak. ....46

**Figure 2-13:** Overlaid chromatograms with formic acid. ....48

**Figure 2-14:** Overlaid chromatograms investigating the potential of 2,2-dimethylbutyric acid. ....48

**Figure 2-15:** <sup>1</sup>H NMR spectra of the starting materials and product in the TMS esterification of butyric acid. ....49

**Figure 2-16:** <sup>1</sup>H NMR characterisation of the FAME reaction of butyric acid. ....50

**Figure 2-17:** GC-FID chromatograms of the methyl esterification reaction starting materials and product. ....51

**Figure 2-18:** Overlaid HPLC traces of acetic acid, butyric acid and isobutyric acid (left) and zoomed in on the analyte peaks (right). ....52

**Figure 3-1:** Left the diffusion of the dyed monomer. Right the <sup>1</sup>H NMR of the hydrogel before and after this addition, stacked. ....56

**Figure 3-2:** Percentage difference in mass of hydrogels exposed to the Light Hammer for varying amounts of time compared to the standard. ....58

**Figure 3-3:** Stacked <sup>1</sup>H NMR of the hydrogels synthesised using different UV exposure times with the highlighted disappearance of the vinyl peaks. ....59

**Figure 3-4:** Overlaid FTIR spectra of the hydrogels produced with different reaction times and the NaAMPS starting material. ....60

**Figure 3-5:** Overlaid TGA data from the hydrogels made using different UV exposure times. ....62

**Figure 3-6:** Stacked <sup>1</sup>H NMR spectra of the polymers produced using different initiator concentrations (relative to standard). ....63

**Figure 3-7:** Larger hydrogel with the wave cured in. ....64

<b>Figure 3-8:</b> ‘Crazed’ larger hydrogel.....	64
<b>Figure 3-9:</b> Standard hydrogel disk using Lighthammer only (left) and a hydrogel square cut from the bigger sheet synthesised using 8-9 minute pre-cure followed by lighthammer (right).....	65
<b>Figure 3-10:</b> UV-vis spectrum of irgacure 1173. ....	65
<b>Figure 3-11:</b> FITC dyed hydrogels (crazed and standard, left and right respectively) under UV light. ....	66
<b>Figure 3-12:</b> LCSM image of a crazed hydrogel. ....	66
<b>Figure 3-13:</b> Comparison of absorption and extraction efficiency of a standard p(NaAMPS) hydrogel and a ‘crazed’ p(NaAMPS) hydrogel.....	67
<b>Figure 3-14:</b> Swelling kinetics of the hydrogels containing different concentrations of crosslinker. Swelling ratio as calculated in eq. 1-1. Yellow highlighted region illustrated on RHS.....	68
<b>Figure 3-15:</b> Four different hydrogel crosslinker concentrations swollen to their maximum. For reference the large jar is 500 ml. Graph of EWC as a factor of crosslinker concentration (right).....	69
<b>Figure 3-16:</b> Storage modulus (') versus frequency of the increasing crosslinker concentration hydrogels. ....	71
<b>Figure 3-17:</b> Storage modulus (at 1 Hz) as a function of increasing crosslinker concentration.....	71
<b>Figure 3-18:</b> Tensile test Stress-strain repeat curve for the four crosslinker concentrations tested. ....	72
<b>Figure 3-19:</b> Young’s modulus as a function of increasing crosslinker concentration. ....	73
<b>Figure 3-20:</b> <sup>1</sup> H NMR of HEA monomer and p(HEA) hydrogels with different initiators concentrations investigated. Black = monomer, red = standard initiator conc. used, green = 10 times standard initiator concentration used. ....	74
<b>Figure 3-21:</b> Initial 6 hour swelling kinetics of the HEA single network. ....	75
<b>Figure 3-22:</b> Comparison of swelling ratios for the two different single networks over time. ....	75
<b>Figure 3-23:</b> P(HEMA) hydrogel synthesised <i>via</i> thermally induced bulk polymerisation as per literature. ....	77

<b>Figure 3-24:</b> P(HEMA) hydrogel as synthesised from aqueous solution (left) and after being dried to the xerogel state (right).....	78
<b>Figure 3-25:</b> standard 3 ml volume hydrogel, 10 wt% p(HEMA) (left), 10 wt% p(HEMA) hydrogel (middle) and 5 wt% p(HEMA) hydrogel (right) all with excess water on top. ....	78
<b>Figure 3-26:</b> Comparison of swelling kinetics for p(NaAMPS), p(HEA) and p(HEMA) (left) and focusing on p(HEA) and p(HEMA) (right). ....	79
<b>Figure 3-27:</b> Sodium alginate gel physically crosslinked using Ca <sup>2+</sup> as the divalent metal ion. ....	80
<b>Figure 3-28:</b> Viscous polymer formed at 15 wt% monomer.....	81
<b>Figure 3-29:</b> Proposed AMPS-graft-alginate reaction product.....	82
<b>Figure 3-30:</b> Acrylamide gel containing sodium alginate (left) and with added Ca <sup>2+</sup> solution (right).....	83
<b>Figure 3-31:</b> Overlaid compression cycles for the p(NaAlg) hydrogel before and after the second (physical) network was crosslinked.....	84
<b>Figure 3-32:</b> Initially synthesised double networks. ....	85
<b>Figure 3-33:</b> Overlaid swelling kinetics of NaAMPS and HEMA single networks as well as the combined double network. ....	86
<b>Figure 3-34:</b> p(NaAMPS)-HEMA after first UV-induced polymerisation but before thermal (HEMA) polymerisation. ....	87
<b>Figure 3-35:</b> Swelling kinetics of the p(NaAMPS-HEMA) pseudo-simultaneous DN compared to the equivalent single networks. ....	88
<b>Figure 3-36:</b> Comparison of the swelling kinetics of two NaAMPS-HEMA DN <sub>s</sub> synthesised <i>via</i> two different routes. ....	89
<b>Figure 4-1:</b> An insight into current, industrial olfactory assessment.....	91
<b>Figure 4-2:</b> Comparison of the average recovery of VFAs from dosed hydrogels using different swelling lengths of swelling time. ....	94
<b>Figure 4-3:</b> Average contact angle of the three materials, normalised to their own starting contact angle. ....	96
<b>Figure 4-4:</b> Contact angle of p(NaAMPS) at two different time points; 2 minutes (left) and 10 minutes (right).....	96

<b>Figure 4-5:</b> Analytical recovery data from the different solvent extractions for comparison.....	98
<b>Figure 4-6:</b> Analytical recovery data from different length of extractions.....	100
<b>Figure 4-7:</b> Overlaid GC chromatograms from the Soxhlet extraction of a hydrogel and a polyester patch.....	101
<b>Figure 4-8:</b> Concentration of three of the malodour acids as percentage of the dosed concentration.....	102
<b>Figure 4-9:</b> Comparison of simple solvent recovery and soxhlet extraction of a hydrogel. ....	103
<b>Figure 4-10:</b> Example total ion count (TIC) chromatograms, supplied by Suprex, from the method development of SFE of hydrogels. ....	104
<b>Figure 4-11:</b> hydrogels after various SFE procedures; 0.2 mol% Hydrogel after 20 min at 90 bar/35 °C (left) And after 20 min at 300 bar/50 °C (right) (a), 1.0 mol% X-linker Hydrogel CO <sub>2</sub> only, 300 bar (b), 2.0 mol% X-linker Hydrogel CO <sub>2</sub> only, 300 bar (c), and 2.0 mol% X-linker Hydrogel CO <sub>2</sub> and acetonitrile, 300 bar (d). All hydrogels are p(NaAMPS) where the mol% refers to the concentration of crosslinker (PEGDA). ....	105
<b>Figure 4-12:</b> Calculated percentage concentration recovered of the five VFAs with calibration curves over a four week stability study at 25 °C.....	107
<b>Figure 5-1:</b> Illustration of the bacterial assay results. ....	112
<b>Figure 5-2:</b> Anonymised data from the olfactory assessment of the hydrogel and textile patch comparison study.....	113
<b>Figure 5-3:</b> Chromatogram of sample containing 18 different identified compounds (pink line) compared to the 'blank' extract (black line) (supplied by Steph Blissett, Unilever Port Sunlight).....	114
<b>Figure 5-4:</b> Overlaid GC-MS chromatograms for participant 2's samples, highlighting the presence of propionic acid and butyric acid (supplied by Steph Blissett, Unilever Port Sunlight). ....	115
<b>Figure 5-5:</b> Stacked example chromatograms of real sweat collected using hydrogels. ....	116
<b>Figure 5-6:</b> Stacked chromatograms comparing a real sweat sample and two VFAs. ....	117

**Figure 5-7:** a) Overlaid fluorescence spectra of quinine at the two different pH. b) the corresponding structures of quinine. c) the corresponding photos of the solutions under the UV lamp with the recorded pH of the solutions. ....118

**Figure 5-8:** a) The quinine ‘gel’ that is yellow in colour. b and c) Photos of the quinine-AMPS polymers that did not form a stable gel network as standard p(AMPS) hydrogels do.....119

**Figure 5-9:** Left: Stacked <sup>1</sup>H NMR spectra of the hydrogels synthesised containing different concentrations of quinine. Right: the same spectra for the gels containing quinine sulfate.....120

**Figure 5-10:** 10 mg /gel quinine fluorescence spectra overlaid. ....120

**Figure 5-11:** Left: Normalised overlaid fluorescence spectra of the three different concentrations of quinine tested to-date. Right is the same spectra using quinine sulfate.....121

**Figure 5-12:** Quinine rehydrated hydrogel (top), under the UV light (bottom left), under the UV light with absorbed model sweat (bottom right).....121

**Figure 5-13:** Normalised fluorescence spectra illustrating that the quinine can be added pre- or post-polymerisation for the same detection result.....122

**Figure 5-14:** a) Worn hydrogels that contain quinine sulfate (left) and no indicators (right) under UV lamp. b) Comparison of worn and unworn halves of a quinine sulfate – containing hydrogel under a UV lamp. ....122

**Figure 5-15:** Normalised overlaid data of the worn quinine sulfate hydrogel and the equivalent model sweat spectra.....123

**Figure 5-16:** Structure of bromophenol blue.....124

**Figure 5-17:** Original standard hydrogel containing BPB (a), with 0.5 ml added model sweat (b), decreased concentration of BPB (c), with 0.5 ml added model sweat (d). ....125

**Figure 5-18:** UV-Vis spectra of a BPB containing hydrogel, before and after the addition of model sweat. ....125

**Figure 5-19:** Unworn (left) and worn (right) hydrogels all containing bromophenol blue.....126

**Figure 5-20:** Overlaid UV-vis spectra of a ‘blank’ BPB hydrogel (- - -), when model sweat is added (---) and the volunteer worn hydrogels (solid line).....127



<b>Figure 5-21:</b> p(HEMA) hydrogels containing bromophenol blue.....	128
<b>Figure 5-22:</b> p(NaAMPS) hydrogels containing ‘New Day’ fragrance at 1 % (v/v) fragrance (a), 0.5 % (v/v) fragrance (b) and no fragrance incorporated (c). .....	129
<b>Figure 5-23:</b> p(NaAMPS) hydrogels containing ‘White Willow’ fragrance at 0.1 % (v/v) fragrance (a), 0.5 % (v/v) fragrance (b) and 1 % (v/v) fragrance (c). .....	129
<b>Figure 7-1:</b> The Light Hammer®. ....	141
<b>Figure 7-2:</b> Output spectrum of 10” Fusion UV Electrodeless Bulb; H bulb (13 mm). .....	143
<b>Figure 7-3:</b> UV nail lamp that was used as an alternative UV light source.....	143
<b>Figure 7-4:</b> Side-by-side Soxhlet extraction set-up.....	147
<b>Figure 7-5:</b> Demonstration of hydrogel <i>in situ</i> in the UV-vis spectrometer.....	151

## List of Schemes

<b>Scheme 1-1:</b> General equations for the stages of free radical polymerisation.....	12
<b>Scheme 1-2:</b> Sequential IPN formation. Where M denotes monomer, I = initiator, X = Crosslinker. Black is the first network and red is the second. Filled circles are crosslinking points. Adapted from Interpenetrating Networks: An Overview. <sup>71</sup> .....	14
<b>Scheme 1-3:</b> Simultaneous IPN formation. Where M denotes monomer, I = initiator, X = Crosslinker. Black is the first network and red is the second. Filled circles are crosslinking points. Adapted from Interpenetrating Networks: An Overview. <sup>71</sup> .....	14
<b>Scheme 2-1:</b> General reaction of a volatile fatty acid to form the TMS ester.....	49
<b>Scheme 3-1:</b> Sadeghi <i>et al</i> proposed mechanistic pathway for synthesis of alginate-AMPS hydrogel. <sup>17</sup> .....	82
<b>Scheme 3-2:</b> pseudo-simultaneous IPN synthesis; both reaction mixtures are present prior to first network polymerisation but the reactions are carried out in sequence. Where M denotes monomer, I = initiator, X = Crosslinker. Black is the first network and red is the second. Filled circles are crosslinking points. ....	87

## List of Tables

<b>Table 1-1:</b> Comparison of boiling points <sup>96</sup> of straight chain saturated acids and their methyl esters. <sup>94</sup> .....	18
<b>Table 1-2:</b> Pictorial table of esters and the associated odour. <sup>97</sup> .....	18
<b>Table 1-3:</b> List of indicators recommended by Koh et al. with information collated from Bates. <sup>120,121</sup> .....	23
<b>Table 2-1:</b> Detectors and their associated detection limits. <sup>1</sup> .....	32
<b>Table 2-2:</b> Details of SIM mode analysis of short chain VFAs from Wu <i>et al.</i> The target ions used for quantification are highlighted. <sup>5</sup> .....	34
<b>Table 2-3:</b> Column information adapted from Practical Gas Chromatography A Comprehensive Reference. <sup>6</sup> .....	36
<b>Table 2-4:</b> Functional Groups and potential interactions. <sup>8</sup> .....	37
<b>Table 2-5:</b> Elution time and calculated minimum concentration for the 12 volatile compounds used. ....	47
<b>Table 3-1:</b> Infrared Spectroscopy characterisation of p(NaAMPS) and NaAMPS monomer. <sup>3</sup> .....	61
<b>Table 4-1:</b> Average uptake percentage and associated standard deviation ( $\sigma$ ) over absorption time where n = 3.....	93
<b>Table 4-2:</b> Average contact angles of a water droplet, on the three materials tested, over time. ....	95
<b>Table 4-3:</b> Percentage recovery from liquid-liquid liquid extraction based on GC peak areas. ....	99
<b>Table 4-4:</b> Mass data for preliminary stability test.....	106
<b>Table 5-1:</b> Summary of the results of the bacterial assay on pig skin test. N.B. T4 uninoculated (with and without hydrogel) account for failure to achieve total sterility of the pig skin, <i>via</i> radiation, prior to testing. ....	111
<b>Table 7-1:</b> Volatile compounds used. ....	136
<b>Table 7-2:</b> Starting materials for synthesis of p(NaAMPS) hydrogels.....	138
<b>Table 7-3:</b> p(HEMA) thermal polymerisation materials.....	139

## Table of Abbreviations

Abbreviation	Definition
A	peak area
AAm	acrylamide
AIBN	2,2-azobis(2-methylpropionitrile)
AMPS	2-Acrylamido-2-methylpropane sulfonic acid
amu	Atomic mass unit
APS	ammonium persulfate
A.U.	Arbitrary units
b.p.	boiling point
BPB	Bromophenol blue
cfu	Colony forming units
cfu/cm <sup>2</sup>	colonies found per square cm
CI	chemical ionisation
cm	centimetres
cm <sup>2</sup>	square centimetres
Da	Daltons
DMA	Dynamic Mechanical Analysis
DN(s)	double network(s)
ECG	electrocardiogram
EI	electron ionisation
EWC	equilibrium water content
FAME(s)	fatty acid, methyl ester(s)
FDA	US Food and Drug Administration
FFA(s)	free fatty acid(s)
fg	femtograms
fg s <sup>-1</sup>	Femtograms per second
FITC	fluorescein isothiocyanate
GC	gas chromatography
GC-FID	gas chromatography flame ionisation detector
GC-MS	gas chromatography mass spectrometry
GC-MS-O	gas chromatography mass spectrometry olfactometry
h	hour
<sup>1</sup> H NMR	proton nuclear magnetic resonance
HEA	2-Hydroxyethyl acrylate
HEMA	2-Hydroxyethyl methacrylate
HPLC	high performance liquid chromatography
Hz	hertz
IPN(s)	interpenetrating polymer network(s)
ID	Internal diameter
IR	infrared
K	Kelvin

LOD	limit of detection
LLOD	Lower limit of detection
LSCM	laser scanning confocal microscopy
m	metre
MBA	<i>N,N'</i> -methylenebisacrylamide
ml	millilitre
mm	millimetre
m min <sup>-1</sup>	metres per minute
mg l <sup>-1</sup>	milligrams per litre
mol dm <sup>-3</sup>	mole per cubic decimetre
mol%	Molar percent
mmol dm <sup>-3</sup>	millimole per cubic decimetre
m/z	Mass to charge ratio
N	Newtons
NaAMPS	2-Acrylamido-2-methylpropane sulfonic acid, sodium salt
NaAlg	sodium alginate
ng	nanograms
nl	nanolitre
NMR	nuclear magnetic resonance
OD	Optical density
Pa	pascals
p(AMPS)	poly(2-Acrylamido-2-methylpropane sulfonic acid)
p(HEA)	hydroxyethyl acrylate
p(HEMA)	poly(Hydroxyethyl methacrylate)
PBS	Phosphate-buffered saline
PDMS	poly(dimethyl polysiloxane)
PET	poly(ethylene terephthalate)
PEG	poly(ethylene glycol)
PEGDA	poly(ethylene glycol) diacrylate
pg	picograms
pg s <sup>-1</sup>	Pictograms per second
PhBr	bromobenzene
PLOT	porous layer open tubular
ppm	parts per million
PTR-MS	proton-transfer-reaction mass spectrometry
RF	response factor
RGB	red, green and blue light
RI	refractive index
SCFA(s)	short-chain fatty acid(s)
sCO <sub>2</sub>	supercritical carbon dioxide
SEC	size exclusion chromatography
SIM	single ion monitoring
SWE	subcritical water extraction
SFC	supercritical fluid chromatography

SFE	supercritical fluid extraction
SPME	solid phase microextraction
SR	Swelling ratio
TD	thermal desorption
TEMED	tetramethylethylenediamine
TGA	thermogravimetric analysis
TIC	total ion count
TMS	trimethylsilyl
TSBT	Tryptone soy broth with Tween
UV	ultraviolet
UV-Vis	Ultraviolet-visible
VA-057	2,2'-Azobis[N-(2-carboxyethyl)-2-methylpropionamide]tetrahydrate
VFA(s)	Volatile fatty acid(s)
VOC(s)	volatile organic compound(s)
vol%	Volume percent
w	amount of analyte
WCOT	wall coated open tubular
$W_d$	dry mass
$W_e$	equilibrium swollen state mass
$W_s$	swollen mass
wt%	Weight percent
$\mu$ l	microlitre

## Abstract

This thesis is concerned with the preparation, and subsequent application of, hydrogels as devices for analysing axillary malodour in order to test the efficacy of antiperspirant / deodorant products. Using the well documented ability of hydrogels to absorb water and small molecules, the absorption, storage and subsequent extraction of a model sweat was investigated. Ten volatile fatty acids, one unsaturated aldehyde and one thiol were used in an aqueous solution to represent malodorous sweat in order to investigate the plausibility of such a device.

Quantitative analysis of the malodorous compounds was carried out *via* GC-FID, with unknown compound identification carried out *via* GC-MS. Qualitative analysis was acquired with the addition of pH indicators such as bromophenol blue and quinine to the hydrogel device.

The physical properties of the hydrogels were also probed by investigating a range of crosslinker concentrations and alternative hydrogel materials. The swelling kinetics in deionised water and the mechanical properties were investigated by dynamic mechanical analysis and Universal tester.

Bacterial studies illustrated the hydrogels' suitability for *in vivo* testing which then illustrated that the model protocol could be transferred to natural samples.

# 1. Introduction

An axilla is one of the most densely populated areas of the skin; there are over 10 million bacteria living in the underarm. Wilson reported, in a study of healthy males and females,  $6.9 \times 10^5$  cfu/cm<sup>2</sup> and  $8.9 \times 10^5$  cfu/cm<sup>2</sup> respectively (number of colonies found per square cm), when counting total aerobes in the axillae.<sup>1</sup> Soap alone is not enough to combat the potentially unpleasant problem of body odour that can often affect self-esteem. As a result, antiperspirants and deodorants are a large global business. Statista estimate the size of the global antiperspirant and deodorant market in 2018 to be worth US\$72.7 billion<sup>2</sup> and estimate that Unilever had 26.6 % of the market share worldwide in the same year.<sup>3</sup>

The terms antiperspirant and deodorant are often used interchangeably but they have different purposes. Antiperspirants are worn to reduce the volume of sweat that reaches the skin surface in the axilla, whilst deodorants limit the concentration of malodorous compounds as they contain antimicrobial ingredients, where any product can perform one or both of these functions. It is proposed that by using the analytical techniques discussed in this thesis, the efficacy of a deodorant; *i.e.* its ability to limit the production of these malodours, can be determined by monitoring the concentration of volatile fatty acids in the axilla.

The axilla malodour arises from a combination of volatile fatty acids (VFAs), thioalcohols and steroids. These are by-products of the metabolism of proteins and lipids secreted in sweat by the bacteria that is found on the skin, and it is these that are malodorous rather than what is secreted directly (Figure 1-1).<sup>4-6</sup> In their review, de lacy Costello *et al.* suggest that there is a total of 532 volatile organic compounds reportedly emanating from the skin.<sup>7</sup> This thesis focuses on a sample of 10 VFAs, one unsaturated aldehyde and one thioalcohol in a mixed aqueous solution to mimic sweat when testing sampling devices and analytical techniques.



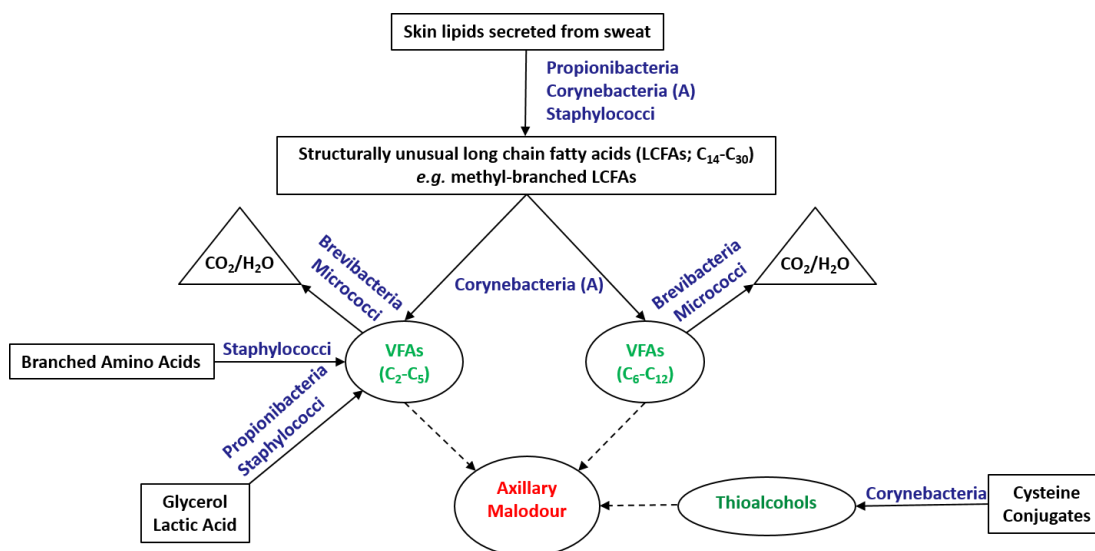


**Figure 1-1:** Formation of malodour by axillary bacteria adapted from James *et al.*<sup>5</sup>

Currently there is no method in place for the quantitative analysis of the effectiveness of an antiperspirant/deodorant concerning the malodour produced in the axilla, however, Dormont *et al.* published a useful review on previous related work, which indicated that no method applied alone allows trapping of the whole human scent.<sup>8</sup> They even went further as to suggest more than one method would need to be simultaneously applied in order to sample the whole scent profile from the human skin.

The “Official, Standardised and Recommended Methods of Analysis”, although outdated now, only had methods referenced for fatty acids in buttermilk and gave reference for them in only one bodily fluid; blood.<sup>9</sup>

## 1.1 Literature and Unilever’s Current Methods

The industrial standard for testing the efficacy of a deodorant is to employ ‘sniffers’ to mark the strength of the malodour in volunteers’ underarms out of five on a ten point scale. This is carried out under regulated conditions whilst allowing people to carry on their daily lives so as to get as close to realistic data to the everyday lives of the end user; the consumer.

An alternative used to monitor antiperspirant efficacy is to attach textile patches to underarms of t-shirts and weigh these after wearing for a set period to determine the mass of sweat produced. Even for this limited information storing is a difficulty

as the patches are immediately vacuum-packed and stored at -80 °C in order to avoid bacterial growth / loss of sweat.

## 1.2 Collection Media

Prada *et al.* demonstrated that contact sampling is better than non-contact sampling in both the range of volatiles collected and also the mass of scent collected.<sup>10</sup> Furthermore, they found that cellulosic type materials (*e.g.* cotton) provided the widest range of functional groups collected, and the largest mass of scent. This has been previously suggested to be a combination of differing volatilities of the compounds and the structure of the collection materials themselves. Obendorf *et al.* elucidated that the distribution of chemicals varied within cotton and poly(ethylene terephthalate) (PET) fibres. They are only found on the external surface of the PET whereas cotton fibres have a more complex structure with capillary forces and pore structures influencing the adsorption of liquids.<sup>11</sup> In addition, cotton is very hydrophilic with strong polar interactions. These are capable of forming bonds with the acidic molecules. Equally, McQueen *et al.* discussed the hydrophobic nature of polyester fabric which has no hydrogen bonding groups available, and therefore tends to be more oleophilic, with an affinity for the longer chain malodour precursors.<sup>12</sup>

Conversely, polyester-type materials appear optimal for the collection of acidic volatiles, however, this could be related to polyester being a better environment for the continuous production of volatile fatty acids *via* bacterial biotransformation even after the removal from volunteers, as hypothesised by McQueen *et al.* who observed an increase in short chain fatty acids after 7 days storage at room temperature.<sup>12</sup> Currently used polyester swatches have several drawbacks. These drawbacks include the inability to control the stability of the sample, which requires the samples to be vacuum-packed and stored at -80 °C to limit bacterial growth alongside the loss of the volatile components of sweat to the environment. Moreover, there is no standardised fabric of choice across the industry. Furthermore, there is currently no method for the recovery of the malodourous compounds from the polyester swatches, instead these are sniffed and graded on a 1-5 scale of strength and also weighed to determine the mass of sweat produced. The medium within which a

fabric containing collected sample is stored is also influential to the results of analysis along with the conditions at which it is stored. Hudson *et al.* found that glass was better for storage of cotton samples so that the results of the analysis were most similar to if they were analysed immediately, compared to storage in polymeric or aluminized materials, however, the heat-sealing process applied to some of these methods may have been partly responsible for some of the difference. Additionally, excessive exposure of samples to UVA/UVB lights leads to greater number of methyl esters and aldehydes being detected in the headspace analysis.<sup>13</sup> It is of note that these studies were undertaken in order to determine the reliability of the use of canine scent evidence in forensic science<sup>10,13,14</sup> rather than to test deodorant capabilities.

Axilla patches that have been patented over the last 25 years are mostly for odour control.<sup>15,16</sup> These are likely to contain active ingredients such as antiperspirants, deodorant elements or antimicrobial agents, and have no associated analytical element. Another patent was issued in 2006 for a much more complicated device including a circulation element and a sampling element such as an SPME fibre or a PDMS-coated stirrer bar for analysis by thermal desorption.<sup>17</sup>

Currently, sweat analysis is carried out for medical purposes. For example, in disease diagnosis, chloride concentration can be analysed as a test for cystic fibrosis. Due to the wide range of biomarkers available in sweat, it has also been shown to be a promising biofluid for use in the diagnosis of cancer and schizophrenia.<sup>18</sup> More recently, sweat has been investigated as an alternative to finger-prick blood testing for people with diabetes. A recent review of continuous glucose monitoring technology suggested that while there is a correlation between glucose concentrations in the blood and sweat, glucose concentration decreases from blood to skin surface and therefore the limit of detection, accuracy and precision of measurements using sweat samples remains a challenge.<sup>19</sup>

One product that has been commercially available for nearly 30 years is the PharmChek® sweat patch,<sup>20</sup> which is FDA approved and permissible as evidence in court for the detection of illicit drugs and their metabolites. This is a relatively basic non-occlusive patch consisting of an absorbent pad with an adhesive backing,<sup>21</sup>

something that is interesting as a possible device for collection of the malodorous components of sweat as is the goal of this research.

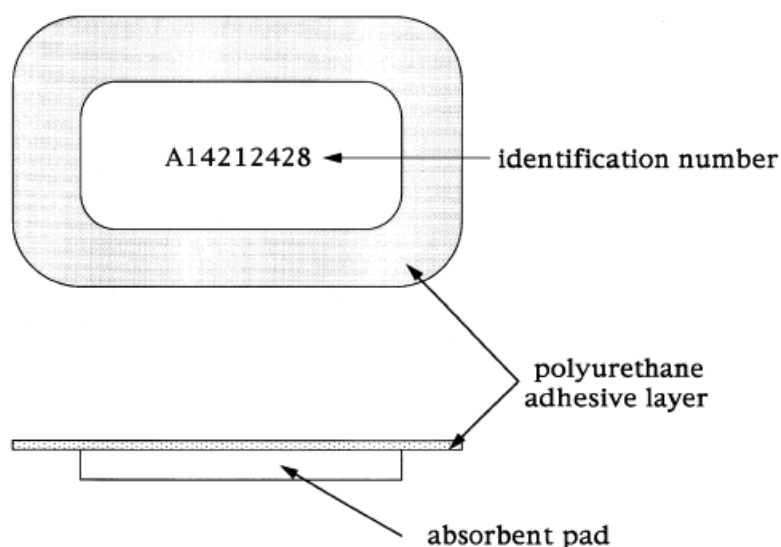


**Figure 1-2:** Representation of the PharmChek<sup>®</sup> patch reproduced from Kintz *et al.*<sup>21</sup>

Twenty years ago, Schoendorfer was granted a patent for a method and apparatus for determination of chemical species in perspiration.<sup>22</sup> Unlike hydrogels, this was a dissolvable patch rather than one that required extraction. Although it was used for analysis, it was designed to monitor controlled drug (e.g. cocaine) metabolites as a less invasive technique than blood sampling and was looking for volatiles such as ethanol (rather than VFAs).

Ten years later, Savelev *et al.* were granted a patent for a more complicated sampling device.<sup>17</sup> This was a device that enclosed a volume above the skin surface. It contained a sampling element, examples being an SPME fibre or a PDMS-coated stir bar. Both SPME fibres and PDMS-coated stir bars have appeared in other literature as sampling materials for this application and are completely different to the current solvent extraction method employed with the hydrogel as they would be transferred directly in to an analytical device (e.g. GC-MS) for analysis preferably by a transfer method such as thermal desorption. Furthermore, the device included a mechanical element which encouraged the circulation of the entrapped air. This is not something that is part of the hydrogel device.

A third patent came in the same year, from Villain, who created a disposable underarm patch.<sup>16</sup> This was a kidney-shape design made of 'flexible' material with the intention of protecting the wearer's clothing from sweat stains. There is no mention of recovering from the device for any sort of analysis of the sweat. This was also prior art in the patent of Van Bavel.

In 2013, Van Bavel *et al.* were granted a patent for a disposable, self-adherent odor-control patch.<sup>15</sup> This was for the same application as that of Villain. Although it was probably polymeric, there was no mention of hydrogels. It also included an odour-control agent (e.g. activated carbon / zeolite / clay / silica / cyclodextrin) and potentially other additives.

### 1.2.1 Hydrogels

The aim of this project requires an absorbent material to form part of the collection device, one possible material for such a device is a hydrogel. Hydrogels are superabsorbent cross-linked polymer networks which can be >90 % water. This makes them viscoelastic and, with a soft consistency and high porosity, often similar to animal tissue.<sup>23</sup> There are many patents and literature references for hydrogels being used in a wide range of medical and personal applications such as on ECG electrodes,<sup>24</sup> contact lenses,<sup>25,26</sup> wound care<sup>27</sup> and transdermal drug delivery<sup>28,29</sup> as well as a much wider range of applications, making them ideal for their use in this novel application. As demonstrated in Figure 1-3, the interest in hydrogel research has grown exponentially over recent decades.<sup>30,31</sup>

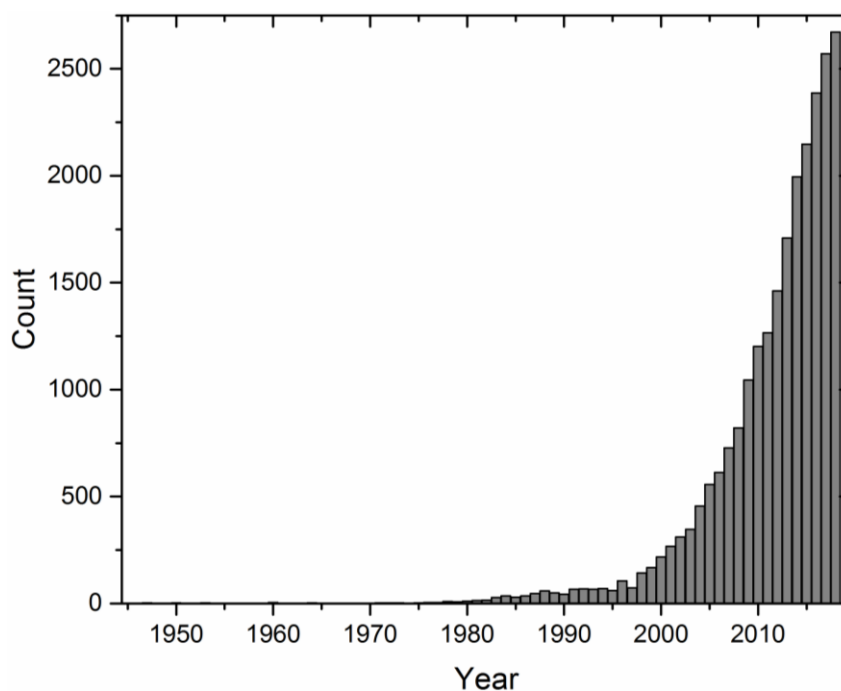


**Figure 1-3:** Results by year from the search term 'hydrogels' on pubmed.<sup>31</sup>

The applications of hydrogels are often either for absorption (in the case of wound dressings) or release (transdermal drug delivery), but thus far no studies have been found which report an application requiring both. Most of the characteristics required of a wound dressing hydrogel are relevant to this application as the device will also remain on the skin for extended periods of time; maintain natural skin moisture level and temperature, demonstrate good gas permeability, are able to be supplied sterile and be easy to apply then remove.<sup>32</sup>

Some polymers commonly used for the synthesis of hydrogels both as homopolymers or copolymers include: poly(vinyl alcohol), poly(*N*-vinyl-2-pyrrolidone), poly(ethylene glycol), poly(*N*-isopropylacrylamide), poly(acrylic acid) and polyurethanes,<sup>33</sup> however, these will not be focussed on in this work.

Another monomer widely used in the production of hydrogels is 2-acrylamido-2-methylpropane sulfonic acid (AMPS, Figure 1-4) and its sodium salt, NaAMPS.<sup>23,27,34–39</sup> It is suitable for use in human contact devices and widely used as such, however, according to Kabiri *et al.* the synthesis of full-AMPS hydrogels is yet to be reported.<sup>35</sup>

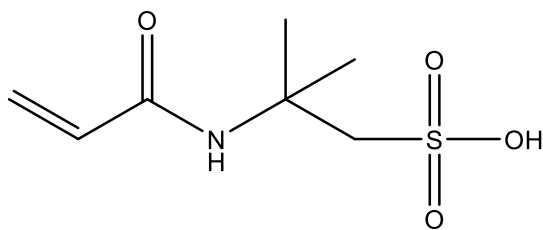


**Figure 1-4:** Structure of AMPS monomer.

A further possible monomer is hydroxyethyl methacrylate (HEMA). The use of HEMA was first reported for this use in the 1960s by Wichertle and Lim,<sup>25,40</sup> around the time that ‘plastics’ for biomedical applications were first being studied. At that time the main challenge was the lack of materials akin to biological tissue, a property that, these days, hydrogels are well known for. HEMA also produces biocompatible hydrogels and is commonly used in the synthesis of contact lenses known as soft contact lenses. It also affords different structural and mechanical properties to a hydrogel. Unlike p(AMPS) hydrogels, these will only swell to ~40 % water.<sup>41</sup> This is something investigated in Chapter 3 of this thesis.

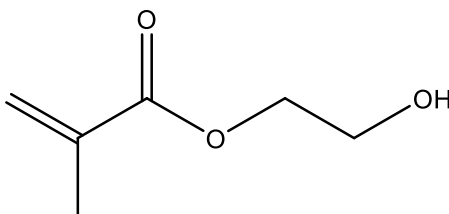


**Figure 1-5:** Structure of HEMA monomer.

#### 1.2.1.1 Swelling

Hydrogels can absorb most solvents as opposed to dissolution when placed in solvent due to their chemical or physical crosslinks. The degree of swelling is one of the most important parameters when designing and synthesising hydrogels for medical applications such as the delivery and release of drugs.<sup>42</sup> Thus, the kinetics of the swelling and, similarly, deswelling equilibrium of hydrogels have been studied; originally this was published by Peppas in two consecutive articles defining a simple equation for description of solute release.<sup>43,44</sup> In the first of the two articles, he reports that drug release can be modelled by Fickian’s diffusion mechanism for polymeric devices of various geometries (equation 1-1, below).

$$\frac{M_t}{M_\infty} = kt^n \quad (1-1)$$

Where  $M_t/M_\infty$  is the fractional solute release,  $t$  is the release time,  $k$  is a constant incorporating characteristics of the macromolecular network system and the drug, and  $n$  is the diffusional exponent which is indicative of the transport mechanism. For disks or tablets (the shape of a hydrogel), depending on the ratio of diameter to thickness, the Fickian diffusion mechanism is described by  $0.43 < n < 0.50$ .

In the second article, Peppas describes how swellable devices can still be modelled using equation 1-1 as long as the equilibrium swelling ratio is not higher than 1.33 (25 % water content by volume).

Meanwhile, other research has been carried out in an attempt to determine the length of time necessary to reach swelling equilibrium.<sup>27,42</sup> Kabiri *et al.* reported a 0.2 g sample of polymer was left for two hours in 500 ml of water in order to reach equilibrium whilst Taleb *et al.* reported HEMA/AMPS hydrogels required 10 hours to reach swelling equilibrium under irradiated conditions. Taleb *et al.* used equation 1-2, where  $w_s$  and  $w_d$  are the mass of the swollen sample and the dried sample respectively, to calculate the water uptake as a percentage until equilibrium was reached.

$$\text{Water uptake (\%)} = \frac{W_s - W_d}{W_d} \times 100 \quad (1-2)$$

Although gravimetric methods are the most widely used methods to calculate water content and swelling kinetics in literature, they are not the only methods available. Similar calculations can be performed using volumetric methods.<sup>45</sup> Alternatively, the water content can be related to the refractive index of the material. As the RI of water is known (1.33), as a hydrogel becomes more hydrated, the RI of the material will tend towards this number. Conversely, as it is dehydrated, the RI will increase. By carrying out the RI measurements on a series of hydrogels with known water content, a calibration curve can be created to be used on unknown samples. As illustrated by, Efron and Brennan, this calibration curve does not change regardless of the polymeric material investigated.<sup>46</sup>



Research into the effect of drying methods of hydrogels on their swelling capacity has also been reported.<sup>35</sup> Although Kabiri *et al.* concluded that oven-drying was the most cost-effective, and therefore favourable industrial method, this would not work for the application in this project as it is assumed the VFAs would evaporate first. Other methods including non-solvent dewatering, room-temperature drying and freeze drying have been reported. Freeze-drying has been used to prepare hydrogels for scanning electron microscopy (SEM) analysis.<sup>39</sup>

#### 1.2.1.2 Oxygen Permeability

Oxygen permeability is useful for sweat collection devices as it allows the aerobic respiration of the skin bacteria as in the natural state, thus keeping the environment as realistic as possible and therefore the efficacy data of deodorant products akin to without the hydrogel device being there.

Oxygen permeability of hydrogels increases logarithmically with increase in hydration irrespective of polymer type,<sup>29,46,47</sup> where, as discussed, water content can be measured and calculated in several ways. This is likely due to water having a greater oxygen permeability than the polymer and, as hydration increases, the water has a greater influence. The relationship between EWC and oxygen permeability has been found to be:<sup>48</sup>

$$Dk = 1.67e^{0.0397EWC} \quad 1-3$$

Where D is the diffusivity of the material, k is the oxygen solubility and EWC is the equilibrium water content of the material.<sup>49</sup> The units of Dk are known as Barrer (a non-SI unit for gas permeability used in the contact lens industry).<sup>50</sup> A high Dk value suggests a high oxygen transmittance where  $Dk < 12$  are considered a low value.<sup>51</sup> Due to oxygen permeability also being dependent on the thickness of the material, the transmissibility level (Dk per thickness) is more commonly used and expressed as Dk/t. Where hydrogels use the water to transport oxygen, the maximum Dk/t is approximately 40. Silicone hydrogels have a higher oxygen permeability ( $> 100Dk/t$ ) as the silicone molecules are better than the water molecules at the transportation of oxygen.<sup>52</sup>

#### 1.2.1.3 Smart gels

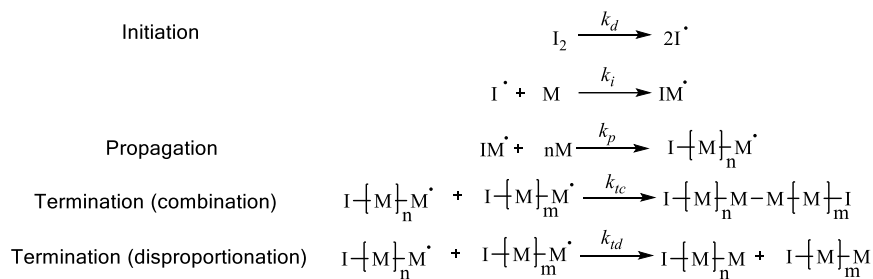
'Smart gels' are environmentally sensitive hydrogels; they react to chemical (*e.g.* pH changes and solvent exchange) or physical stimuli (*e.g.* temperature, light, electric forces, magnetic forces, and mechanical forces). These types of hydrogel are already being used in medical applications including transdermal drug delivery which suggests that the recovery of the volatile components of sweat is possible *via* one, or a combination, of these stimuli.<sup>53</sup>

For example, according to Taleb *et al.*, the SO<sub>3</sub>H groups on the AMPS can readily dissociate to form SO<sub>3</sub><sup>-</sup> "mobile ions" that can create an osmotic pressure difference between the gel and the solvent which leads to an enhancement in swelling.<sup>42</sup> As a result of this, the uptake and release from an AMPS containing hydrogel can be pH controlled. Bao *et al.* reported that when using the sodium salt form of the AMPS or taking the hydrogel above pH = 9, excess Na<sup>+</sup> causes a "charge screening effect" and therefore a decrease in the swelling equilibrium. This led to them reporting an optimum pH for degree of swelling of pH = 5.<sup>54</sup>

#### 1.2.1.4 Polymerisation

Generally, hydrogels can be synthesised 2-ways; either by crosslinking the water-soluble, linear polymer post-polymerisation using radiation, heating or a crosslinking agent, or *via* 'three-dimensional polymerisation' which is the polymerisation of the chosen monomer in the presence of a multi-functional crosslinking agent.<sup>55</sup> It is the latter that will be focused on in this work.

Hydrogels can be synthesised *via* photo-initiated radical polymerisation. They can be produced in the dry state *via* a bulk process (*e.g.* soft contact lenses<sup>47</sup>) or *via* solution polymerisation using water or other solvents to dilute the system as a way of controlling heat transfer and other properties of the hydrogels produced.<sup>56</sup> Although this may lead to some uncontrollability, it is often a preferred synthetic route.



**Scheme 1-1:** General equations for the stages of free radical polymerisation.

Irgacure 1173 (2-hydroxy-2-methylpropiophenone, Figure 1-6) is a hydroxyacetophenone which is a Type I photoinitiator. This means it is a unimolecular photoinitiating system, *i.e.* no coinitiator or catalyst is required instead, typically one bond is broken *via* homolytic cleavage to form a pair of radicals. Whereas with type II initiators, hydrogen abstraction is used to create two radicals on separate molecules *e.g.* benzophenone.<sup>57,58</sup> Hydroxyacetophenones usually absorb shorter wavelength UV-A radiation than benzophenones (300-350 nm).

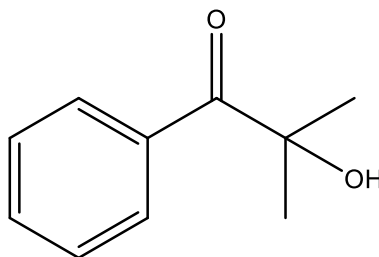


**Figure 1-6:** Structure of Irgacure 1173.

#### 1.2.1.5 Copolymers

Most hydrogel literature found is on copolymers *i.e.* they contain two or more different monomers within the one network. Ahmed suggests that at least one is a hydrophilic component, and that they can be arranged in a random, block or alternating configuration along the chain of the polymer network.<sup>56</sup> For example, the hydrogel copolymer composition patent by Munro and Boote,<sup>59</sup> and in the literature; AMPS and *N*-isopropylacrylamide,<sup>60</sup> Poly(acrylamidoxime-*co*-AMPS),<sup>61</sup> AMPS, *N*-vinylpyrrolidone and acrylic acid,<sup>62</sup> HEMA and acrylic acid,<sup>63,64</sup> and many more. Copolymers of AMPS and HEMA have been reported by Taleb *et al.* and, more recently, Elgueta *et al.*<sup>42,65</sup>

This method of combining monomers has not been investigated in this research.

### 1.2.1.6 Interpenetrating Polymer Networks

Another method of combining more than one monomer is interpenetrating polymer networks (IPNs) which are composed of two polymer networks within one material. There can be many benefits of double networks compared to single networks depending on the specific constituent combinations, Figure 1-7. This allows for flexibility in tuning the properties of the materials. The synthetic route to these double networks is dependent on the network required, that is what monomeric species to use.

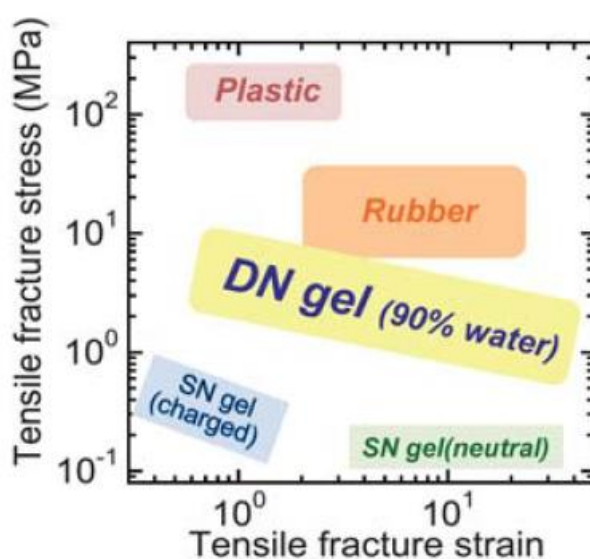
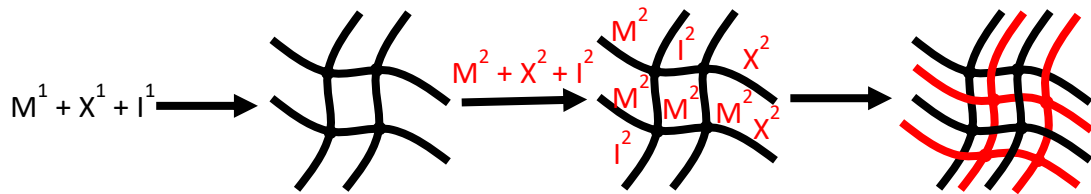


**Figure 1-7:** Comparison of the mechanical strength of various polymeric materials taken from Gong where DN = double network and SN = single network.<sup>66</sup>

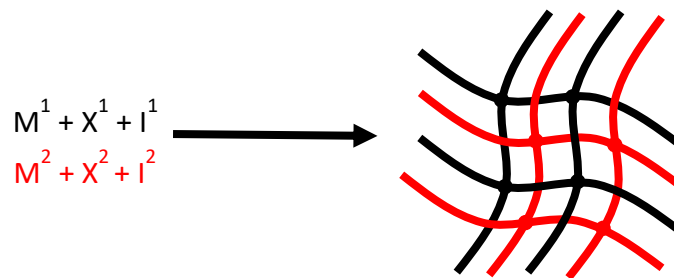
According to Peak *et al.* double networks (DNs) consist of two interpenetrating and covalently crosslinked polymer networks with Gong *et al.* suggesting that these networks illicit opposing properties.<sup>67</sup> This can be achieved *via* a 2-step synthetic process, known as sequential IPNs, whereby one network is formed then the resultant gel is soaked in the monomer of the second network before a second polymerisation is carried out, Scheme 1-2.<sup>68,69</sup> This itself can be an issue as not only is it comparatively time consuming compared to a 1-pot synthesis, but it also relies on the second monomer being readily and uniformly absorbed by the first network. A good example for this first network are polyelectrolytes, e.g. 2-acrylamido-2-methyl-1-propanesulfonic acid (AMPS). According to Chen *et al.*, this was first double

network, reported in 2003 by Gong *et al.* using a combination of acrylamide and AMPS.<sup>68,70</sup>



**Scheme 1-2:** Sequential IPN formation. Where M denotes monomer, I = initiator, X = Crosslinker. Black is the first network and red is the second. Filled circles are crosslinking points. Adapted from *Interpenetrating Networks: An Overview*.<sup>71</sup>

Alternatively, IPNs can be synthesised *via* a one-pot process known as simultaneous IPNs, Scheme 1-3.<sup>69,71</sup> Here, both sets of monomer, crosslinker and initiator are included in one solution prior to polymerisation which may take advantage of two different, noninterfering initiation methods.



**Scheme 1-3:** Simultaneous IPN formation. Where M denotes monomer, I = initiator, X = Crosslinker. Black is the first network and red is the second. Filled circles are crosslinking points. Adapted from *Interpenetrating Networks: An Overview*.<sup>71</sup>

Gel networks can be covalently or physically crosslinked. Covalent bonds require the use of a chemical crosslinker during polymerisation whilst physical crosslinking can be achieved with either natural polymers (*e.g.* polysaccharides such as alginate) or synthetic polymers, post-polymerisation of linear chains, by modification to form hydrogen-bonds, Van der Waals interactions or ionic bonding.

Covalently-crosslinked gel networks are typically stronger than the physically crosslinked networks, however, in covalent networks, once the bonds are broken, they cannot be recovered. Conversely, physically crosslinked networks often break more easily, however, this is often reversible once no longer under stress. A DN does not have to be purely covalent or physical, it can be a combination of one of each type. This allows for even more diversity of material properties. Depending on the combination of double network types used, the increase in strength compared to a single network gel will occur *via* a different mechanism. Gong reported that covalent

– covalent DNs are strengthened *via* the ‘sacrificial bond’ mechanism.<sup>66</sup> Here, bonds of one network break in order to ‘protect’ the other network and in doing so leave pockets of the initial network intact along with dissipating the energy from the stress. In this case it is the AMPS network that breaks protecting the acrylamide network of the original AMPS-AAm material.

A similar mechanism occurs in a chemical-physical double network, except here it is the weaker, physical network that breaks and, unlike in the covalent-covalent system, this is reversible. These are known as hybrid DNs. Chen *et al.* proposed a ‘chain pulling-out mechanism’ for these hybrid double networks.<sup>72</sup> This can allow for strength to be maintained over a number of cycles compared to the covalent-covalent networks that will likely see a decrease in strength in subsequent mechanical test cycles.

### **1.3 Analytical Method Development**

As the products of bacterial metabolism, VFAs are found in many scenarios and as such their analysis is needed in many areas, not just human (and animal) body fluids,<sup>7,73–75</sup> such as: wastewater,<sup>76,77</sup> landfill leachates,<sup>78,79</sup> food<sup>80,81</sup> and other environmental systems. Analysis of sweat is carried out for many reasons including: medical diagnoses and testing,<sup>74,82</sup> forensic science applications<sup>7,10,13,14,83</sup> and drug testing.<sup>18</sup>

According to Anderson and Yang, volatile fatty acids (VFAs) analysis can be carried out *via* a number of methods including titration, (steam) distillation and chromatography,<sup>84</sup> where Fernandez *et al.* suggest chromatography (gas, liquid, anion exchange and ion exclusion) and capillary electrophoresis.<sup>85</sup> Anderson and Yang described a new alkalinity test to determine total volatile fatty acid concentration as their favoured method as distillation is time consuming and gas chromatography requires more expensive instruments. They also suggested a more direct titration method from several decades earlier,<sup>86</sup> however, both of these would only elicit total VFA concentration. For this reason, titration is not applicable to our application as it does not elicit as much information as chromatography methods would. However, they did demonstrate comparable concentrations *via* their titration

method and a GC method suggesting it could be useful as a pre-screening method. Furthermore, their analyte samples are larger as they are sampling anaerobic digesters, whereas it is very difficult to (naturally) collect a large enough sample of sweat (not absorbed) for this to be viable.

Carboxylic acids for axillary odour investigations have also been analysed by proton-transfer-reaction mass spectrometry (PTR-MS).<sup>87</sup> This relies on the chemical ionisation of the acids primarily to the protonated carboxylic acid ions ( $\text{RCOOHH}^+$ ). This is a relatively simple technique for the detection and quantification of compounds in a mixture although does not provide exact identification though identification can be suggested based on the molecular weight as there is low fragmentation occurring with this soft ionisation technique. With the use of a bell jar sampling device, von Hartungen *et al.* reported successful measurements of short-chain fatty acids (SCFAs) direct from the underarm *via* headspace extraction. Notably, they stated no quantifiable effect by the treatment with an antiperspirant, however, this was a very small study where the authors noted very little adherence to protocol by the participants.

### 1.3.1 Chromatography

Analysis of free VFAs (note: not the ester derivatives), predominantly by gas chromatography (GC) and high performance liquid chromatography (HPLC), both with and without mass spectrometry (-MS), is widely reported from as far back as the 1960s.<sup>88</sup> This includes samples recovered from human sources such as plasma and saliva.<sup>89</sup> Furthermore, this was also applied to sweat samples by Perry *et al.*, although these samples were collected under 'forced' conditions (volunteer was sat in a large plastic bag with the addition of heating).<sup>90</sup>

A further example of forced conditions is the use of pilocarpine. This is a molecule with a variety of medicinal applications. Its side effect of excessive sweat production is exploited in biomedical sweat testing. It is introduced to the patient *via* iontophoresis (diffusion of ions driven by an electric current) and was first reported by Gibson and Cooke in 1959 who also discussed the problems (including fatalities!) associated with the bag method.<sup>91</sup>

These forced conditions were deemed necessary because, naturally, humans only produce relatively small volumes of sweat, where, the aim of this research is to create a device that is more feasible to use in a more realistic situation, and therefore with a more realistic quantity collected, consequently the sensitivity of the analytical technique must be considered. Fleming *et al.* carried out the GC of human biological specimens using a polar column with a mixed solvent that was partially acidified, where the method development for this project was based on this research.<sup>89</sup> Concentrations of VFAs from various bodily fluids have been quantified using linear regression analysis based on the integrated areas of the peaks compared to the linear calibration in relation to the internal standard.<sup>73</sup> In 1975, Hauser and Zabransky used GC to determine the presence of VFAs in order to identify the presence of anaerobic bacteria.<sup>92</sup> It is this methodology that we aim to use as a method to quantify the efficacy of an antiperspirant / deodorant product.

The advantage of using GC in combination with mass spectrometry (GC-MS), as when using any combination of analytical techniques, is that it provides more information than if the two techniques were used separately, as a result of this it is a widely used technique. In the case of GC-MS, the addition of molecular splitting patterns, along with database identification, gives more definitive proof of the compounds' identities rather than relying on a comparison of elution times (as in GC-FID) as there can be more than one compound with the same elution time. GC-MS has been a popular analytical technique for the analysis of fatty acids since the 1980s. A literature survey of this area indicates that most of this work was carried out on ester derivatives. The most obvious reason for this is that derivatization increases the volatility of the fatty acids. Due to the polar hydroxyl groups on the free acids, intermolecular hydrogen bonding can occur, therefore increasing the boiling point of the free acids.<sup>93</sup> Masking these groups, *e.g.* by derivatisation, therefore increases volatility by removing these intermolecular interactions as is illustrated in Table 1-1.<sup>94</sup> In addition, the esters tend to smell more favourable than the free acids, with esters being responsible for many fruit aromas which may make the esterified forms more appealing to handle, Table 1-2.<sup>95</sup>



**Table 1-1:** Comparison of boiling points<sup>96</sup> of straight chain saturated acids and their methyl esters.<sup>94</sup>

IUPAC name	common name	Free acid		methyl ester	
		melting point (°C)	boiling point (°C)	melting point (°C)	boiling point (°C)
methanoic	formic	8	101	—	32
ethanoic	acetic	17	118	—	56
propanoic	propionic	-21	141	—	80
butanoic	butyric	-8	162	—	102
pentanoic	valeric	-35	184	—	127
hexanoic	caproic	-2	205	—	150
heptanoic	enanthic	-9	223	—	172
octanoic	caprylic	16	240	—	193

**Table 1-2:** Pictorial table of esters and the associated odour.<sup>97</sup>

**Esters**  
Table of esters and their smells

from the carboxylic acid (second word)	from the alcohol (first word)										
	methyl 1 carbon	ethyl 2 carbons	propyl 3 carbons	2-methyl propyl- 4 carbons	butyl 4 carbons	pentyl 5 carbons	hexyl 6 carbons	benzyl benzene ring	heptyl 7 carbons	octyl 8 carbons	nonyl 9 carbons
<b>methanoate</b> 1 carbon	ETHEREAL	BACARDI		ETHEREAL							?
<b>ethanoate</b> 2 carbons											
<b>propanoate</b> 3 carbons											?
<b>2-methyl propanoate</b> 4 carbons, branched		ETHEREAL	BACARDI								?
<b>butanoate</b> 4 carbons											?
<b>pentanoate</b> 5 carbons					ETHEREAL				?	?	
<b>hexanoate</b> 6 carbons											
<b>benzoate</b> benzene ring									?		
<b>heptanoate</b> 7 carbons					?					?	
<b>salicylate</b> from salicylic acid								DIFFERENT PEOPLE PERCEIVE DIFFERENTLY	?		?
<b>octanoate</b> 8 carbons											
<b>nonanoate</b> 9 carbons									?		?
<b>cinnamate</b>											?
<b>decanoate</b> 10 carbons									?	?	?

The most common esters employed are methyl, benzyl and trimethylsilyl (TMS) esters.<sup>98–103</sup> However, derivatisation is time consuming and the aim of this project is to develop a method of analysing the free fatty acids (FFAs) as this is more efficient and cost effective and, as mentioned above, has already been reported for standalone GC. Despite this, in order to test this hypothesis for our own circumstances, derivatization and analysis was briefly investigated (Chapter 2 section 2.2)

### **Sample preparation**

In 2015, Jadoon *et al.* indicated that, unlike with other bodily fluids, generally sweat is directly analysed without the need for extraction.<sup>18</sup> One form of GC-MS commonly used for analysis of VFAs is solid-phase micro-extraction –GC-MS (SPME-GC-MS).<sup>104</sup> The advantage of this technique is that it analyses the volatiles in the air above the solid sample in the vial which is ideal for volatiles. In addition, this is more useful for smaller volume / less concentrated samples as there is no further dilution by the addition of solvent for recovery. Dormont *et al.* hypothesised that the extraction method effects which parts of the scent profile are detected.<sup>8</sup> The example they give is that Curran *et al.* use SPME as their extraction technique<sup>104</sup> but do not detect thiols known to be part of malodour whereas when using solvent extraction (*e.g.* Zeng *et al.* and Natsch *et al.*<sup>105</sup>) the key compounds were detected.

A further extraction method that can be combined with GC-MS is thermal desorption. This is where the analytes are extracted from the solid substrate using a combination of heat and an inert gas flow to carry the volatiles to the GC. According to Agilent, this is reliably up to 95 % efficient compared to solvent extraction techniques which are reported to be 30 – 80 % efficient.<sup>106</sup>

When not using either of these solid phase extraction techniques, the extraction method to be used has to be considered in order to minimise loss of analyte pre-analysis. Prada *et al.* compared supercritical fluid extraction (SFE), subcritical water extraction (SWE), Soxhlet extraction and the use of an autoclave on various brands of sterile pads and cottons.<sup>83</sup> They found that even with sterilization, headspace analysis of ‘blank’ gauze pads still revealed the presence of volatile organic

compounds (VOC) limiting the analysis results. They concluded that, of the methods tested, SFE resulted in the complete removal of VOCs from the sorbent materials under optimised conditions and therefore this was the best of those tested. The drawback of SFE is that there is a limit to the amount of water that can be introduced into the system because of the cooling that occurs, as the water will likely freeze and cause blockages.

Supercritical Fluid Extraction (SFE, not to be confused with supercritical fluid chromatography – SFC) is a technique that most commonly uses supercritical carbon dioxide (sCO<sub>2</sub>) as the extraction solvent. A supercritical fluid is one that is above its critical temperature and pressure. For carbon dioxide, these are 304 K and 72.8 bar respectively (Figure 1-8).<sup>107,108</sup> Cardea *et al.* reported the use of sCO<sub>2</sub> to dry hydrogels, removing all solvent to form scaffolds for tissue engineering applications.<sup>109</sup> This is something that will be investigated in Chapter 4.

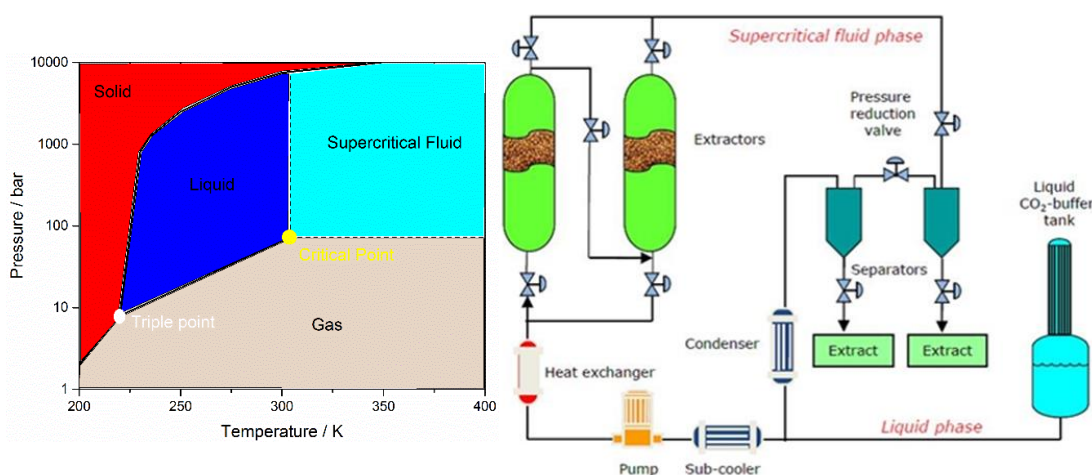


**Figure 1-8:** Left diagram of the phases of carbon dioxide by temperature / pressure. Right schematic of supercritical fluid extraction apparatus.

Furthermore, Kanda *et al.* used a six hour long Soxhlet extraction to remove foot sweat samples from socks for GC-MS analysis. They found that although all samples contained SCFAs, only those with a strong foot odour contained isovaleric acid.<sup>104,110</sup>

A further analytical technique that is used for the analysis of malodour is olfactometry.<sup>111</sup> In olfactometry, odours are pushed down a tube to an opening made for someone to place their nose and sniff. The ‘sniffers’ then pick from an extensive list of descriptive words such as that put together by Harper in 1968<sup>112</sup> as their rating.

This was used in conjunction with GC by Dravnieks to create an odorgram; a GC chromatogram annotated with the assigned descriptors, and is still used in such a manner or in conjunction with GC-MS (GC-MS-O) to this day (see Figure 1-9). Interestingly, Dravnieks used the Kovats index (converts retention times to system independent constants by comparing them to the elution of known *n*-alkanes) for his GC data. This is the only use I am aware of, even though it was first coined by Ervin Kováts in 1958, as it appears not to have been widely adopted.<sup>113</sup> The advantage of GC-MS-O is that the individual malodour components in a mixed sample will elute at different times and therefore can be smelled separately. Olfactometry is most similar to the real life sniff panels which, although somewhat outdated, is still necessary to understand consumer perception of fragrances and the success of antiperspirant / deodorant products created in an industrial setting. This is because GC or GC-MS can only identify / quantify the compounds involved in a sample, they cannot determine the significance of a compound to the overall smell.



**Figure 1-9:** A GC-Olfactometer.

As evidence for this necessity, in 1996, Behan *et al.* reported how the skin changes perfume.<sup>114</sup> They found that there is some evidence for changes in perfume ingredients in the underarm and suggested this was probably due to microbially catalysed reactions. They did this *via* monitoring 'underarm headspace' followed by thermal desorption GC. They reported the hydrolysis of esters within microbially rich areas such as the axilla and that the product of this could be useful perfume ingredients in their own right. It is also stated that this did not occur in the rest of

their experiments carried out on the forearm. This could be of further interest as it means the fragrance may last longer than if the alcohol was applied directly. Interestingly, they also noted the appearance of a large number of peaks 'extraneous to the experiment' which could be accounted for by sampling untreated axillae. I suggest this is likely to be components observed in other literature, including the volatile malodorous compounds of interest within this research.

HPLC of VFAs from human and animal samples of multiple biological materials was carried out by Stein *et al.* and Wagner and co-workers in the 1990s.<sup>75,115</sup> Just prior to this, Chen and Lifschitz reported achieving similar results by HPLC compared to the usually preferred GC when analysing VFAs.<sup>116</sup> HPLC is advantageous compared to GC if subsequent manipulation of the separated VFAs is desired. Furthermore, it is easier to collect the separated VFAs when they are still in liquid form compared to the gas form which would require condensation.<sup>115</sup> Stein *et al.* made an unusual solvent choice of sulphuric acid.<sup>75</sup> This resulted in a reportedly highly sensitive and reproducible detection method by UV without the need for esterification. Wagner and coworkers used a common solvent ratio of 15 to 85 % acetonitrile to water for short chain fatty acids.<sup>115</sup> This is investigated in Chapter 2.

The analysis of antiperspirant / deodorants should also be investigated. Previously, GC-MS was carried out by Rastogi,<sup>117,118</sup> however, they did not attempt the analysis of deodorant components and VFAs simultaneously which could be a challenge if elution times are too similar.

#### 1.3.1.1 Qualitative, visual analysis

A further possible application would be to include indicators for elements of sweat in the device for a more instantaneous output (visual, *e.g.* colour change), for example a pH indicator as sweat is generally acidic in nature due to the presence of volatile fatty acids. On a slightly more simplistic level, colorimetric data is a powerful tool for gathering data from people's skin.

Lambers *et al.* suggested that the natural skin pH is an average of below 5, especially without the use of soap and other cosmetics or even tap water (typical pH *ca.* 8).<sup>119</sup> It has also been documented that the acidic skin surface (often referred to as the

acidic mantle) helps the bacteria attach to the skin surface. However, their study was carried out on the volar forearm but they also suggested that the pH of occluded areas, such as the axilla, is likely to be slightly higher. These areas are often referred to as ‘holes’ in the acid mantle.

Koh *et al.* used a multitude of colour-change indicators within one microfluidic device to simultaneously determine many features of sweat.<sup>120</sup> This colourimetric sensing allowed assessment of rate and volume of sweating, pH and concentrations of chloride, lactate and glucose. They used anhydrous cobalt (III) chloride to chelate with the water in sweat to form the hexahydrate complex; a colour change from blue to purple. In sweat, pH is often considered an index of hydration state. Meanwhile, universal pH indicators including dyes such as bromothymol blue, methyl red and phenolphthalein were suggested as they all cover a ‘medically relevant’ pH range.

**Table 1-3:** List of indicators recommended by Koh *et al.* with information collated from Bates.<sup>120,121</sup>

Indicator	pH transition	Visible transition
Bromothymol blue	6.0-7.6	Yellow-blue
Bromophenol blue	3.0-4.6	Yellow-blue
Methyl red	4.4-6.0	Red-yellow
phenolphthalein	8.0-10.0	Colourless-red

This was illustrated in 1961 by Tashiro *et al.* who used bromophenol blue to visualise finger prints after Manuila had used it to investigate sweating in the human axilla some 10 years earlier,<sup>122,123</sup> furthermore, in 2013, Liu *et al.* used quinine as a pH-responsive chemfluorescence indicator for the detection of human body sweat odour,<sup>124</sup> however, this was not used directly as a biosensor. Instead, the samples were collected then sprayed onto the quinine-containing gels and the fluorescent results captured using a specialised camera. This is no more user friendly than traditional sampling.

Also in 2013, Oncescu *et al.* published a paper that included a smartphone-based app. for the colorimetric detection of biomarkers in sweat.<sup>82</sup> However, this involved a purpose-built case for the smartphone for test strips to be inserted into an optical

reading system after being placed on, for example, the forehead to collect a sweat sample. This was designed for monitoring the pH in relation to sodium ion concentration as a guide to hydration levels of the test subject with a view to monitoring during exercise. It is a step in the right direction for point-of-care monitoring using a non-invasive sample collection method but improvements need to be made so that less specialist phone modifications are required. These smartphone-based technologies can be quite complex in nature, using lab-on-a-chip technology such as microfluidics and transmitting data to a smart phone.

Previous work in the Haddleton group has used the substitution reaction of thiols onto dibromomaleimide for stabilisation;<sup>125–127</sup> this reaction invokes a yellow product, from colourless starting solutions, which also fluoresces, allowing for the reaction to be monitored, and potentially be quantitatively analysed by UV / fluorescence spectroscopy.<sup>128</sup>

In 2016, Park *et al.* illustrated the use of polydiacetylenes for sweat-pore mapping of fingerprints.<sup>129</sup> This was an advancement as it is a photo-curable polymer that can be inkjet-printed onto a substrate to make a patch for sampling; a high throughput technique. This gives immediate data through a hydrochromic colour change (blue to red) and was illustrated with the ability to visualise a fingerprint. This can then be analysed further by Raman spectroscopy or a more simple photograph followed by RGB analysis.

### **Recent Advances**

Most recent advances in the field of sweat analysis have been in the development of wearable biosensors.

In 2015, Jadoon *et al.* published a review article on the recent developments in sweat analysis and its applications.<sup>18</sup> This was mainly in comparison of the ease of using sweat as a biofluid, compared to blood samples, for detection of drugs (and their metabolites), ethanol, metals, ions and salts or volatile organic compounds. This application is of most interest to this work but was unfortunately a relatively small part of this review in comparison to drug detection and disease diagnosis. Furthermore, the sweat detection techniques discussed were devices found in

literature previously such as filter paper, occlusive devices and a water-tight sweat collection bag which illustrates the lack of recent progress in this area and therefore the need for this research. They also only discussed traditional analytical techniques, such as chromatography, after solvent-based extraction techniques, where necessary.

In 2014, Dutkiewicz *et al.* published the most relevant article to this project.<sup>130</sup> They used agarose gel probes to collect sweat from the forearm then carried out direct desorption-ionisation into a mass spectrometer (without any separative chromatography). Interestingly, they suggest that the skin-excreted metabolites diffuse into the already trapped water within the hydrogel evidenced by no observed increase in the mass of the probe after sampling and that dry agarose patches are less efficient at trapping metabolites. Furthermore, they were not looking for the malodorous compounds but at the potential use in healthcare and drug testing applications. They also indicated that the probes could be refrigerated for ~20 hours prior to analysis and results would still be valid. However, one of the goals of this project is to avoid refrigeration. Finally, they did not use a model solution to determine the efficiency of recovery from their patch, as they noted there is no suitable *in vitro* model to simulate excretion of metabolites with sweat, but did estimate recovery between 30-68 % depending on compound and concentration.

In 2016, Peng *et al.* published a paper on a new oil/membrane approach for integrated sweat sampling.<sup>131</sup> They claim that the use of the oil layer against the skin reduces analyte concentration (something that had also been reported previously<sup>132</sup>), and also that they could reduce the sample volumes required from  $\mu\text{l}$  to  $\text{nL}$ . This is the most important advancement reported in this paper as sweat is not usually produced in large amounts unless forced conditions are used<sup>90</sup> so for the 'real life' application of my project, this would be extremely beneficial. This oil/membrane approach had previously been used in a more simplistic manner in 1961 by Tashiro *et al.* who used bromophenol blue (a standard colorimetric pH indicator) to visualise finger prints.<sup>122</sup>



In conclusion, there has been very little advancement in the field of simplistic sampling and analysis of sweat especially from an antiperspirant deodorant perspective. However, there is an increase in wearable technology that can provide much data from the content of sweat for medical advances.

During a patent search for prior art to such a device, prior art was found pertaining to both sweat capture devices and hydrogels but our invention is combining the two.

The following chapters of this thesis aim to address the challenges discussed above. Chapter 2 illustrates gas chromatography method development, utilising a model sweat as well as investigating esterification and liquid chromatography. Chapter 3 examines all aspects of the synthesis of p(NaAMPS) and p(HEMA) hydrogels then compares them to more complex double network hydrogels. Chapter 4 then takes these p(NaAMPS) hydrogels and explores their use as a sweat collection device; investigating model sweat absorption, storage and extraction. Finally, Chapter 5 explores the use of the device *in vivo* alongside the inclusion of additives such as fragrances and indicators for qualitative pre-screening.

## 1.4 References

- 1 M. Wilson, *Microbial Inhabitants of Humans: Their Ecology and Role in Health and Disease*, Cambridge.
- 2 Statista, Size of the global antiperspirant and deodorant market from 2012 to 2024 (in billion U.S. dollars), <https://www.statista.com/statistics/254668/size-of-the-global-antiperspirant-and-deodorant-market/>, (accessed October 2018).
- 3 Statista, Unilever's antiperspirants and deodorants market share worldwide from 2012 to 2024, <https://www.statista.com/statistics/254615/unilevers-antiperspirants-and-deodorants-market-share-worldwide/>, (accessed October 2018).
- 4 A. G. James, J. Casey, D. Hyliands and G. Mycock, *World J. Microbiol. Biotechnol.*, 2004, **20**, 787–793.
- 5 A. G. James, C. J. Austin, D. S. Cox, D. Taylor and R. Calvert, *FEMS Microbiol. Ecol.*, 2013, **83**, 527–540.
- 6 A. Natsch, J. Schmid and F. Flachsmann, *Chem. Biodivers.*, 2004, **1**, 1058–1072.
- 7 B. D. L. Costello, A. Amann, H. Al-Kateb, C. Flynn, W. Filipiak, T. Khalid, D. Osborne and N. M. Ratcliffe, *J. Breath Res.*, 2014, **8**, 014001.
- 8 L. Dormont, J. M. Bessièrè and A. Cohuet, *J. Chem. Ecol.*, 2013, **39**, 569–578.
- 9 N. W. Hanson, Ed., *Official, Standardised and Recommended Methods of Analysis*, Second., 1973.
- 10 P. A. Prada, A. M. Curran and K. G. Furton, *J. Forensic Sci.*, 2011, **56**, 866–881.
- 11 S. K. Obendorf, H. Liu, M. J. Leonard, T. J. Young and M. J. Incorvia, *J. Appl. Polym. Sci.*, 2006, **99**, 1720–1723.
- 12 R. H. McQueen, R. M. Laing, C. M. Delahunty, H. J. L. Brooks and B. E. Niven, *J. Text. Inst.*, 2008, **99**, 515–523.
- 13 D. T. Hudson, A. M. Curran and K. G. Furton, *J. Forensic Sci.*, 2009, **54**, 1270–1277.
- 14 P. A. Prada, A. M. Curran and K. G. Furton, *J. Forensic Sci. Criminol.*, 2014, **1**, 1–10.
- 15 D. Van Bavel, C. Ward and A. Wibaux, Eur. Pat., EP2155273B1, 2013.
- 16 S. K. Villain, US Pat., US20060041987, 2006.
- 17 S. Savelev, H. Wang, T. Clare and M. Gosling, Int. Pat., WO2006/111748, 2006.
- 18 S. Jadoon, S. Karim, M. R. Akram, A. K. Khan, M. A. Zia, A. R. Siddiqi and G. Murtaza, *Int. J. Anal. Chem.*, 2015, **2015**, 1–7.
- 19 B. J. Van Enter and E. Von Hauff, *Chem. Commun.*, 2018, **54**, 5032–5045.
- 20 PharmChem Inc., PharmChek® Sweat Patch, <https://pharmchek.com/products/pharmchek-patch>, (accessed January 2019).
- 21 P. Kintz, A. Henrich, V. Cirimele and B. Ludes, *J. Chromatogr. B*, 1998, **705**, 357–361.
- 22 D. W. Schoendorfer, US Pat., US5441048, 1995.
- 23 M. J. Zohuriaan-Mehr and K. Kabiri, *Iran. Polym. J.*, 2008, **17**, 451–477.
- 24 B. R. Eggins, *Analyst*, 1993, **118**, 439–442.
- 25 O. Wichterle and D. Lim, *Nature*, 1960, **185**, 117–118.
- 26 J. J. Nichols, *Contact Lens Spectr.*, 2013, **28**, 24–29.

- 27 K. Nalampang, N. Suebsanit, C. Witthayaprapakorn and R. Molloy, *Chiang Mai J. Sci*, 2007, **34**, 183–189.
- 28 J. J. Perrault, US Pat., US5800685A, 1998.
- 29 R. Pó, *J. Macromol. Sci. Part C Polym. Rev.*, 1994, **34**, 607–662.
- 30 N. Chirani, L. Yahia, L. Gritsch, F. L. Motta, S. Chirani and S. Fare, *J. Biomed. Sci.*, 2015, **4**, 1–23.
- 31 NCBI, Hydrogels, <https://www.ncbi.nlm.nih.gov/pubmed/?term=hydrogels>, (accessed January 2019).
- 32 V. Jones, J. E. Grey and K. G. Harding, *Br. Med. J.*, 2006, **332**, 777–780.
- 33 A. Gupta, M. Kowalczyk, W. Heaselgrave, S. T. Britland, C. Martin and I. Radecka, *Eur. Polym. J.*, 2019, **111**, 134–151.
- 34 S. Durmaz and O. Okay, *Polymer (Guildf)*, 2000, **41**, 3693–3704.
- 35 K. Kabiri, H. Mirzadeh and M. J. Zohuriaan-Mehr, *J. Appl. Polym. Sci.*, 2008, **110**, 3420–3430.
- 36 K. Kabiri, A. Azizi, M. J. Zohuriaan-Mehr, G. B. Marandi, H. Bouhendi and A. Jamshidi, *Iran. Polym. J.*, 2011, **20**, 175–183.
- 37 K. Kabiri, S. Faraji-Dana and M. J. Zohuriaan-Mehr, *Polym. Adv. Technol.*, 2005, **16**, 659–666.
- 38 M. M. Ozmen and O. Okay, *Polymer*, 2005, **46**, 8119–8127.
- 39 N. Sahiner, *Colloid Polym. Sci.*, 2006, **285**, 283–292.
- 40 O. Wichterle and D. Lim, US Pat., US2,976,576, 1961.
- 41 M. F. Refojo, *J. Biomed. Mater. Res. Part A*, 1969, **3**, 333–347.
- 42 M. A. Taleb, D. E. Hegazy and G. A. Mahmoud, *Int. J. Polym. Mater. Polym. Biomater.*, 2014, **63**, 840–845.
- 43 P. L. Ritger and N. A. Peppas, *J. Control. Release*, 1987, **5**, 23–36.
- 44 P. L. Ritger and N. A. Peppas, *J. Control. Release*, 1987, **5**, 37–42.
- 45 I. Yazici and O. Okay, *Polymer*, 2005, **46**, 2595–2602.
- 46 N. Efron and N. Brennan, *Optician*, 1987, **194**, 29–41.
- 47 T. Nakashima, N. Toyoshima and Y. Sasai, US Pat., US4745158, 1988.
- 48 P. B. Morgan and N. Efron, *Contact Lens Anterior Eye*, 1998, **21**, 3–6.
- 49 M. A. Muter, *Int. J. Res. Stud. Biosci.*, 2015, **3**, 152–160.
- 50 S. A. Stern, *J. Polym. Sci. Part B Polym. Phys.*, 1968, **6**, 1933–1934.
- 51 G. Heiting, What Are Contacts Made Of?, <https://www.allaboutvision.com/contacts/faq/contact-materials.htm>, (accessed March 2019).
- 52 Alensa, Oxygen permeability, [www.alensa.co.uk/dictionary/oxygen-permeability.html](http://www.alensa.co.uk/dictionary/oxygen-permeability.html), (accessed March 2019).
- 53 M. Ebara, Y. Kotsuchibashi, R. Narain, N. Idota, Y.-J. Kim, J. M. Hoffman, K. Uto and T. Aoyagi, in *Smart Biomaterials*, Springer, 2014, pp. 9–65.
- 54 Y. Bao, J. Ma and N. Li, *Carbohydr. Polym.*, 2011, **84**, 76–82.
- 55 E. Caló and V. V. Khutoryanskiy, *Eur. Polym. J.*, 2015, **65**, 252–267.
- 56 E. M. Ahmed, *J. Adv. Res.*, 2015, **6**, 105–121.
- 57 J. P. Fouassier and J. Lalevée, *Polymers*, 2014, **6**, 2588–2610.
- 58 J. Lalevée and J. P. Fouassier, *Photopolymerisation Initiating Systems*, 2018.
- 59 H. S. Munro and N. Boote, US Pat., US 2013/0121952 A1, 2013.
- 60 C. Zhang and A. J. Easteal, *J. Appl. Polym. Sci.*, 2007, **104**, 1723–1731.
- 61 O. Hazer, C. Soykan and S. Kartal, *J. Macromol. Sci. Part A*, 2008, **45**, 45–51.

- 62 E. K. Yetimoğlu, M. V. Kahraman, Ö. Ercan, Z. S. Akdemir and N. K. Apohan, *React. Funct. Polym.*, 2007, **67**, 451–460.
- 63 M. T. Am Ende and N. A. Peppas, *J. Control. Release*, 1997, **48**, 47–56.
- 64 M. T. A. M. Ende and N. A. Peppas, 2002, **59**, 1–13.
- 65 E. Elgueta, B. L. Rivas, A. Mancisidor, D. Núñez and M. Dahrouch, *Polym. Bull.*, 2019.
- 66 J. P. Gong, *Soft Matter*, 2010, **6**, 2583–2590.
- 67 J. P. Gong, *Science*, 2014, **344**, 161–163.
- 68 Q. Chen, H. Chen, L. Zhu and J. Zheng, *J. Mater. Chem. B*, 2015, **3**, 3654–3676.
- 69 D. Klempler and L. Berkowski, in *Encyclopedia of Polymer Science and Technology*, ed. H. F. Mark, Wiley-Interscience, 3rd edn., 2007, pp. 279–341.
- 70 J. P. Gong, Y. Katsuyama, T. Kurokawa and Y. Osada, *Adv. Mater.*, 2003, **15**, 1155–1158.
- 71 L. H. Sperling, in *Interpenetrating Polymer Networks*, ed. D. Klempler, L. H. Sperling and L. A. Utracki, ACS, 1994, ch. 1, pp. 3–38.
- 72 Q. Chen, L. Zhu, L. Huang, H. Chen, K. Xu, Y. Tan, P. Wang and J. Zheng, *Macromolecules*, 2014, **47**, 2140–2148.
- 73 B. McArthur and A. P. Sarnaik, *Clin. Chem.*, 1983, **28**, 1983–1984.
- 74 S. K. Pandey and K. H. Kim, *TrAC - Trends Anal. Chem.*, 2011, **30**, 784–796.
- 75 J. Stein, J. Kulemeier, B. Lembcke and W. F. Caspary, *J. Chromatogr. B Biomed. Sci. Appl.*, 1992, **576**, 53–61.
- 76 V. A. Vavilin and L. Y. Lokshina, *Bioresour. Technol.*, 1996, **57**, 69–80.
- 77 Q. Wang, M. Kuninobu, H. I. Ogawa and Y. Kato, *Biomass and Bioenergy*, 1999, **16**, 407–416.
- 78 V. A. Vavilin, S. V. Rytov and L. Y. Lokshina, *Bioresour. Technol.*, 1996, **56**, 229–237.
- 79 T. Wu, X. Wang, D. Li, G. Sheng and J. Fu, *Int. J. Environ. Anal. Chem.*, 2008, **88**, 1107–1115.
- 80 N. Innocente, S. Moret, C. Corradini and L. S. Conte, *J. Agric. Food Chem.*, 2000, **48**, 3321–3323.
- 81 O. Pinho, I. M. P. L. V. O. Ferreira and M. A. Ferreira, *Anal. Chem.*, 2002, **74**, 5199–5204.
- 82 V. Oncescu, D. O'Dell and D. Erickson, *Lab Chip*, 2013, **13**, 3232–3238.
- 83 P. Prada, A. Curran and K. Furton, *Anal. Methods*, 2010, **2**, 470–478.
- 84 G. K. Anderson and G. Yang, *Water Environ. Res.*, 1992, **64**, 53–59.
- 85 R. Fernández, R. M. Dinsdale, A. J. Guwy and G. C. Premier, *Crit. Rev. Environ. Sci. Technol.*, 2016, **46**, 209–234.
- 86 R. DiLallo and O. E. Albertson, *J. (Water Pollut. Control Fed.)*, 1961, **33**, 356–365.
- 87 E. von Hartungen, A. Wisthaler, T. Mikoviny, D. Jaksch, E. Boscaini, P. J. Dunphy and D. M. Tilmann, *Int. J. Mass Spectrom.*, 2004, **239**, 243–248.
- 88 C. W. Gehrke and W. M. Lamkin, *Agric. Food Chem.*, 1961, **9**, 85–88.
- 89 S. E. Fleming, H. Traitler and B. Koellreuter, *Lipids*, 1987, **22**, 195–200.
- 90 T. L. Perry, S. Hansen, S. Diamond, B. Bullis, C. Mok and S. B. Melancon, *Clin. Chim. Acta*, 1970, **29**, 369–374.
- 91 L. E. Gibson and R. E. Cooke, *Pediatrics*, 1959, **23**, 545–549.
- 92 K. J. Hauser and R. J. Zabransky, *J. Clin. Microbiol.*, 1975, **2**, 1–7.

- 93 D. R. Knapp, *Handbook of Analytical Derivatization Reactions*, Wiley, 1979.
- 94 W. H. Brown and J. March, Carboxylic acid, <https://www.britannica.com/science/carboxylic-acid>, (accessed January 2018).
- 95 R. J. Ouellette and J. D. Rawn, in *Organic Chemistry: Structure, Mechanism, and Synthesis*, First., 2014, pp. 699–746.
- 96 I. Brondz, *Anal. Chim. Acta*, 2002, **465**, 1–37.
- 97 J. Kennedy, table-of-esters-and-their-smells, <https://jameskennedymonash.wordpress.com/2013/12/13/infographic-table-of-esters-and-their-smells/>, (accessed January 2018).
- 98 W. Onkenhout, P. F. van der Poel and M. P. van der Heuvel, *J. Chromatogr.*, 1989, **494**, 133.
- 99 U. Hintze, H. Röper and G. Gercken, *J. Chromatogr. A*, 1973, **87**, 481–489.
- 100 A. Kuksis, J. J. Myher, L. Marai and K. Geher, *Anal. Biochem.*, 1976, **70**, 302–312.
- 101 W. Welz, W. Sattler, H. J. Leis and E. Malle, *J. Chromatogr.*, 1990, **536**, 319.
- 102 U. Caruso, B. Fowler, M. Erceg and C. Romano, *J. Chromatogr.*, 1991, **562**, 147.
- 103 Y. J. Yang, M. H. Choi, M. J. Paik, H. R. Yoon and B. C. Chung, *J. Chromatogr. B. Biomed. Sci. Appl.*, 2000, **742**, 37–46.
- 104 A. M. Curran, S. I. Rabin, P. A. Prada and K. G. Furton, *J. Chem. Ecol.*, 2005, **31**, 1607–1619.
- 105 A. Natsch, S. Derrer, F. Flachsmann and J. Schmid, *Chem. Biodivers.*, 2006, **3**, 1–20.
- 106 Agilent and Markes, THERMAL DESORPTION Introduction and Principles, <http://www.chem.agilent.com/cag/country/principles.pdf>, (accessed July 2016).
- 107 R. Marriott, in *Natural Food Additives, Ingredients and Flavourings*, eds. D. Baines and R. Seal, Woodhead Publishing Limited, 2012, pp. 260–278.
- 108 Suprex, Extraction & Fractionation, <http://www.suprex.uk/extraction-and-fractionation>, (accessed February 2017).
- 109 S. Cardea, L. Baldino, I. De Marco, P. Pisanti and E. Reverchon, *Chem. Eng. Trans.*, 2013, **32**, 1123–1128.
- 110 F. Kanda, E. Yagi, M. Fukuda, K. Nakajima, T. Ohta and O. Nakata, *Br. J. Dermatol.*, 1990, **122**, 771–776.
- 111 A. Dravnieks, *J. Soc. Cosmet. Chem.*, 1975, **26**, 551–571.
- 112 R. Harper, D. G. Land and N. M. Griffiths, *Br. J. Psychol.*, 1968, **59**, 231–252.
- 113 E. Kováts, *Helv. Chim. Acta*, 1958, **41**, 1915–1932.
- 114 J. M. Behan, A. P. Macmaster, K. D. Perring and K. M. Tuck, *Int. J. Cosmet. Sci.*, 1996, **18**, 237–246.
- 115 A. B. Kroumova and G. J. Wagner, *Anal. Biochem.*, 1995, **225**, 270–276.
- 116 H. Chen and C. Lifschitz, *Clin. Chem.*, 1989, **35**, 74–76.
- 117 S. C. Rastogi, J. D. Johansen, P. Frosch, T. Menné, M. Bruze, J. P. Lepoittevin, B. Dreier, K. E. Andersen and I. R. White, *Contact Dermatitis*, 1998, **38**, 29–35.
- 118 S. C. Rastogi, *J. High Resol. Chromatogr.*, 1959, **18**, 653–658.
- 119 H. Lambers, S. Piessens, A. Bloem, H. Pronk and P. Finkel, *Int. J. Cosmet. Sci.*, 2006, **28**, 359–370.
- 120 A. Koh, D. Kang, Y. Xue, S. Lee, R. M. Pielak, J. Kim, T. Hwang, S. Min, A. Banks,

- P. Bastien, M. C. Manco, L. Wang, K. R. Ammann, K.-I. Jang, P. Won, S. Han, R. Ghaffari, U. Paik, M. J. Slepian, G. Balooch, Y. Huang and J. A. Rogers, *Sci. Transl. Med.*, 2016, **8**, 366–165.
- 121 R. G. Bates, *determination of pH Theory and Practice*, Wiley-Interscience, Second., 1973.
- 122 G. Tashiro, M. Wada and M. Sakurai, *J. Invest. Dermatol.*, 1961, **36**, 3–4.
- 123 L. Manuila, *Dermatology*, 1950, **100**, 304–309.
- 124 C. Liu, Y. Furusawa and K. Hayashi, *Sensors Actuators, B Chem.*, 2013, **183**, 117–123.
- 125 J. Collins, J. Tanaka, P. Wilson, K. Kempe, T. P. Davis, M. P. McIntosh, M. R. Whittaker and D. M. Haddleton, *Bioconjug. Chem.*, 2015, **26**, 633–638.
- 126 M. W. Jones, R. A. Strickland, F. F. Schumacher, S. Caddick, J. R. Baker, M. I. Gibson and D. M. Haddleton, *J. Am. Chem. Soc.*, 2012, **134**, 1847–1852.
- 127 M. P. Robin, P. Wilson, A. B. Mabire, J. K. Kiviaho, J. E. Raymond, D. M. Haddleton and R. K. O’reilly, *J. Am. Chem. Soc.*, 2013, **135**.
- 128 M. P. Robin and R. K. O’Reilly, *Chem. Sci.*, 2014, **5**, 2717–2723.
- 129 D. H. Park, W. Jeong, M. Seo, B. J. Park and J. M. Kim, *Adv. Funct. Mater.*, 2016, **26**, 498–506.
- 130 E. P. Dutkiewicz, J. Lin, T. Tseng, Y. Wang and P. L. Urban, *Anal. Chem.*, 2014, **86**, 2337–2344.
- 131 R. Peng, Z. Sonner, A. Hauke, E. Wilder, J. Kasting, T. Gaillard, D. Swaille, F. Sherman, X. Mao, J. Hagen, R. Murdock and J. Heikenfeld, *Lab Chip*, 2016, **16**, 4415–4423.
- 132 T. C. Boysen, S. Yanagawa, F. Sato and K. Sato, *J. Appl. Physiol.*, 1984, **56**, 1302 LP-1307.

## 2. Chromatography

Currently, there is no industrial standard method for the identification and quantification of malodorous compounds from the axilla as a measure of the efficacy of antiperspirant / deodorant products. Chromatography, especially gas chromatography, is a relatively low cost, widely available technique that could meet this requirement.

### 2.1 Gas Chromatography

Gas chromatography (GC) is a common and well-established analytical technique used to separate and analyse mixtures of compounds. Depending on the detector used, this can be useful for identifying unknown compounds and determining concentrations. It is an interactive chromatography; it involves separation *via* a combination of polarity and boiling points of the compounds, due to the use of a column with a stationary phase and a heating method.

Typically, upon injection of a liquid sample, it is vaporised before being carried down the column by the mobile phase, also known as the carrier gas. This is most commonly hydrogen, helium or nitrogen. In this work, the GC-FID uses hydrogen and the GC-MS uses helium. Separation then takes place in the column, followed by detection *via* the chosen detector, Table 2-1.

**Table 2-1:** Detectors and their associated detection limits.<sup>1</sup>

Detector	Approximate detection limit	Linear range
Thermal Conductivity	400 pg ml <sup>-1</sup> (propane)	>10 <sup>5</sup>
Flame Ionisation	2 pg s <sup>-1</sup>	>10 <sup>7</sup>
Electron Capture	5 fg s <sup>-1</sup>	10 <sup>4</sup>
Flame Photometric	<1 pg s <sup>-1</sup> (phosphorous) <1 pg s <sup>-1</sup> (sulfur)	>10 <sup>4</sup> >10 <sup>3</sup>
Nitrogen-phosphorous	100 fg s <sup>-1</sup>	10 <sup>5</sup>
Sulfur chemiluminescence	100 fg s <sup>-1</sup> (sulfur)	10 <sup>5</sup>
Photoionisation	25-50 pg (aromatics)	>10 <sup>5</sup>
Fourier Transform Infrared	200 pg – 40 ng	10 <sup>4</sup>
Mass Spectrometry	25 fg – 100 pg	10 <sup>5</sup>

The most common detectors are flame ionisation detector (FID) and mass spectrometry (MS). Although Table 2-1 reports general detection limits for these detectors, Fernandez *et al.* demonstrated the range of LOD reported in literature since the 1990s specifically for VFAs.<sup>2</sup> They indicate that for FID, this ranges from 10 mg l<sup>-1</sup> to less than 1x10<sup>-3</sup> mg l<sup>-1</sup> (both valeric acid). For mass spectrometry, this was reported as 1 mg l<sup>-1</sup> (acetic acid) to 1x10<sup>-6</sup> mg l<sup>-1</sup> (valeric acid), with the linear dynamic ranges of 3 to 4 orders of magnitude for both. These will depend on factors such as sample matrix and pre-treatment employed in each case.

In flame ionisation detectors, analytes are burned under the carrier gas, H<sub>2</sub>, and air. Hydrocarbons produce CH radicals while carbonyls and carboxyls produce CHO<sup>+</sup>. FID is insensitive to any other (non-C-H) group. For compound identification, flame ionisation detection relies on comparison of the retention time of known compounds. A second method traditionally employed is relating the retention time to those of straight chain alkanes known as Kovats' index.<sup>3</sup>

Gas chromatography-Mass spectrometry (GC-MS) can provide both quantitative and qualitative information. By comparison of the mass spectra to internal databases, compounds can be identified with more reliability than when using a GC-FID. Here the mass spectrometry detector is typically quadrupole (1, 2, or 3 in series) and the compounds are fragmented by electron ionisation (EI) or chemical ionisation (CI). This is ideal for the investigation of unknown compounds. A general m/z scan (*e.g.* 40-400 amu) can give a poor signal to noise ratio, which can be problematic for quantitation, however, if the compounds are known, selected ion monitoring (SIM) may be used. Dodds *et al.* compared the use of GC-FID with EI GC-MS for analysis of fatty acid methyl esters (FAMES)<sup>4</sup> and Wu *et al.* highlighted the use of SIM mode for analysis of volatile fatty acids (VFAs).<sup>5</sup>



**Table 2-2:** Details of SIM mode analysis of short chain VFAs from Wu *et al.* The target ions used for quantification are highlighted.<sup>5</sup>

VFAs	Retention time (minutes)	Retention Window (minutes)	Selected ions (m/z)
C <sub>2</sub>	8.96±0.01	8.00-10.00	43, 45, 60
C <sub>3</sub>	10.82±0.02	10.00-11.20	29, 45, 74
<i>i</i> -C <sub>4</sub>	11.42±0.01	11.20-12.00	41, 43, 73
<i>n</i> -C <sub>4</sub>	12.68±0.01	12.00-13.20	60, 73
<i>i</i> -C <sub>5</sub>	13.50±0.00	13.20-14.00	29, 57, 74
<i>n</i> -C <sub>5</sub>	14.85±0.03	14.00-15.20	60, 73
C <sub>5</sub> (d <sub>9</sub> - <i>n</i> C <sub>5</sub> )	14.63±0.02	14.00-15.20	45, 63

Note: each retention time value is the mean value ± standard deviation (n=5).

As illustrated in Figure 2-1, where there is a large amount of co-elution in the total ion count (TIC) chromatogram that quantification would be impossible, SIM mode allows for complete peak separation. This not only leads to better signal to noise but can also allow faster methods as peak overlap is no longer an issue. This is further highlighted in Figure 2-2, where the peaks in the 74 m/z chromatogram can be attributed to C<sub>3</sub> and *i*-C<sub>5</sub>.

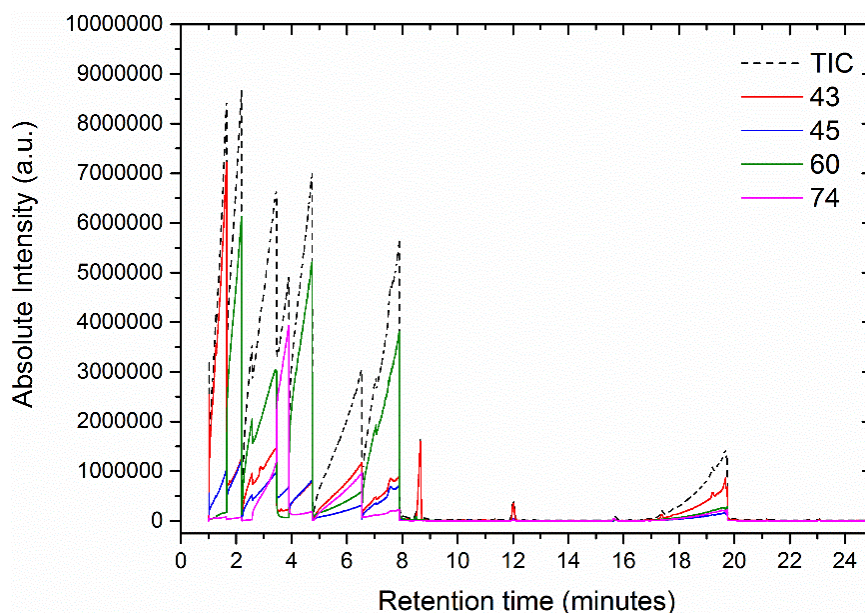


**Figure 2-1:** Overlaid SIM and TIC chromatograms.

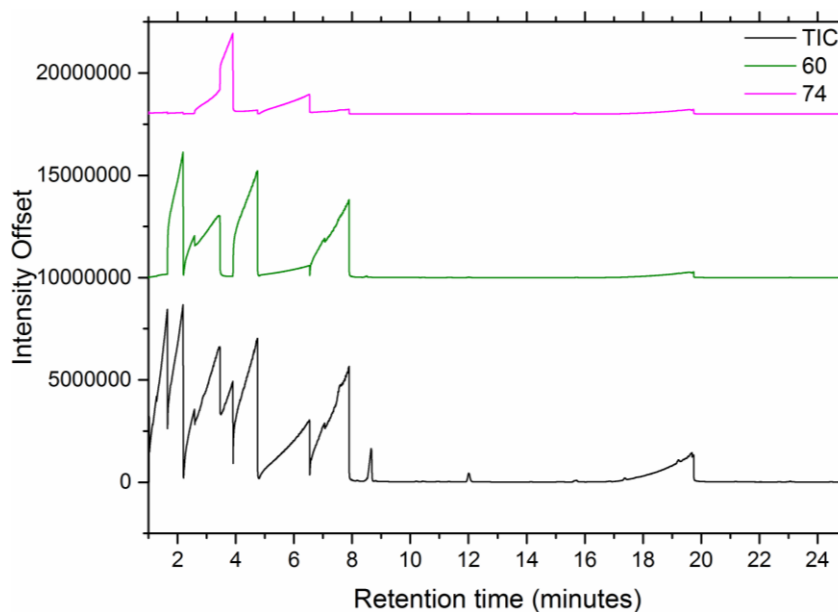


**Figure 2-2:** Highlighting the ability to differentiate between *i*-C<sub>5</sub> and *n*-C<sub>5</sub> by using SIM mode.

### 2.1.1 Column

There are two general types of columns that have been employed in gas chromatography since its inception; packed columns and capillary columns. Capillary columns can be further divided into wall coated open tubular (WCOT) columns and porous layer open tubular columns (PLOT), Figure 2-3, where the difference is whether the inner wall lining is a high boiling liquid (WCOT) or a porous layer of a solid absorbent (PLOT).<sup>6</sup>

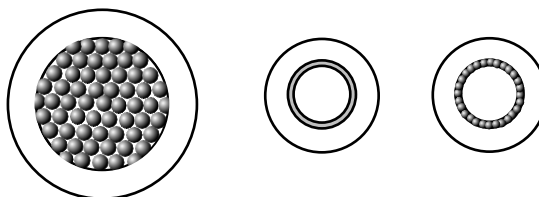


**Figure 2-3:** Illustration of the different types of column available for gas chromatography; packed (left), WCOT (middle) and PLOT (right).<sup>6</sup>

**Table 2-3:** Column information adapted from Practical Gas Chromatography A Comprehensive Reference.<sup>6</sup>

Column type	Packed Column	WCOT	PLOT
Stationary Phase	a) Porous support impregnated with a liquid b) Adsorbent particles	Thin film of a high boiling point liquid	Porous layer of a solid adsorbent
Retention Mechanism	a) Partition b) Adsorption	Partition (solubility)	Adsorption
Length	0.5 – 6 m	5- 100 m	5 – 30 m
Inner diameter	2 - 4 mm	0.1 -0.6 mm	0.2 – 0.6 mm
Particle size	100 – 300 $\mu\text{m}$	N/A	5 – 50 $\mu\text{m}$
Film thickness	N/A	0.1 – 10 $\mu\text{m}$	N/A
Column material	Copper, stainless steel, glass, quartz	Glass, fused silica (quartz) with polyimide coating, fused silica coated with stainless steel	

Today, WCOT columns are the most commonly used column type (>80 % of all applications). The first paper on GC analysis of acids using a capillary column was published by Lipsky in 1959.<sup>7</sup> This thesis uses only capillary columns made of fused silica.

As well as the material that forms the stationary phase, other factors to consider are the thickness of this stationary phase, the inner diameter of the column and the length of the column. Increasing the thickness of the stationary phase increases the retention time of compounds which increases the resolution of fast-eluting peaks. Resolution also increases proportionally to the square root of the column length. Finally, narrower column inner diameters also provide increased resolution. All these factors must be considered in combination.

**Table 2-4:** Functional Groups and potential interactions.<sup>8</sup>

Functional groups	Dispersion/induction	Dipole	H-bond
Methyl	Strong	None	None
Phenyl	Very Strong	None	Weak
Cyanopropyl	Strong	Very Strong	Medium
Trifluoropropyl	Strong	Medium	Weak
Polyethylene glycol	Strong	Strong	Moderate

Initially, GC was carried out using an Agilent DB-1ms non-polar column where the stationary phase is poly(dimethyl siloxane) (PDMS). This is regarded as a good general purpose column whereby separation relies more on the respective boiling points of the analytes than the chemistry due to very little interactions with the stationary phase.

As reported by Fleming *et al.* amongst others, a polar column was used for the analysis of volatile fatty acids.<sup>9</sup> In this work, a Restek Stabilwax column (stationary phase polyethylene glycol) was employed. It is suggested that with the non-polar column, separation is reliant on boiling point of the analytes whereas with this polar column, hydrogen bonding to the stationary phase will play a major role. The increase in column length is a major factor in the separation of the analytes, Figure 2-4. The polar PEG column elicits sharper, taller peaks compared to the non-polar column, making this more ideal for quantification.

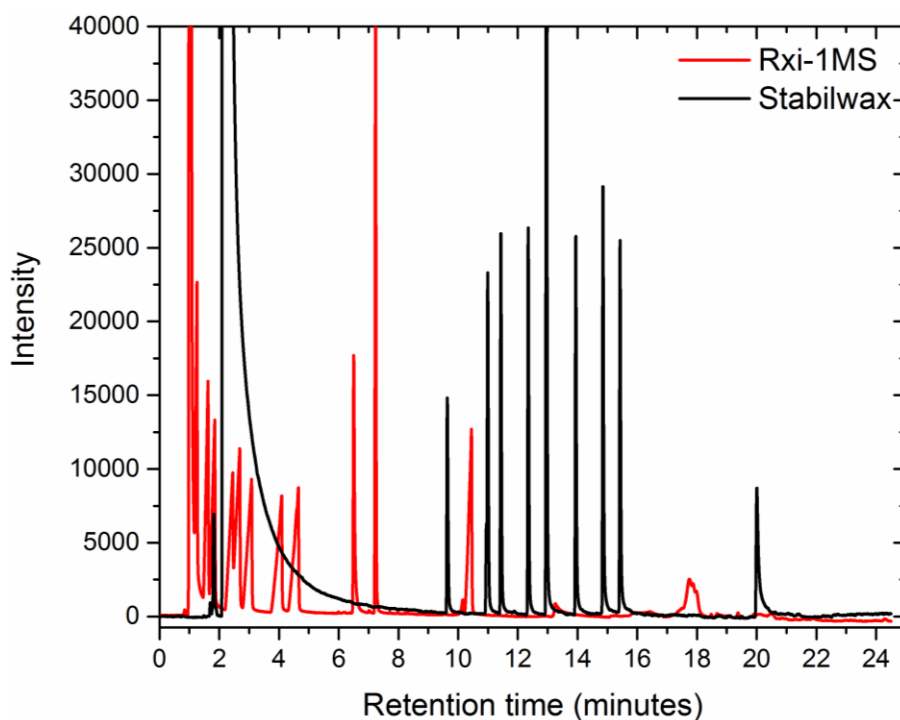


**Figure 2-4:** Comparison of the effect of column material and length on the separation of analytes by comparing chromatograms from a non-polar 15 m length column (Rxi1MS) and a polar 30 m length column (Stabilwax) both on the GC-FID using the Fleming oven heating method.

### 2.1.2 Heating Method

Gas chromatography can be run isothermally or using a temperature program. At a constant temperature, more volatile components will elute close together and less volatile components will have very long retention times or not elute at all if too low an isothermal program. With a temperature gradient, analytes will elute with an even distribution across the chromatogram, with the more volatile compounds eluting faster.

The heating method chosen, alongside the column type, is key to the separation of the compound mixture. The ideal method will be as fast as possible for efficient data acquisition but this can be hindered if there is a large number of compounds to be separated or if the compounds are of very similar nature. Therefore a compromise between these two factors must be made. For example, the original method used in this work was a very quick method ( $40\text{ }^{\circ}\text{C min}^{-1}$ , total run time  $\sim 8$  minutes) as the application was concentration determination of a single compound within a mix of 2 or 3 including solvent. In the case of this application, this was not suitable. As illustrated in the chromatogram, most of the compounds were co-eluting which is

not suitable for quantification, Figure 2-5. Therefore, a longer method (slower heating gradient) was necessary to try and split the 12 different compounds in the model sweat used throughout this research, Figure 2-6.<sup>9</sup>

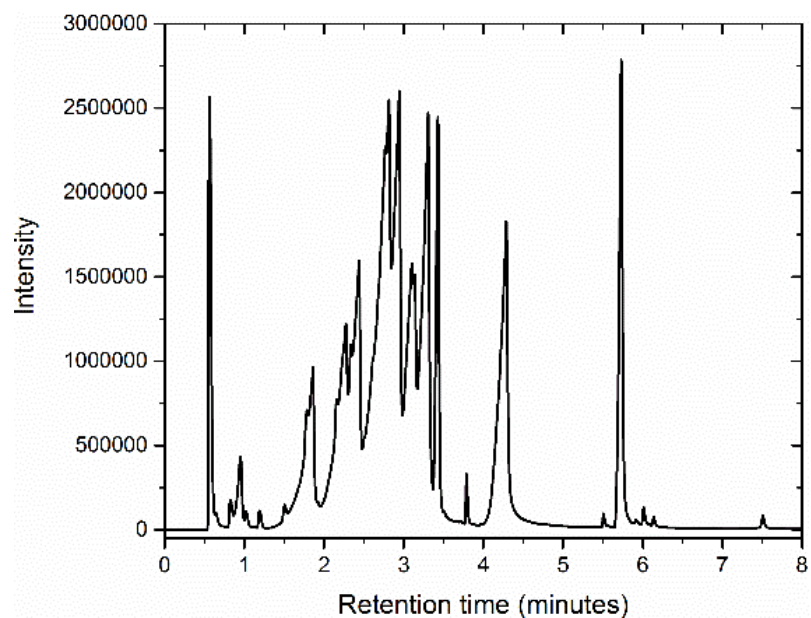


**Figure 2-5:** GC-FID chromatogram of the attempt to separate the 12 malodour compounds using the original, fast method.

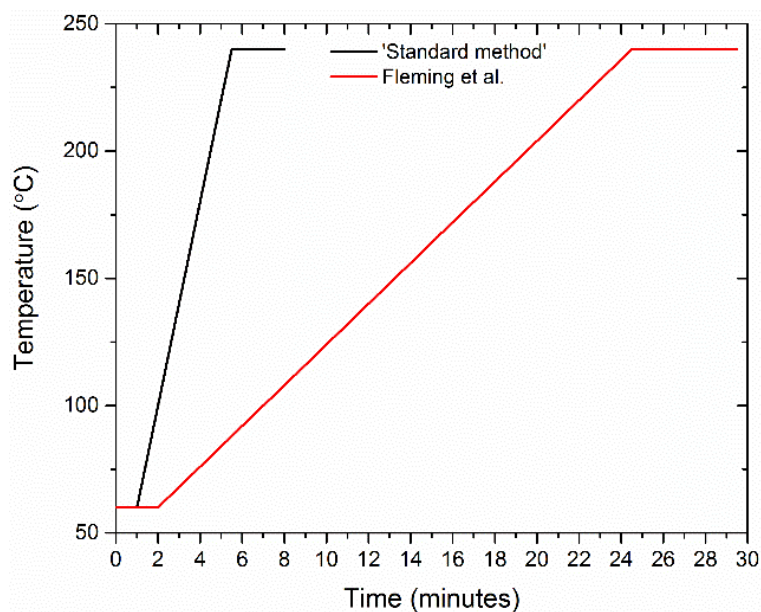


**Figure 2-6:** Comparison of the heating profiles employed in the different GC-FID methods.

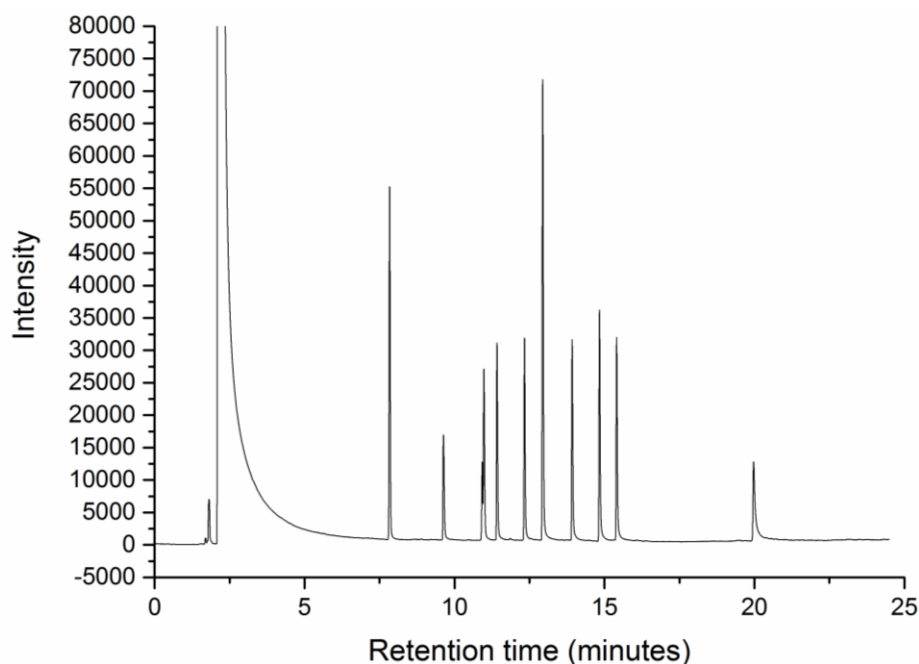


**Figure 2-7:** Chromatogram illustrating improved separation using the slower heating rate method.

Although this proved effective with the polar column on the GC-FID system, further method development was required for the GC-MS which had a shorter, non-polar column, Figure 2-8.

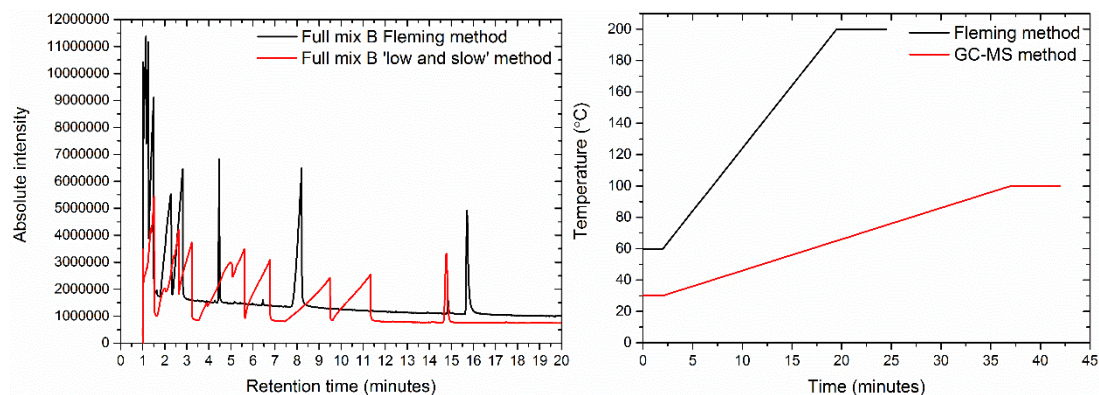


**Figure 2-8:** TIC chromatograms for the two different column oven heating methods tested, where the black line uses the same method as successfully used on the longer, polar column on the GC-FID (left). Corresponding heating profiles (matching colours) where the Fleming method (GC-FID standard) heats from 60 to 200 °C at 8 °C min<sup>-1</sup> whereas the new method is from 35 to 100 °C at 2 °C min<sup>-1</sup> (right). All other conditions remained the same.

### 2.1.3 Solvent

Solvents are used as a vehicle to transfer the analytes to the column. Ideally, a highly volatile, low boiling point solvent that all analytes are soluble in would be used. Special attention should be paid if the analytes are very highly volatile themselves as there can be overlap with the solvent peak (in the case of FID) or analyte peaks will not be seen by the detector, in the case of mass spectrometry, as they could appear before the detector is switched on, the time known as solvent cut time (the delay between sample injection and detector starting, usually 1-2 minutes, to protect the detector from saturation damage by the solvent).

Initially a co-solvent system reported by Fleming *et al.* was investigated whereby they found that using 1 N HCl in the presence of 80 % of an organic solvent provided the optimum results.<sup>9</sup> However, aqueous-containing solvent systems are not suitable for extraction from a hydrogel due to hydrogel absorption, therefore this would require further steps in recovery / analysis which is not ideal.

The solvent that could be used for the gas chromatography was limited based on the interaction with the hydrogels during the extraction procedure. This meant that aqueous-based solvent systems and similarly polar organic solvents were ruled out as they are absorbed by the hydrogel (where water has a normalised relative polarity of 1.000<sup>10</sup>). Therefore, relatively non-polar solvents, which still had relatively low boiling points, were chosen. Based on this, acetonitrile (0.460, b.p. 81.6 °C) and ethyl acetate (0.228, 77 °C) were deemed good candidates.

A further factor involved in solvent choice was the potential for side reactions during the gas chromatography analysis. For example, Brondz reported if methanol was used during the analysis of the volatile fatty acids it could result in the formation of FAMES,<sup>11</sup> then the heating cycle could initiate methyl esterification of the analytes, complicating the analysis (2.2.1 Fatty Acid Methyl Esters (FAMES)). Based on this information, the solvent was changed from methanol to acetonitrile. As illustrated by Figure 2-9, this change in solvent did not affect the chromatography.



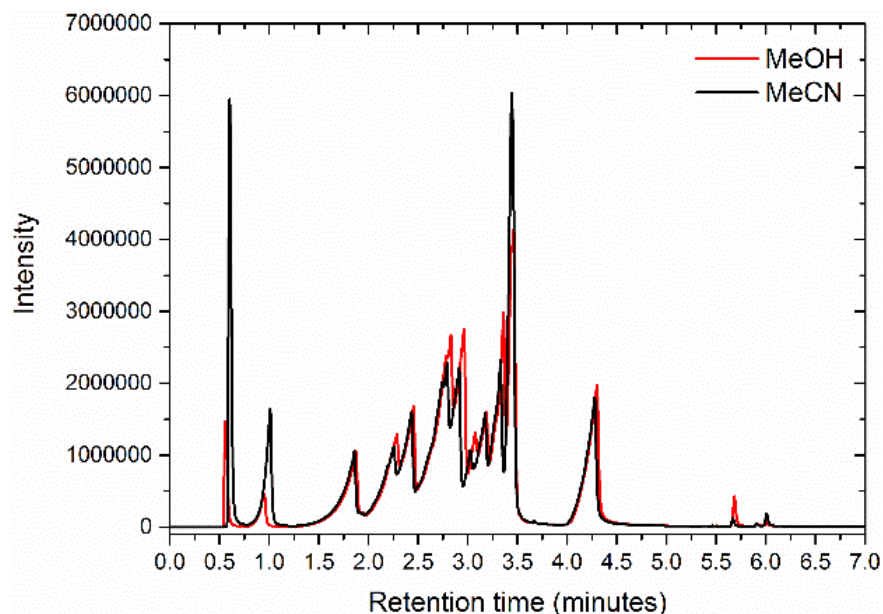


**Figure 2-9:** Overlaid chromatograms illustrating that changing the eluent did not affect the chromatography.

## 2.1.4 Quantification including Calibration

Quantification can be achieved using either the peak height or the peak area, however, peak area is used in this thesis as it avoids many of the potential problems associated with the use of peak height. These include changing temperatures, change in gas flow, peak tailing and overloading of the column or detector. Common methods of quantification are discussed in the following subsections.

### 2.1.4.1 Response Factor

Equivalent concentrations of different analytes yield different peak areas hence the need for individual calibrations for each analyte. Calculating the response factor (RF) is the most simple of these:

$$RF = \frac{w}{A} \quad (2-1)$$

where  $w$  is amount of analyte and  $A$  is the associated peak area. The peak area of a sample of unknown concentration can then be simply multiplied by this RF value to calculate the concentration.

#### 2.1.4.2 *Area Percent*

This is a relative quantification method that allows the comparison of different analytes within a mixture by comparing the peak area of an individual analyte with the total of the peak areas of all analytes. It has a severe limitation in that it only works effectively if the mixture comprises of only chemically similar compounds. This method can be used to check purity but is not recommended for use in trace analyses.

#### 2.1.4.3 *Calibrations*

##### **External standard**

An external standard calibration relies on a calibration curve of peak area vs known concentration for a series of concentrations, over the range to be analysed, being created.

##### **Internal standard**

An internal standard calibration relies on the addition of another compound (of known concentration) to the mixture to be analysed prior to analysis. Ideally, this would be a compound that is similar to the compounds of interest but that does not co-elute with anything already present in the mixture. Deuterated forms of the analytes are often chosen<sup>12</sup> but may still co-elute, this would be better for use on a GC-MS. If this is added pre-extraction (where such procedures are carried out), then it can elucidate information on the efficiency of the extraction procedure if that is not otherwise known. In the case of this work, this was not necessary due to most work being carried out by dosing with a mixture of known concentration for research purposes.

Bromobenzene (PhBr) is widely used as an internal standard in gas chromatography analysis of volatile organic compounds from wastewater and other environmental monitoring.<sup>13</sup> As this work did not rely on the internal calibration alone for concentration calibrations, it was less important that the chosen standard was of similar chemical and physical properties to the analyte. Instead it was chosen as there was good separation between PhBr, the solvent peak and the analyte peaks and

therefore useful for monitoring consistent detector response of the instrument over time.

This work takes advantage of both an internal and an external calibration simultaneously.

### **Standard Addition method**

An alternative is the standard addition method. A mixture is analysed before and after being spiked with a known concentration of one of the analytes that is already present in the sample, where the difference in peak area gives a reference.

#### *2.1.4.4 Internal Standard Ratios*

Calibration curves were created for use in determining unknown concentrations of VFAs within samples by linear regression. Calibration curves were only produced for five of the VFAs as the others overlapped in the chromatogram and therefore the individual peak area could not be determined, Figure 2-10. The peaks that are used are highlighted by the orange boxes on the overlaid chromatograms in Figure 2-11. The axes in Figure 2-10 are labelled as ratios. The y-axis is the ratio of the peak area of the VFA of interest divided by the peak area of the PhBr internal standard. Similarly, the x-axis is the ratio of the concentration of the VFA divided by the concentration of the PhBr which is kept constant between samples at  $0.04 \text{ mol dm}^{-3}$ . This is implemented following the analysis of Fleming *et al.*<sup>9</sup> and is useful to account for any fluctuation in performance of the GC instrument over time.

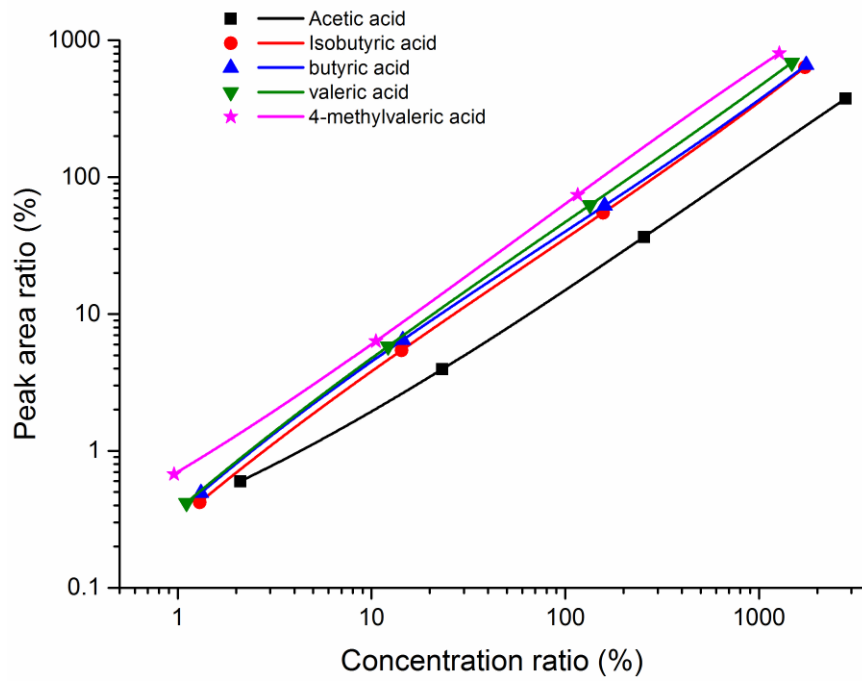


Figure 2-10: Calibration curves of the 5 separated VFAs.

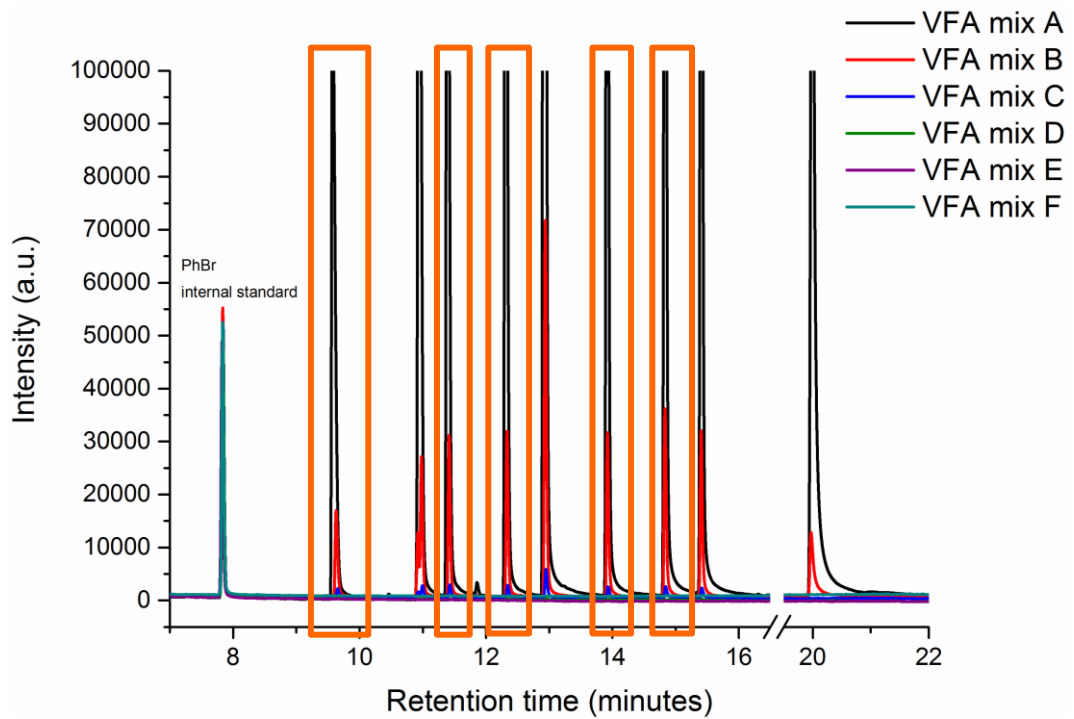
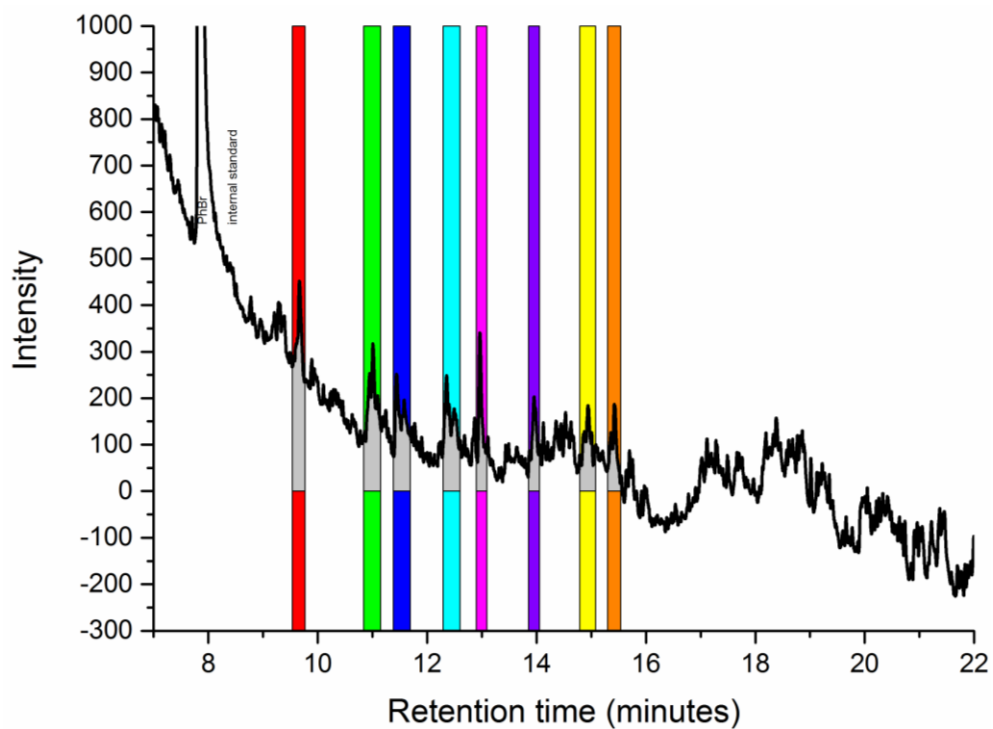


Figure 2-11: Overlaid chromatogram of the serial dilution highlighting the VFAs of interest.

The lower limit of detection (LLOD) was also determined using the same serial dilution samples. This is reported as the calculated concentration of the last sample in the serial dilution where its peak in the chromatogram can be separated from any background noise, Figure 2-12. For all but one of the VFAs used, the calculated lower detectable concentration is between 0.03 – 0.10 mmol dm<sup>-3</sup>, these are displayed in Table 2-5 along with the respective elution times. The lowest detectable limit of 4-ethyloctanoic acid is approximately 100 times more concentrated than the other VFAs although this is most likely due to one or more of the following; the GC method, column conditions or an inappropriate solvent choice.



**Figure 2-12:** Chromatogram of lowest concentration determinable peak.

**Table 2-5:** Elution time and calculated minimum concentration for the 12 volatile compounds used.

<b>Volatile Compound</b>	<b>Elution time (minutes)</b>	<b>Calculated minimum concentration (mmol dm<sup>-3</sup>)</b>
Acetic acid	9.6	0.0904
Propionic acid	10.9	0.0694
Trans-2-nonenal	10.9	0.0312
Isobutyric acid	11.4	0.0558
Butyric acid	12.3	0.0566
2-methylbutyric acid	12.9	0.0474
Isovaleric acid	12.9	0.0469
Valeric acid	13.9	0.0476
4-methylvaleric acid	14.9	0.0411
Hexanoic acid	15.4	0.0413
3-mercapto-1-hexanol	15.4	0.0376
4-ethyloctanoic acid	20.0	3.29

Following a review of the literature, the following compounds were found to be used as internal standards during VFA analysis: valeric acid,<sup>14,15</sup> biphenyl acid,<sup>16</sup> heptanoic acid,<sup>17</sup> 2,2-dimethylbutyric acid,<sup>18</sup> isobutyric acid, 2-methylpentanoic acid and benzoic acid,<sup>19</sup> n-heptadecanoic acid,<sup>20</sup> d<sub>3</sub>-stearic acid,<sup>21</sup> hexanoic acid,<sup>22</sup> and diethylacetic acid.<sup>23</sup> Immediately, valeric acid and isobutyric acid can be discounted as they are already present as malodours in sweat and make up part of the model sweat utilised in this thesis. Two of the other acids were investigated as options for an internal standard that was chemically more similar to the analytes than bromobenzene. Firstly, formic acid was assessed. However, due to the mechanism of FID, it is very low sensitivity compared to similar compounds of longer carbon chain. As reported by Agilent, formic acid has a retention time after acetic acid<sup>24</sup> (*ca.* 10 minutes) and therefore adds to an already busy area of the chromatogram which is not ideal, Figure 2-13.

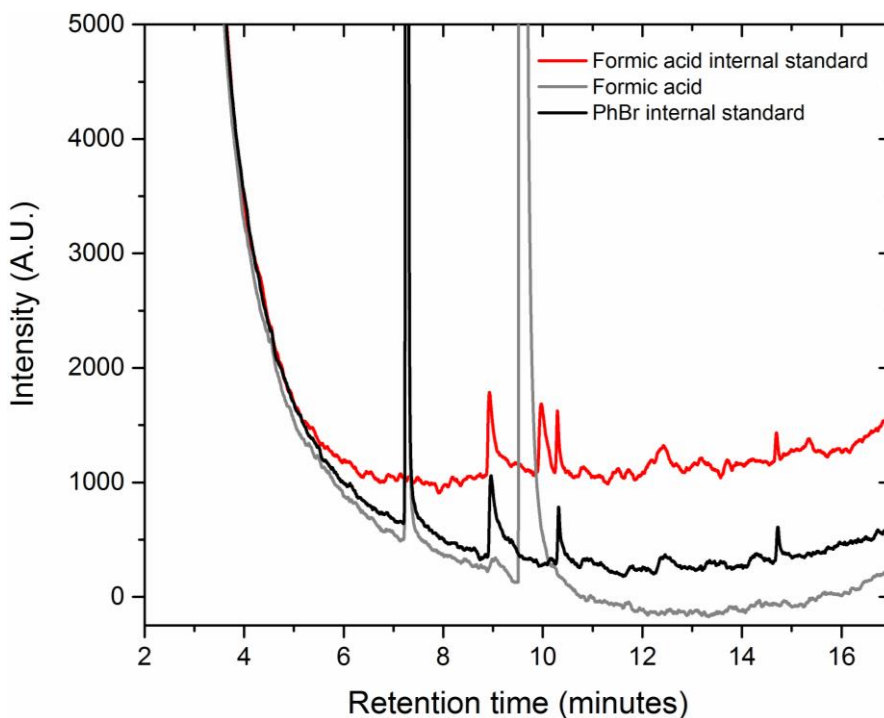


**Figure 2-13:** Overlaid chromatograms with formic acid.

As suggested by Stein *et al.*, 2,2-dimethylbutyric acid was also analysed. As observed in Figure 2-14, 2,2-methylbutyric acid has a much stronger signal and a retention time after those of the analytes.

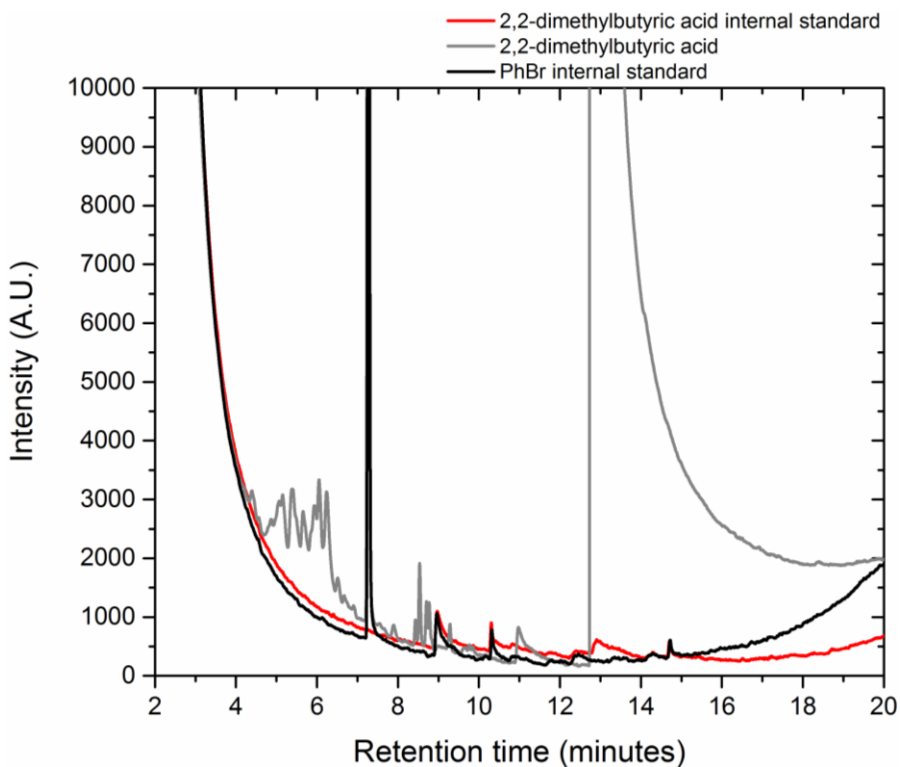
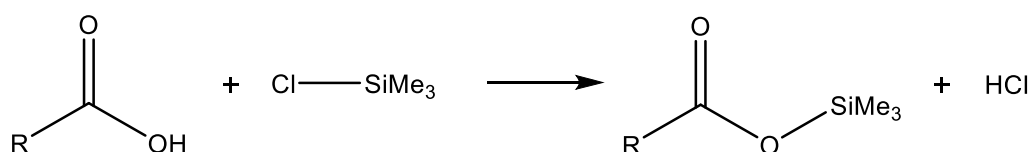


**Figure 2-14:** Overlaid chromatograms investigating the potential of 2,2-dimethylbutyric acid.

## 2.2 Esterification

As discussed in Chapter 1, most literature analysis of volatile fatty acids, is carried out on the esters due to the associated increase in volatility.<sup>25</sup>

The ideal esterification method, for this application, would be carried out at room temperature with minimal additional reagents required so as it is possible to be done within the hydrogel patch at the point of sweat absorption. One method attempted was the formation of the trimethyl silyl (TMS) ester, Scheme 2-1.



**Scheme 2-1:** General reaction of a volatile fatty acid to form the TMS ester.

The successful conversion of butyric acid in this reaction was followed by <sup>1</sup>H NMR, Figure 2-15. The disappearance of the hydroxyl proton that is clearly visible in the butyric acid spectrum is a clear indication of successful conversion.

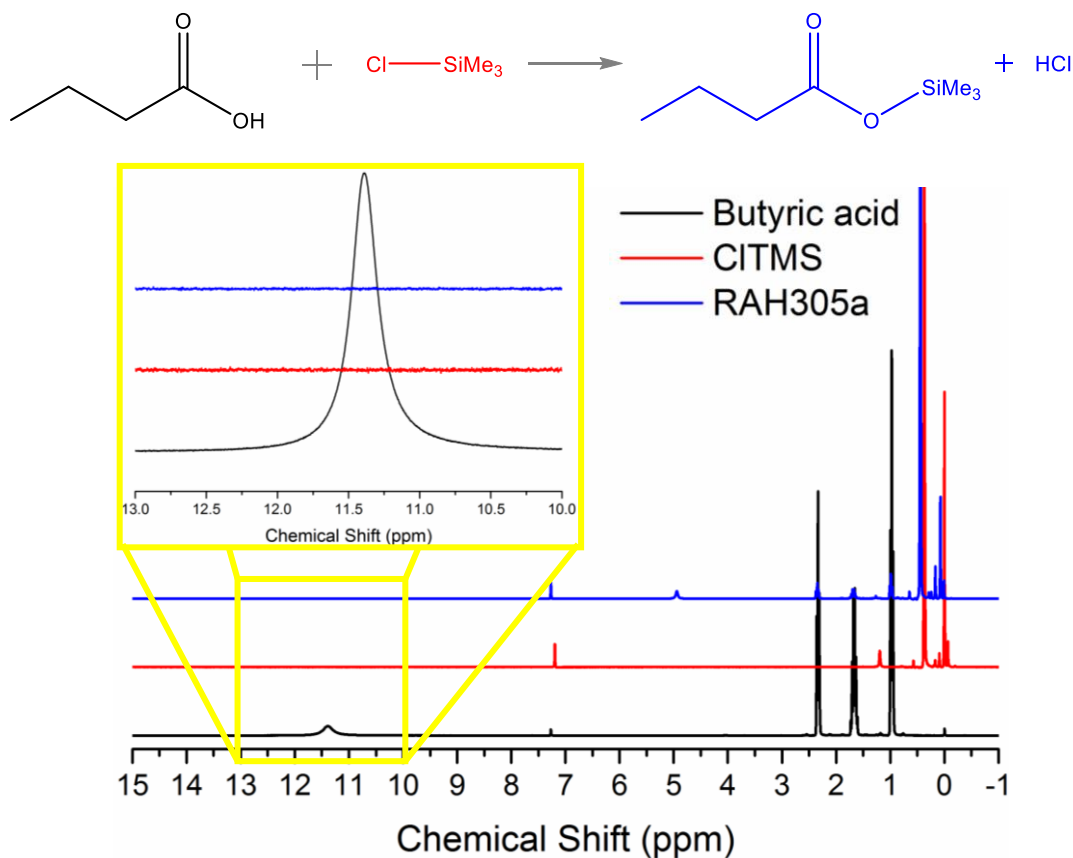


**Figure 2-15:** <sup>1</sup>H NMR spectra of the starting materials and product in the TMS esterification of butyric acid.



### 2.2.1 Fatty Acid Methyl Esters (FAMES)

This was carried out based on the procedure reported by Kanda *et al.*<sup>26</sup> where 0.5 % p-toluene sulfonic acid (catalyst) methanol solution is added to the VFA and heated to 100 °C for an hour, Figure 2-16 where R = Bu. Although the elevated temperature is undesirable, the literature procedure was attempted to determine initial success before decreasing the temperature could be investigated. The disappearance of the hydroxyl hydrogen combined with the appearance of the methyl ester peak in the proton NMR of the free acid and the esterification product respectively, indicates the reaction was successfully performed.

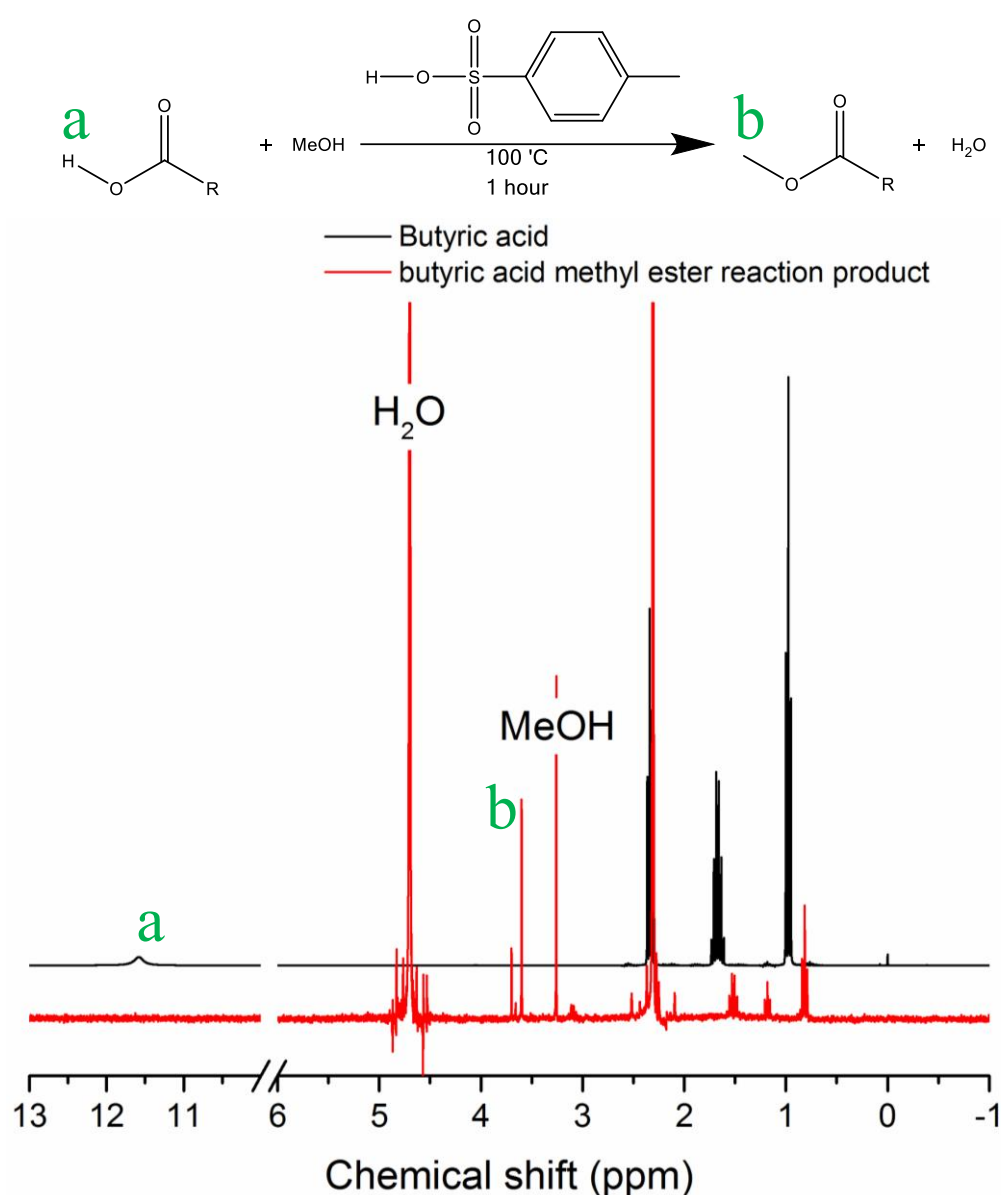
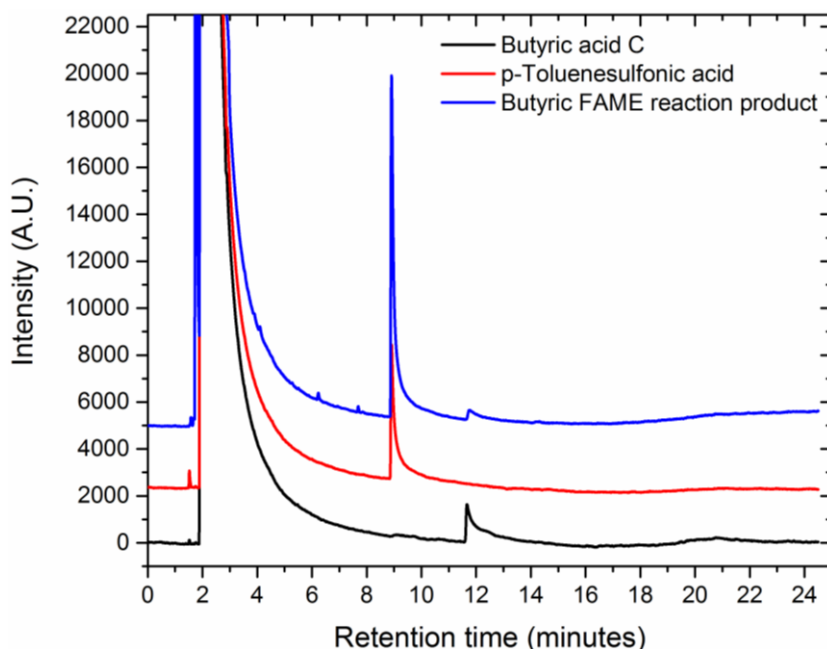


Figure 2-16: <sup>1</sup>H NMR characterisation of the FAME reaction of butyric acid.

However, the malodorous nature of the materials used renders this process non-ideal for this application. The smell given off by the reaction suggests that the butyric acid was evaporating rather than being converted which would not be helpful for quantification of malodorous compounds which is the intended application. Further, the comparison of the GC chromatograms of the starting materials and product mostly reveal the catalyst plus a peak at the same retention time as the free butyric acid with no definitive peak for the product observed. It would be expected that the methyl ester product would appear earlier in the chromatogram than the free acid as it is known that esterification lowers the boiling point compared to free acids as it disrupts the hydrogen bonding that would otherwise occur.<sup>25</sup> It is possible that the two low intensity peaks at 6 and 8 minutes could be attributed to this but this would require further investigation, Figure 2-17. Alternatively, the decrease in boiling point to approximately 102 °C after conversion would suggest that it is possible that the butyric acid is converted to the ester then evaporates as the reaction temperature is 100 °C.



**Figure 2-17:** GC-FID chromatograms of the methyl esterification reaction starting materials and product.

Due to the reasons described above, plus esterification adding an additional step to the procedure and as a result, potentially leading to the loss of analytes, esterification has not been used in this research and, instead chromatography will be carried out on the free fatty acids.

### 2.3 High Performance Liquid Chromatography (HPLC)

A method described by Kroumova and Wagner for the separation of free short chain fatty acids by HPLC was investigated as an alternative to gas chromatography. Analysis was carried out using a UV detector set at 205 nm. The solvent is a mix of acetonitrile and acidified water which would mean modifying extraction solvent post-extraction as discussed previously. Moreover, this method resulted in butyric acid and isobutyric acid eluting at almost identical times (Figure 2-18), suggesting that further method development would be required to optimise separation, thus GC remained the main analytical technique as there was no real advantage to using HPLC over the work already carried out by GC. This is in agreement with the findings of the review by Fernandez *et al.*<sup>2</sup>

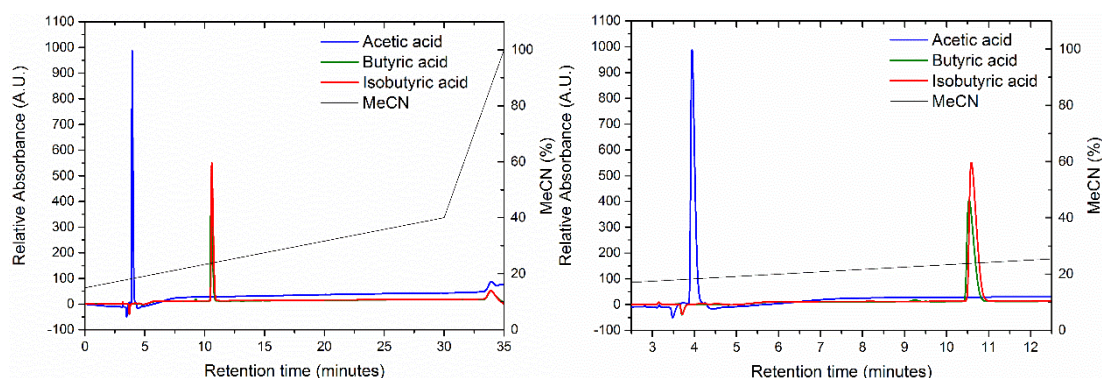


**Figure 2-18:** Overlaid HPLC traces of acetic acid, butyric acid and isobutyric acid (left) and zoomed in on the analyte peaks (right).

## 2.4 Conclusion

Based on the analytical method development presented above, unless otherwise stated, the conditions employed throughout this research are the use of a GC-FID (Shimadzu GC2014 with AOC20 autosampler) with a polar, PEG stationary phase column such as a Restek Stabilwax-DA (30 m length, 0.32 mm ID and 0.25  $\mu\text{m}$  film thickness) with hydrogen as carrier gas (supplied from an external hydrogen generator). The heating profile will be 8  $^{\circ}\text{C min}^{-1}$  from 60  $^{\circ}\text{C}$  (2 minutes) to 220  $^{\circ}\text{C}$  (5 minutes) to analyse free 'model sweat' (10 free fatty acids, one thioalcohol and one aldehyde) unless otherwise discussed. Furthermore, calibration will be carried out externally, prior to analysis and all calibrants and analyte samples will include an internal standard, PhBr, which will be spiked, at a known concentration, for ratios of the concentrations and peak areas to be used in calculations.

GC-MS and HPLC will not be focussed on throughout the remainder of the thesis, instead GC-FID has been used for concentration determinations.

## 2.5 References

- 1 D. C. Harris, in *Quantitative Chemical Analysis*, Freeman, seventh., pp. 528–555.
- 2 R. Fernández, R. M. Dinsdale, A. J. Guwy and G. C. Premier, *Crit. Rev. Environ. Sci. Technol.*, 2016, **46**, 209–234.
- 3 E. Kováts, *Helv. Chim. Acta*, 1958, **41**, 1915–1932.
- 4 E. D. Dodds, M. R. McCoy, L. D. Rea and J. M. Kennish, *Lipids*, 2005, **40**, 419–428.
- 5 T. Wu, X. Wang, D. Li, G. Sheng and J. Fu, *Int. J. Environ. Anal. Chem.*, 2008, **88**, 1107–1115.
- 6 K. Dettmer-Wilde and W. Engewald, Eds., *Practical Gas Chromatography A Comprehensive Reference*, Springer, 2014.
- 7 S. R. Lipsky, R. A. Landowne and J. E. Lovelock, *Anal. Chem.*, 1959, **31**, 852–856.
- 8 D. Rood, *The Troubleshooting and Maintenance Guide for Gas Chromatographers*, 4th edn., 2007.
- 9 S. E. Fleming, H. Traitler and B. Koellreuter, *Lipids*, 1987, **22**, 195–200.
- 10 C. Reichardt, *Solvents and Solvent Effects in Organic Chemistry*, Wiley-VCH, 4th edn., 2010.
- 11 I. Brondz, *Anal. Chim. Acta*, 2002, **465**, 1–37.
- 12 O. Pinho, I. M. P. L. V. O. Ferreira and M. A. Ferreira, *Anal. Chem.*, 2002, **74**, 5199–5204.
- 13 United States Environmental Protection Agency, Method 8270D.
- 14 V. Mahadevan and L. Stenroos, *Anal. Chem.*, 1967, **39**, 1652–1654.
- 15 T. L. Perry, S. Hansen, S. Diamond, B. Bullis, C. Mok and S. B. Melancon, *Clin. Chim. Acta*, 1970, **29**, 369–374.
- 16 J. M. Levy, L. E. Wolfram and J. A. Yancey, *J. Chromatogr.*, 1983, **279**, 133–138.
- 17 A. E. Van den Bogaard, M. J. Hazen and C. P. Van Boven, *J. Clin. Microbiol.*, 1986, **23**, 523–530.
- 18 J. Stein, J. Kulemeier, B. Lembcke and W. F. Caspary, *J. Chromatogr. B Biomed. Sci. Appl.*, 1992, **576**, 53–61.
- 19 J. W. Mayhew and S. L. Gorbach, *Appl. Environ. Microbiol.*, 1977, **33**, 1002–1003.
- 20 T. Masui, M. Fujishima, Y. Mori, T. Shinka and I. Matsumoto, *Int. J. Mass Spectrom. Ion Phys.*, 1983, **48**, 225–228.
- 21 Y. J. Yang, M. H. Choi, M. J. Paik, H. R. Yoon and B. C. Chung, *J. Chromatogr. B. Biomed. Sci. Appl.*, 2000, **742**, 37–46.
- 22 F. J. Sansone and C. S. Martens, *Mar. Chem.*, 1981, **10**, 233–247.
- 23 B. McArthur and A. P. Sarnaik, *Clin. Chem.*, 1983, **28**, 1983–1984.
- 24 W. Liu and C. Wang, Determination of Formic Acid in Acetic Acid for Industrial Use by Agilent 7820A GC, *Agilent Application Brief*, 2009.
- 25 D. R. Knapp, *Handbook of Analytical Derivatization Reactions*, Wiley, 1979.
- 26 F. Kanda, E. Yagi, M. Fukuda, K. Nakajima, T. Ohta and O. Nakata, *Br. J. Dermatol.*, 1990, **122**, 771–776.

### 3. Hydrogel Synthesis

Standard p(NaAMPS) hydrogels are synthesised according to a procedure described previously within the Haddleton group.<sup>1</sup> Briefly, 2-acrylamido-2-methyl-1-propanesulfonic acid sodium salt (monomer), poly(ethylene glycol) diacrylate (crosslinker), 2-hydroxy-2-methylpropiophenone (photoinitiator) and water are mixed in batch before aliquots are transferred to silicone moulds and passed under a UV light source *via* a conveyor belt ( $\sim 5 \text{ m min}^{-1}$ ) five times to complete the synthesis (full details, Chapter 7). This chapter describes all parts of the process in order to optimise its synthesis for potential industrial scale synthesis and application. Attention will then focus on the mechanical properties of the hydrogel and further comparison with more sophisticated double network materials.

#### 3.1 Gel Proton NMR Method Development

Typically, in polymer research, NMR is a very common analytical method used to probe monomer conversion, however, solution state NMR relies on the analyte samples being soluble in a deuterated solvent to obtain data. Where often for synthesised polymers a suitable solvent can be found, the crosslinked materials presented in this thesis are a considerable challenge. However, solid state NMR or non-solution samples for solution NMR are possible but are less readily available and leads to broader peaks and lower resolution.

With this knowledge it was decided to test solution-state NMR on gel samples. Practically it is challenging to get a pre-made hydrogel into a standard size 5 mm NMR tube homogeneously therefore it was determined that the hydrogels could be synthesised for NMR analysis with some minor modifications to the standard procedure. Namely, the water would be replaced with D<sub>2</sub>O and that the synthesis would be carried out on 1 ml aliquots directly in NMR tubes rather than the silicon moulds.<sup>2</sup> Studies were carried out to determine the viability of relying on solution NMR of a gel to illustrate the vinyl proton peaks. Firstly, a study was carried out whereby extra monomer was added to a hydrogel that had been passed under the UV lamp 50 times post polymerisation (and original analysis, see section 3.2.2) and

left to allow the hydrogel to absorb the monomer. This was in order to prove viability of observing the monomer by NMR if it is trapped in the gel matrix.

In order to show that the monomer was being absorbed far enough into the gel for it to be in the NMR window, red food colouring was added to the NaAMPS monomer before addition to the gel (Figure 3-1). It is worth considering that, where 0.1 ml of 50 % monomer was added, clearly not all of the material had permeated the gel (evidenced by the food dye – Figure 3-1). This suggests the concentration of monomer detected by the gel NMR is < 10 %. Figure 3-1 illustrates the  $^1\text{H}$  NMR spectra of the 50 passes gel before and after the extra dyed monomer was added. As can be observed, the vinyl protons are visible in the monomer-doped sample but not before doping, suggesting that if vinyl peaks are not observed in later analyses that quantitative conversion has occurred.

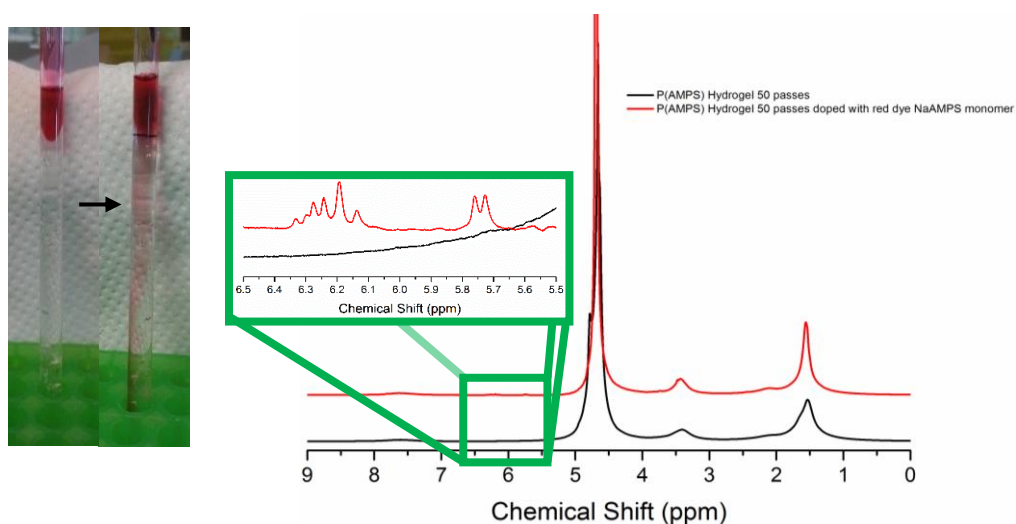


**Figure 3-1:** Left the diffusion of the dyed monomer. Right the  $^1\text{H}$  NMR of the hydrogel before and after this addition, stacked.

This indicated that it took  $\sim 24$  hours for absorption through the gel, something which is interesting for the swelling method employed for the doping of the gels with model sweat for further research (Chapter 4), however, in this NMR tube study, absorption will likely be slower due to the decreased surface area compared to the standard 3 cm diameter discs.

## 3.2 Curing Efficiency

As the goal of this work is to fulfil an industrial need, there was cause to investigate adapting the synthetic process to prepare larger (and possibly thinner) sheets of the hydrogel. Ideally, it would also only require one pass (instead of the standard five) under the Light Hammer (a high-powered UV lamp). One pass refers to once along the conveyor belt under the UV lamp. The conveyor belt speed is set to  $5 \text{ m min}^{-1}$  which equates to approximately 7 seconds of UV exposure per pass. Therefore the standard reaction is *ca.* 35 seconds.

### 3.2.1 Gravimetry

Standard 3 ml p(NaAMPS) hydrogels were prepared using a different number of passes on the conveyor belt under the UV lamp, effectively investigating UV exposure time required to complete the reaction. The mass of the gels formed was recorded and compared to the mass of the 'standard' five passes gels. There is a significant difference in mass between one and five passes observed, Figure 3-2. This is likely caused by evaporation of water due to increased exposure to increased temperature caused by the powerful UV source. Unsurprisingly, 50 passes illustrates a further, significant mass decrease. This suggests that minimising the number of passes is beneficial not only for industrial scale synthesis but also to maintain the hydrated state and preventing phenomena such as the crazing discussed later in this chapter. Therefore, the conversion of monomer needs to be investigated to determine whether five passes are necessary or whether one is sufficient for quantitative conversion.



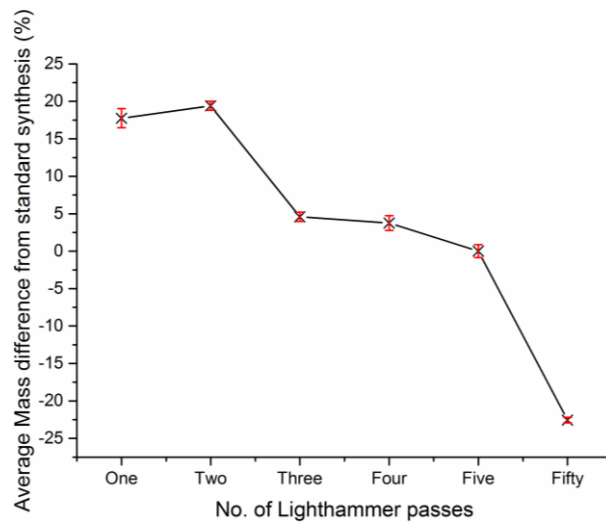


**Figure 3-2:** Percentage difference in mass of hydrogels exposed to the Light Hammer for varying amounts of time compared to the standard.

### 3.2.2 Proton NMR analysis

The kinetics of this polymerisation were then assessed by NMR using the solution method validated in Section 3.1. As discussed, the polymerisations had to be carried out *in situ* as it is not feasible to get the gel into an NMR tube after polymerisation, nor could a suitable solvent be found due to the crosslinked nature of the product. For the same reason, there is no molecular weight data from SEC as this technique also requires solubility. As can be seen in Figure 3-3, the vinyl protons at 5.75 and 6.25 ppm are only visible in the starting material, which is evidence of quantitative conversion of the monomer, even after one pass.

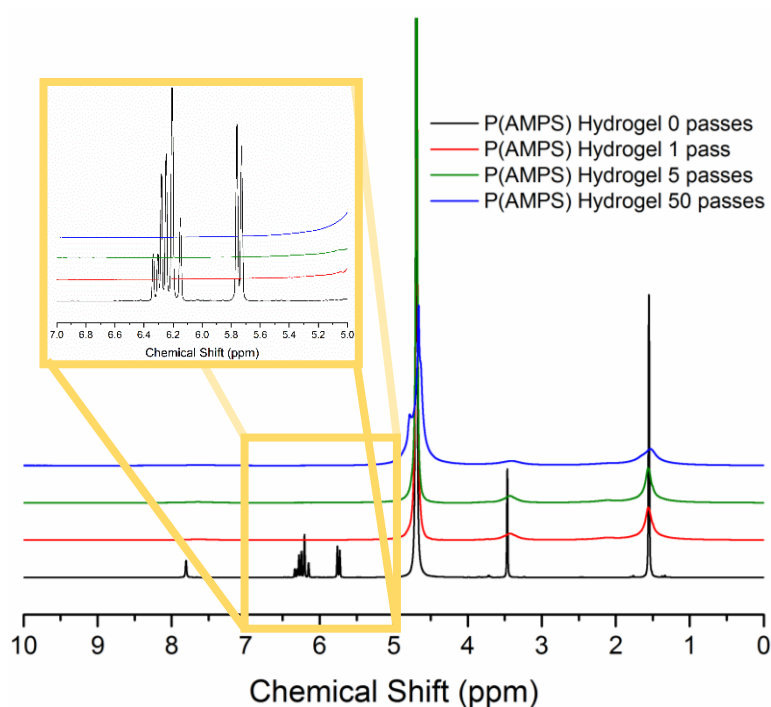


**Figure 3-3:** Stacked  $^1\text{H}$  NMR of the hydrogels synthesised using different UV exposure times with the highlighted disappearance of the vinyl peaks.

### 3.2.3 Infrared Spectroscopy

The overlaid FTIR spectra confirm the disappearance of the vinyl groups, Figure 3-4, as previously illustrated by NMR (Figure 3-3). The key peaks are highlighted on the spectra with the main differences being related to the vinyl groups of the monomer and their disappearance in the polymers. With the C=C stretch at 1635-1620  $\text{cm}^{-1}$  and the terminal vinyl protons appearing as the multiple peaks at 3100-3010  $\text{cm}^{-1}$ . The other key peaks that identify NaAMPS, as reported by Zhang and Eastal are presented in Table 3-1.<sup>3</sup>

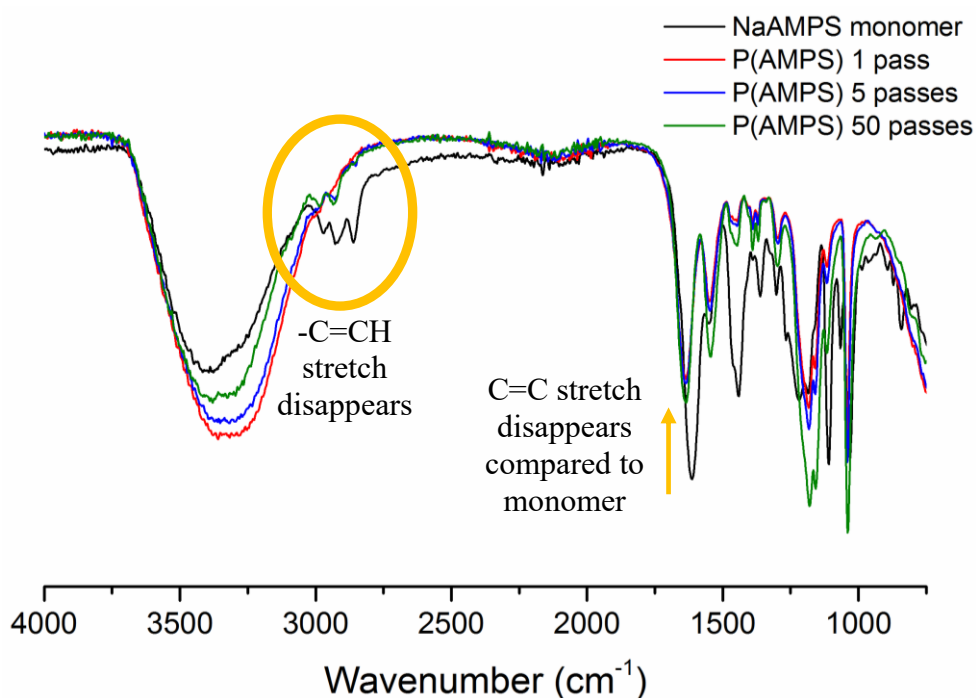


**Figure 3-4:** Overlaid FTIR spectra of the hydrogels produced with different reaction times and the NaAMPS starting material.

**Table 3-1:** Infrared Spectroscopy characterisation of p(NaAMPS) and NaAMPS monomer.<sup>3</sup>

Wavenumber (cm <sup>-1</sup> )	Functional group
3500-3200	N-H stretch, amide group (overlaps with O-H from water)
3435-3469	N-H vibrations
3100-3010	=CH stretch
1652	Secondary amide carbonyl groups
1635-1620	Vinyl C=C stretch
1552-1557	Secondary N-H deformation (in the solid state)
1224-1225	SO <sub>2</sub> asymmetric stretch
1180	C-N stretch
1039	SO <sub>3</sub> symmetric stretch
623-624	C-S stretch

Further work could be to analyse the xerogels so as to minimise the water peak, effectively removing the water from the sample, or investigate the possibility of using Raman spectroscopy as it is blind to water.

### 3.2.4 TGA

TGA analysis shows similar transitions for all samples (Figure 3-5), indicating that the same polymer networks form regardless of the total polymerisation time. Moreover, it can be seen in the initial mass loss, which is predicted to be loss of water, that the fifty passes contains less water than both the one and five pass equivalents which is in agreement with the gravimetric data discussed previously. The second transition is suggested to be a result of desulfonation but may also be attributed to backbone degradation.<sup>4,5</sup> With Aggour *et al.* suggesting two degradation steps at 182 °C and 303 °C and that there was 28 % residual left at 550 °C which is in keeping with the observed step-changes in the thermograms.<sup>6</sup>

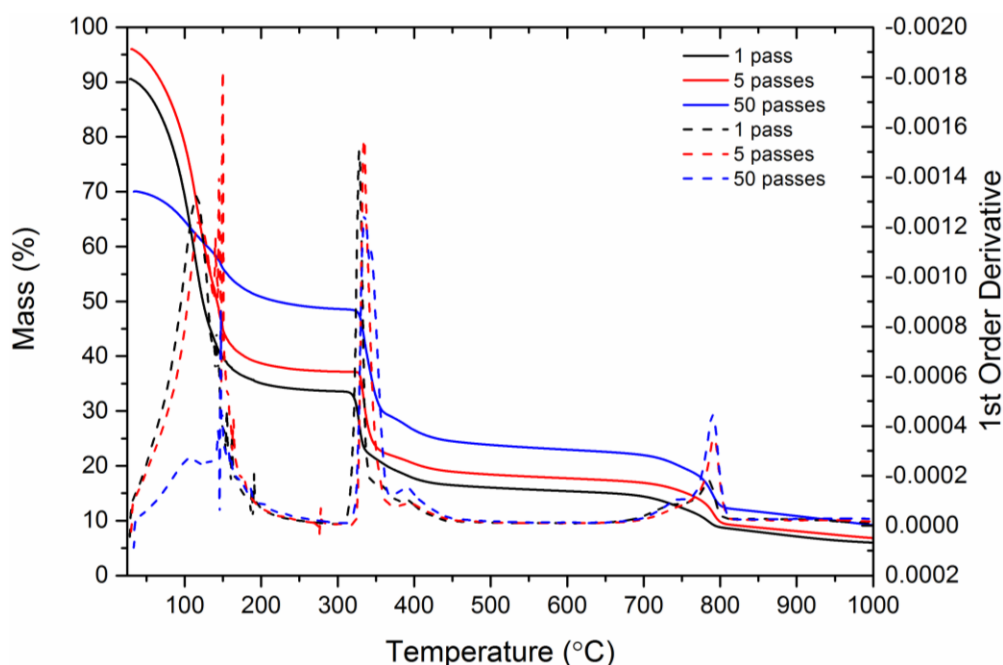


**Figure 3-5:** Overlaid TGA data from the hydrogels made using different UV exposure times. – are the percentage mass loss curves. - - - are the first derivatives of the mass loss curves. Differences in starting mass percentage may be attributed to water loss after sample preparation (whilst in autosampler queue).

### 3.3 Initiator Concentration

A further study was then carried out using decreased initiator concentrations. Physical differences in the materials produced were observed; the 20 vol% initiator sample became gel like in appearance after 2-3 passes on the conveyor belt under the UV lamp compared to the standard material which appears gel-like after 1 pass. The 2 vol% initiator material required 10 passes to form some gel and was still not a homogenous material, with some liquid remaining, after 25 passes. As predicted, the intensity of the vinyl peaks increases with decreasing initiator concentration, Figure 3-6. This is evidence that the initiator concentration is appropriate for quantitative conversion, whilst also further evidencing that this method is suitable for monitoring the conversion in the UV exposure study discussed previously.

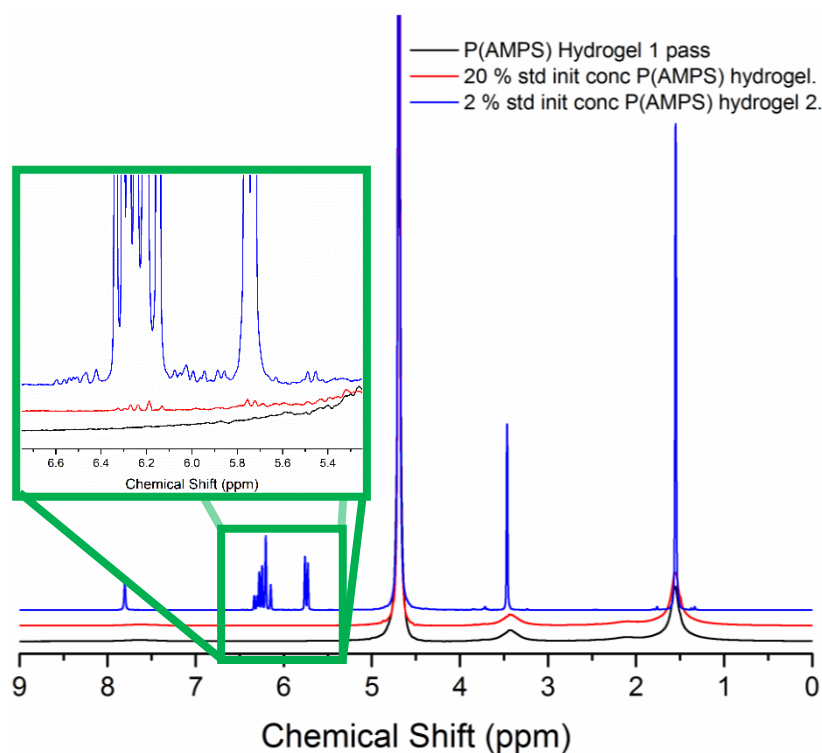


**Figure 3-6:** Stacked <sup>1</sup>H NMR spectra of the polymers produced using different initiator concentrations (relative to standard).

### 3.4 UV Sources

The standard procedure relies on a LightHammer®, a UV lamp (h bulb) with a conveyor belt passing under it to control exposure to seconds at a time. When first attempting to scale up from a ~7 cm<sup>2</sup> disc to a 15.5 cm by 10.0 cm rectangle (both 0.5 cm thick) it was noticed that the conveyor belt was creating a wave which was instantaneously cured into a gel of uneven thickness, Figure 3-7.



**Figure 3-7:** Larger hydrogel with the wave cured in.

#### 3.4.1 Crazeing

To avoid this wave, a UV “nail lamp” was employed to polymerise the sample whilst keeping the sample static, however, due to increased exposure time to elevated temperature (50 °C<sup>7</sup>) compared to the few seconds per pass under the Light Hammer this caused a phenomenon known as ‘crazing’, Figure 3-8. This is where water evaporation from the hydrogel causes cracks in the upper face of the hydrogel, which gives it the appearance of crazy paving.



**Figure 3-8:** ‘Crazed’ larger hydrogel.

In an attempt to overcome these undesirable morphologies, using a combination of the nail lamp and the Light Hammer was investigated. The goal was to carry out a ‘pre-cure’ under the nail lamp; long enough that gel formation began but not long enough for crazing to begin, before passing it under the Light Hammer to complete polymerisation without a wave forming.

The optimum time for this was found to be 8 – 9 minutes pre-cure, Figure 3-9, however, this is not ideal for industrial scale-up as it adds more steps to the synthetic procedure.

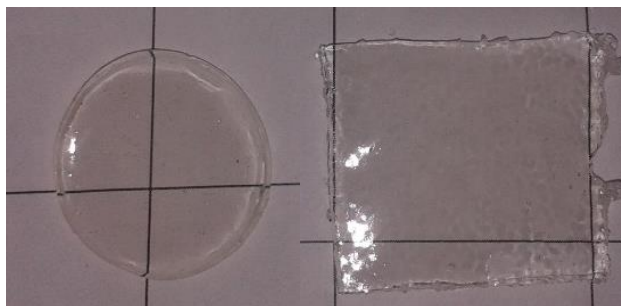


**Figure 3-9:** Standard hydrogel disk using Lighthammer only (left) and a hydrogel square cut from the bigger sheet synthesised using 8-9 minute pre-cure followed by lighthammer (right).

A further UV light source was also investigated; a UVP CL-1000 Ultraviolet Crosslinker. This was unsuccessful, likely due to the wavelength of the bulb being higher energy than that in the nail lamp (~254 nm compared to ~360 nm).<sup>8</sup> As can be seen in Figure 3-10, the UV spectrum of the initiator indicates no activity from the initiator below ~260 nm, therefore it is the wavelength of the bulb that is key to a successful polymerisation.

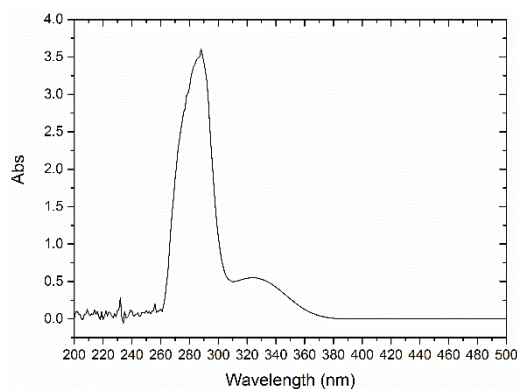


**Figure 3-10:** UV-vis spectrum of irgacure 1173.

When polymerisation was further attempted using a UV crosslinker machine, this time with a 365 nm wavelength bulb, a standard p(NaAMPS) 3 ml gelled within 30 minutes. However, the increased exposure time resulted in crazing as noted previously when using the nail lamp. The strength of the UV radiation and resident time in the heated environment are clearly key factors in the synthesis of hydrogels of successful morphology.



### 3.4.1.1 Laser Scanning Confocal Microscopy

Laser Scanning Confocal Microscopy (LSCM) was carried out in order to observe the structure of these crazed hydrogels. Initially, the hydrogels were soaked in a solution of fluorescein isothiocyanate (FITC), Figure 3-11, before being imaged using an LSCM<sup>9</sup> whereby the crazed structure is clearly visible, Figure 3-12.

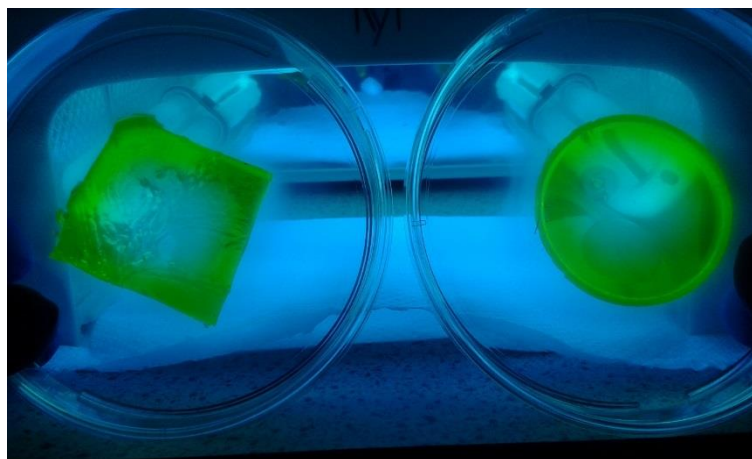


**Figure 3-11:** FITC dyed hydrogels (crazed and standard, left and right respectively) under UV light.

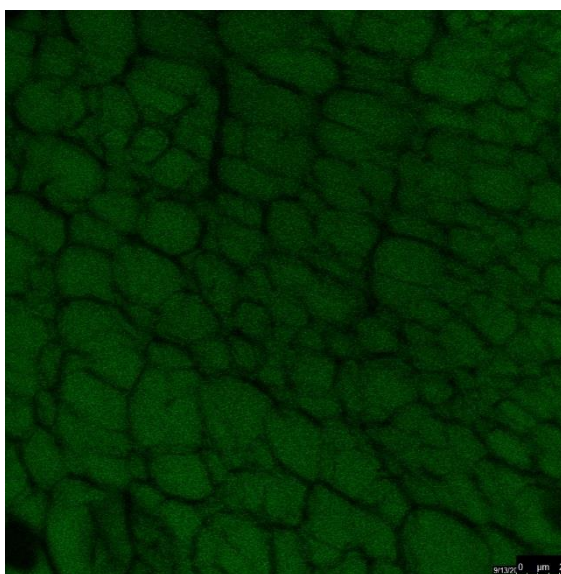


**Figure 3-12:** LSCM image of a crazed hydrogel.

### 3.4.1.2 Dosing and recovery

A standard dosing, absorption and recovery procedure study was carried out on this crazed hydrogel to determine if the crazing affected the end application. Figure 3-13 demonstrates that the standard hydrogel and the crazed version show comparable recovery across all five acids included, suggesting that the crazing is only an aesthetic issue. Further work would be required to determine if a difference in the surface and texture is a problem *in situ*, that is, does it change contact with the axilla, potentially reducing absorption efficiency. However, subsequent optimisation of swelling and extraction is carried out on the standard hydrogels, not the crazed version.

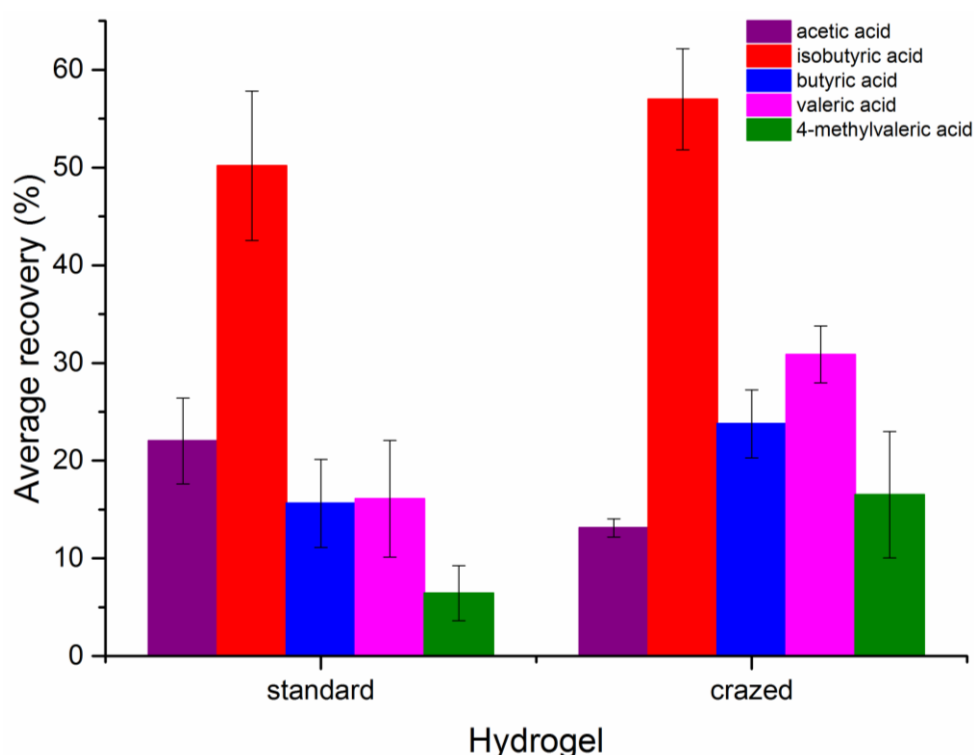


**Figure 3-13:** Comparison of absorption and extraction efficiency of a standard p(NaAMPS) hydrogel and a 'crazed' p(NaAMPS) hydrogel.

## 3.5 Crosslinker Concentration study

The standard crosslinker used in this work is poly(ethylene glycol) diacrylate ( $M_n \sim 575$  g mol<sup>-1</sup>) used at 0.2 mol%. This study investigated 0.2, 0.4, 1.0 and 2.0 mol% in order to determine the effect of crosslinker concentration on the mechanical and physical properties of the p(NaAMPS) hydrogel in order to investigate the possibility of improving the hydrogels' resilience under the increased pressures and temperatures applied during supercritical fluid extraction (Chapter 4).

### 3.5.1 Swelling Kinetics

Throughout this work, swelling kinetics have been carried out on hydrogels that have been dehydrated. These materials will be referred to as xerogels; dry gels prepared by evaporating the pore liquid (“xero” rooted from Greek meaning “dry”).<sup>10</sup>

Swelling is a critical property for the use of the hydrogel as part of a device for sampling and analysing sweat. The method is described in Chapter 7, with the swelling ratio based on the equation reported by Nalampang *et al.*<sup>11</sup>:

$$\text{Swelling ratio} = SR = \frac{W_s - W_d}{W_d} \quad (3-1)$$

where  $W_s$  and  $W_d$  are the mass of the swollen and the dry hydrogel respectively. This is illustrated in Figure 3-14 for the crosslinker level study hydrogels whereby increasing crosslinker concentration both decreases the maximum swelling ratio (equilibrium water content, see below) and slows the swelling kinetics; observations that were also previously reported by Nalampang *et al.*<sup>11</sup>

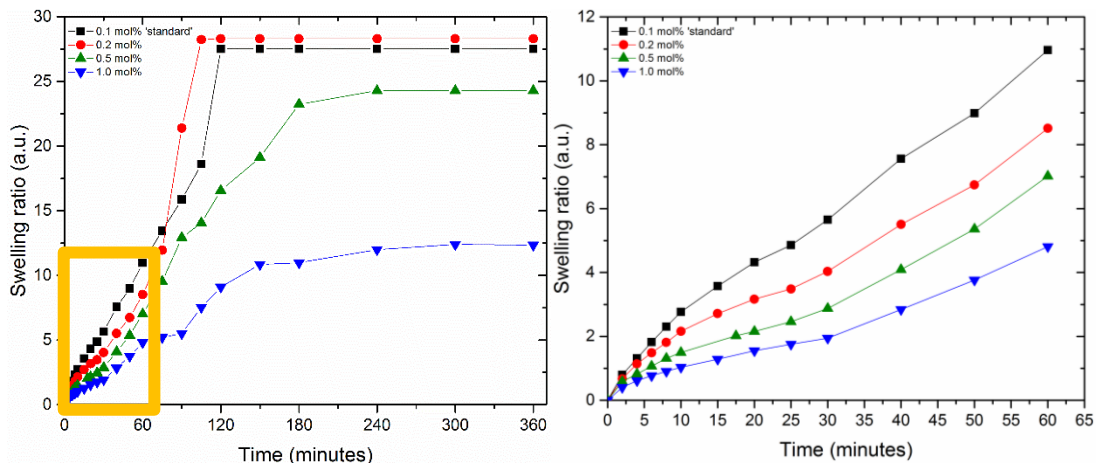


**Figure 3-14:** Swelling kinetics of the hydrogels containing different concentrations of crosslinker. Swelling ratio as calculated in eq. 1-1. Yellow highlighted region illustrated on RHS.

The maximum volume of water absorbed by a hydrogel (from the xerogel state) can also be calculated and is conventionally reported as a percentage of the water in the whole mass known as equilibrium water content (EWC):

$$EWC = \frac{W_e - W_d}{W_e} \times 100 \quad (3-2)$$

where  $W_e$  is the mass of the hydrogel at equilibrium swollen state.

There is a clear negative correlation between increasing concentration of crosslinker (PEGDA) and decreasing EWC, Figure 3-15. This is also depicted in the image where the hydrogels are arranged from lowest to highest concentration of crosslinker (left to right) and the volumes give a good indication of the swelling properties. The lowest concentration taking up over half of the volume of the 500 ml jar whilst the highest concentration takes up less than half the volume of a 250 ml jar. This has been suggested by Holmes and Stellwagen to be due to the increasing crosslinker concentration leading to decreasing pore size within the gel matrices.<sup>12</sup>

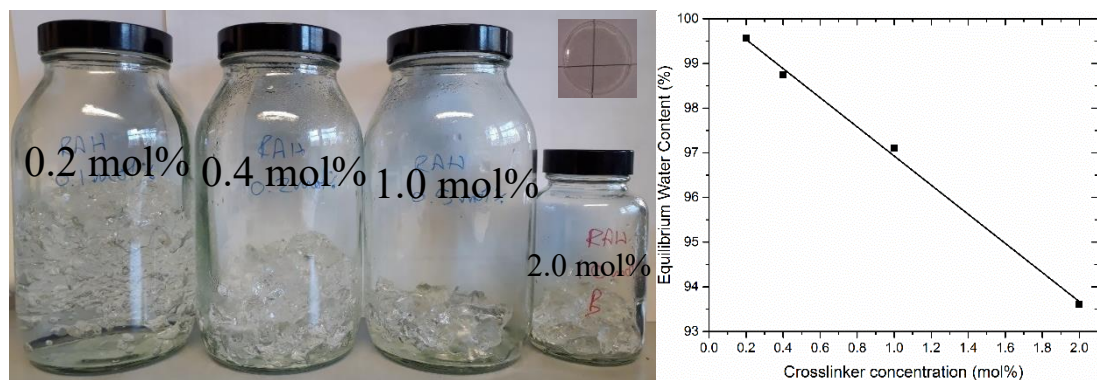


**Figure 3-15:** Four different hydrogel crosslinker concentrations swollen to their maximum. For reference the large jar is 500 ml. Graph of EWC as a factor of crosslinker concentration (right).

Due to the method requiring the surface of the hydrogel to be dried prior to weighing for an accurate mass, some water is lost at every time point. This means that even though the 0.2, 0.5 and 1.0 mol% samples absorb 'all' the water they reach different maximum masses, all of which are less than the initial 50 g of water added to each sample at  $t = 0$ .

Consequently, only the 2.0 mol % sample reached its equilibrium swelling state. Therefore, the kinetics of the other 3 samples were further monitored by adding more water to these now, semi-swollen hydrogels and monitored gravimetrically until they reached their respective equilibrium swelling states, Figure 3-15.

Furthermore, all 4 samples break up to varying degrees, during the kinetic study. This in part is due to the maximum swelling that causes rupturing of the network but also could be exacerbated by the repeated handling / general handling procedure. This meant that not 100 % of the hydrogel was removed from the water at every time point, and not the same pieces / amount of gel were removed at different points. It

also meant that some gel was lost during weighing, as there was transfer between vessels and small bits left on the tissue used to dry the surface.

Conversely, once the hydrogel has broken up significantly, there is a large increase in surface area for water absorption, which is one possible explanation for the significant increase in the rate of water uptake exhibited in the 0.2 mol % hydrogel.

In addition, either the 0.2 or 0.4 mol % sample exhibits anomalous behaviour from 90 minutes. In theory (based on data published by Nalampang and correlation of crosslinker concentration vs. swelling) the 0.2 mol % sample should always have a greater mass than the 0.4 mol % sample (and so on ...) as it should swell to a greater mass and should do so faster. This is the case until 90 minutes but may be attributed to loss of hydrogel through the measurement process errors already discussed.

According to Efron and Brennan, this gravimetric determination of the water content is accurate to approximately  $\pm 2\%$  water content.<sup>13</sup> The main limitation is the removal of surface water prior to weighing the hydrogel. This confirms the challenges we experienced in evaluating gravimetric data, future work could include using a refractometer (inspired by Efron and Brennan) to calculate the water content based on the difference between the measured refractive index of the hydrogel and water.

### 3.5.2 Dynamic Mechanical Analysis

Dynamic mechanical analysis (DMA) was carried out in frequency sweep mode using the tension test geometry to measure hydrogel stiffness with respect to the storage modulus as a function of frequency, Figure 3-16. There is a clear trend between the increase in crosslinker concentration and an increase in storage modulus at every frequency. This is illustrated for 1 Hz in Figure 3-17.

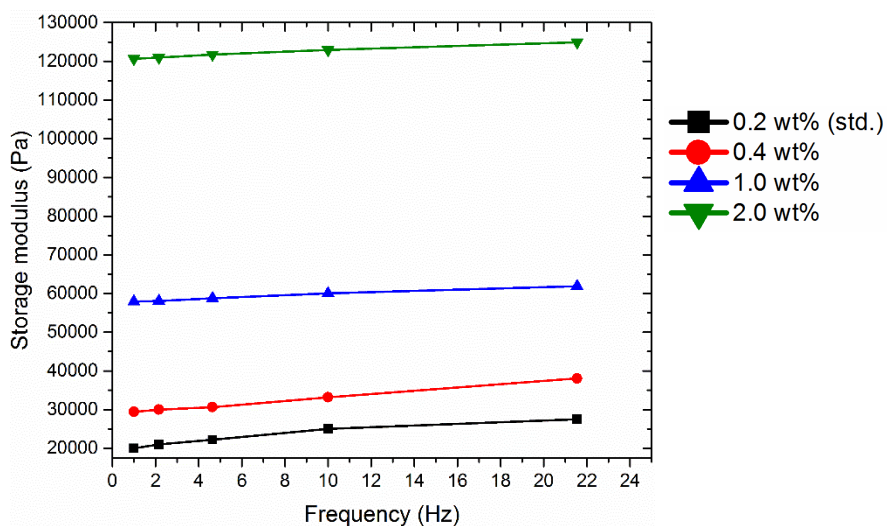


**Figure 3-16:** Storage modulus versus frequency of the increasing crosslinker concentration hydrogels at 25 °C.

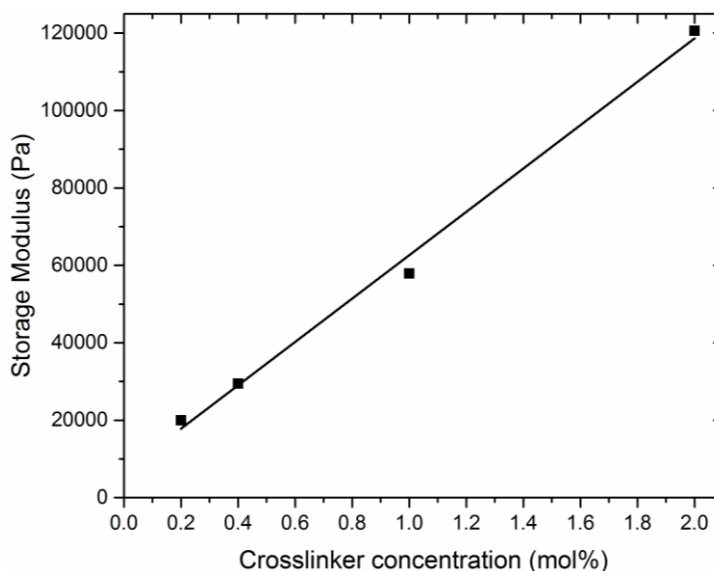


**Figure 3-17:** Storage modulus (at 1 Hz, 25 °C) as a function of increasing crosslinker concentration.

### 3.5.3 Tensile testing

The mechanical properties of the materials containing each of the four crosslinker concentrations tested were measured using a Universal tester in order to determine elongation at break and Young's modulus, Figure 3-18.

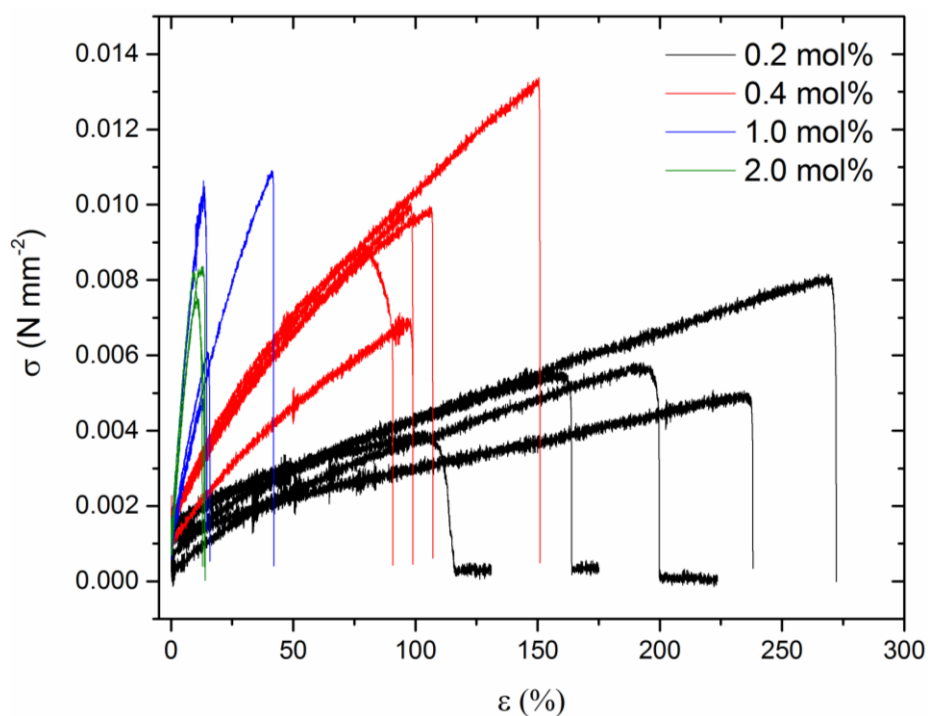


**Figure 3-18:** Tensile test Stress-strain repeat curve for the four crosslinker concentrations tested.

As with the storage modulus from DMA, there is a clear positive correlation between increasing crosslinker concentration and increasing Young's modulus, Figure 3-19. This suggests that the p(NaAMPS) hydrogels exhibit an increase in stiffness with increasing crosslinker concentration.

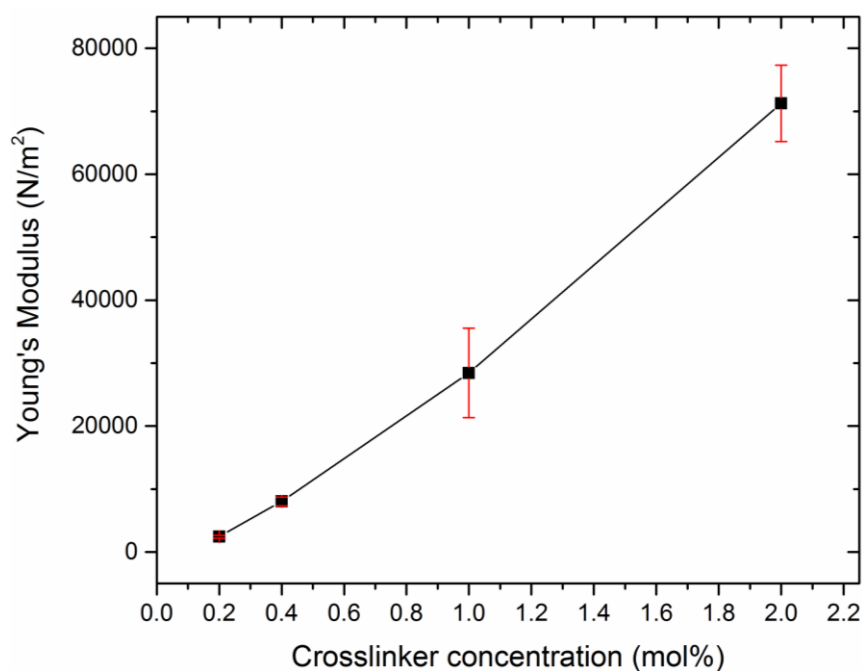


**Figure 3-19:** Young's modulus as a function of increasing crosslinker concentration.

By considering both the absorption capacity and the mechanical data of this series of materials, an optimal crosslinker concentration may be determined depending on the weighting given to the importance of these characteristics, whereby a compromise may be reached.

### 3.6 Other Monomers

#### 3.6.1 2-Hydroxyethyl acrylate

2-Hydroxyethyl acrylate (HEA) was used to synthesise single network hydrogels, initially to compare the properties to the p(NaAMPS) hydrogels with a view to producing covalent-covalent double networks (Section 3.7).

This proved difficult when trying to simply switch monomer in the standard photopolymerisation system used for synthesising p(NaAMPS). <sup>1</sup>H NMR of attempts to carry out these reactions reveals there is still the presence of monomer (*via* the presence of vinyl peaks) evidence that the conversion is lower than ideal, red spectrum, Figure 3-20. A further experiment is overlaid with this whereby ten times the original concentration of initiator was employed. In this case the vinyl peaks have decreased in intensity, suggesting greater monomer conversion as would be



expected, however, the conversion is still not quantitative (green spectrum, Figure 3-20).

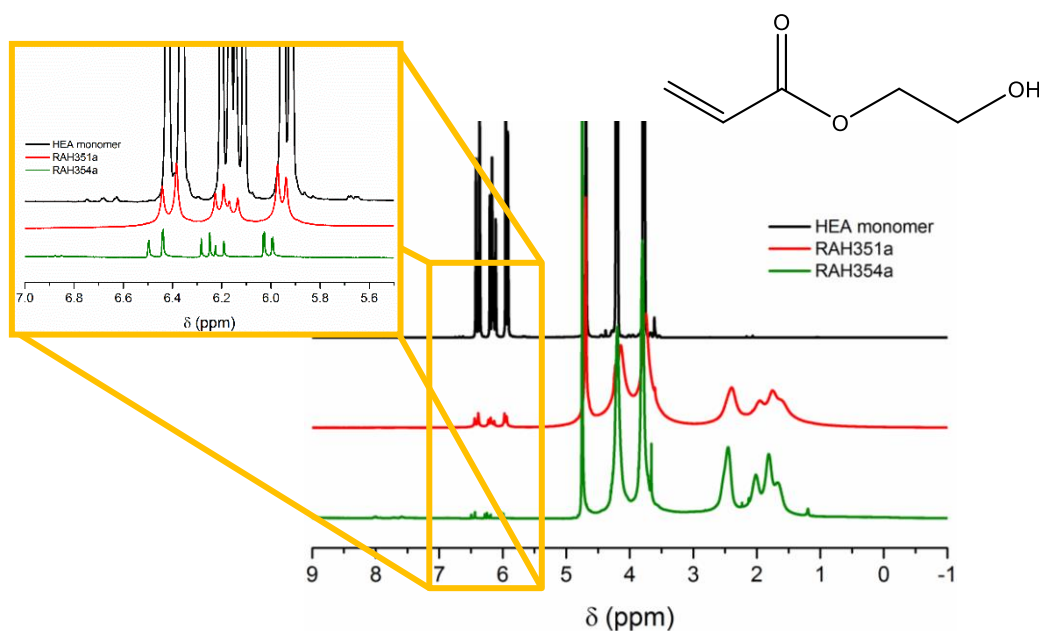


**Figure 3-20:** <sup>1</sup>H NMR of HEA monomer and p(HEA) hydrogels with different initiators concentrations investigated. Black = monomer, red = standard initiator conc. used, green = 10 times standard initiator concentration used.

#### 3.6.1.1 Swelling kinetics

As illustrated in Figure 3-21, gravimetric monitoring of the swelling of an oven dried HEA hydrogel (xerogel) revealed a steady increase in water uptake over time. However, these reactions show slower kinetics than that of a comparable p(NaAMPS) hydrogel, Figure 3-22. Furthermore, the EWC is also much lower than the comparable standard p(NaAMPS) hydrogel as it is 90 % (compared to >99 %). This may be due to the high charge density associated with the sulfonate groups of NaAMPS as it is known that an increasing number of ionic groups increases the swelling capacity.<sup>14</sup>

Notably the p(HEA) xerogel is a flexible material, compared to the standard p(NaAMPS) xerogel which is hard and relatively brittle, suggesting a difference in glass transition temperature. Rault *et al.* reported the glass transition temperature of a p(HEA) homopolymer as ~ 10 °C when investigating its use in IPNs alongside the effect of water content on thermal properties.<sup>15</sup> It is also notable that crosslinking density and molecular weight all effect glass transition temperature, so future work

would require analysis of these hydrogels and their xerogels by DSC in order to obtain accurate data.

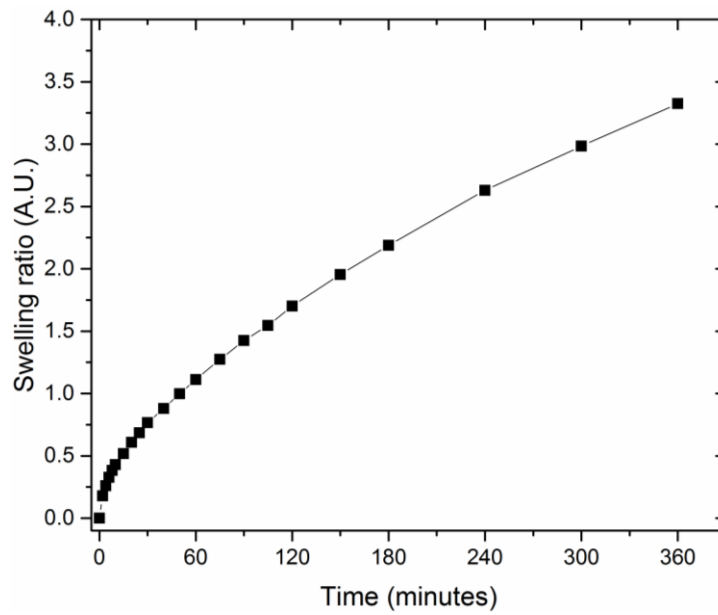


Figure 3-21: Initial 6 hour swelling kinetics of the HEA single network.

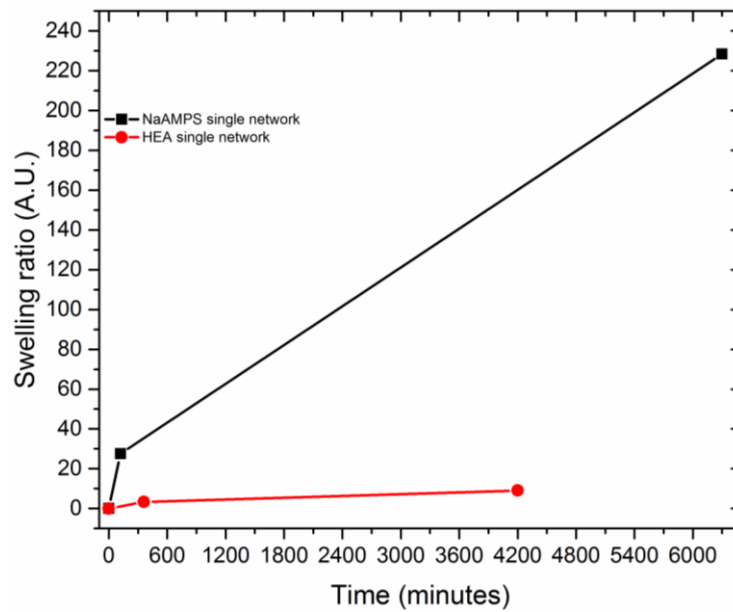


Figure 3-22: Comparison of swelling ratios for the two different single networks over time.

### 3.6.2 Hydroxyethyl methacrylate

Hydroxyethyl methacrylate was evaluated as an alternative to hydroxyethyl acrylate. As mentioned in Chapter 1, a common application for p(HEMA) hydrogels is for contact lenses. Unlike the hydrogels discussed previously, these are often produced in bulk rather than solution, therefore bulk polymerisation of these materials was also attempted. A thermally-initiated polymerisation was also investigated as an alternative to photopolymerisation.

When using the concentration of initiator reported by Al-Shohani (0.45 mmol, 0.6 mol%)<sup>16</sup> for the synthesis of p(HEMA) hydrogels *via* bulk polymerisation, it was observed that the glassy solid formed was full of bubbles, Figure 3-23. It was hypothesised that this was due to the concentration of AIBN being too high causing autoacceleration of the reaction, which is a common disadvantage of the bulk polymerisation process compared to solution polymerisation.

Autoacceleration, also known as the Trommsdorff-Norrish effect, is a process whereby the initiation of the radical initiator (in this case by a thermal input) is an exothermic process. This therefore increases the temperature further within the reaction and encourages more initiation that will keep repeating itself uncontrollably. This is a more common problem in bulk polymerisation than in solution polymerisation as the solvent helps to dissipate this additional heat therefore keeping the temperature better regulated. Furthermore, in this procedure, there is also no stirring involved, which leaves pockets of increased temperature within the mixture. The increase in viscosity as the reaction progresses is also a factor in the heat retention and therefore autoacceleration.

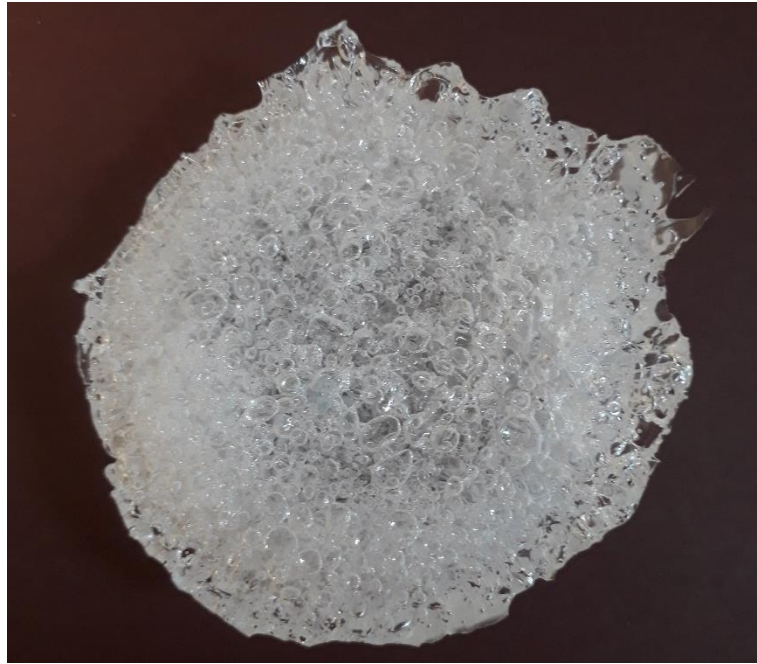


**Figure 3-23:** P(HEMA) hydrogel synthesised *via* thermally induced bulk polymerisation as per literature.

It was also noted that this was a concentration of initiator a factor of 10 greater than is used in the standard p(NaAMPS) hydrogel synthesis (0.065 mol%). Therefore the bulk polymerisation was modified to use the concentration of initiator previously used in the synthesis of p(NaAMPS) hydrogels, however, after 6 hours in the oven at 70 °C (standard procedure, Al-Shohani) instead of a colourless solid forming, as expected, it remained a liquid that appeared transparent but yellow, suggesting this initiator concentration is too low to lead to complete polymerisation. An intermediate concentration of 0.3 mol% was therefore investigated. This proved successful, producing a glassy, transparent, colourless solid with relatively few bubbles. Future investigations could probe the optimum initiator concentration for ideal pHEMA hydrogels.

When p(HEMA) hydrogels are synthesised using a starting aqueous solution (rather than the bulk discussed previously), opaque white hydrogels are formed compared to the bulk produced materials, however, these become colourless and transparent when the water is removed, Figure 3-24. This is due to differences in refractive index of p(HEMA) and water.



**Figure 3-24:** P(HEMA) hydrogel as synthesised from aqueous solution (left) and after being dried to the xerogel state (right).

Lower monomer concentration p(HEMA) hydrogels were also investigated. Compared to the initial 30 wt% hydrogels, these new 10 and 5 wt% hydrogels also formed white opaque hydrogels when thermally polymerised, however, unlike the 30 wt% materials, they appeared to undergo phase separation during the process as there was a significant volume of water remaining on top of the solid at the end of the reaction, Figure 3-25. The standard 3 ml aliquot of the 5 wt% p(HEMA) hydrogel is not displayed in Figure 3-25 as it did not form the anticipated opaque white hydrogel, suggesting that polymerisation did not occur, this is hypothesised to be due to the reaction mixture being too dilute. For the three reactions that did appear to occur, regardless of the volume of solution (and therefore volumes of monomer and water depending on concentration) they achieved an average of 70 % water content ( $\pm 4.58$  %).



**Figure 3-25:** standard 3 ml volume hydrogel, 10 wt% p(HEMA) (left), 10 wt% p(HEMA) hydrogel (middle) and 5 wt% p(HEMA) hydrogel (right) all with excess water on top.

This inability to retain relatively large amounts of water during synthesis is in agreement with the swelling kinetics for standard p(HEMA) hydrogels, where they

were found to not swell to anywhere near the same degree as p(NaAMPS) networks, Figure 3-26. Instead, p(HEMA) displays similar swelling kinetics to p(HEA); significantly slower than p(NaAMPS) with a significantly lower EWC.

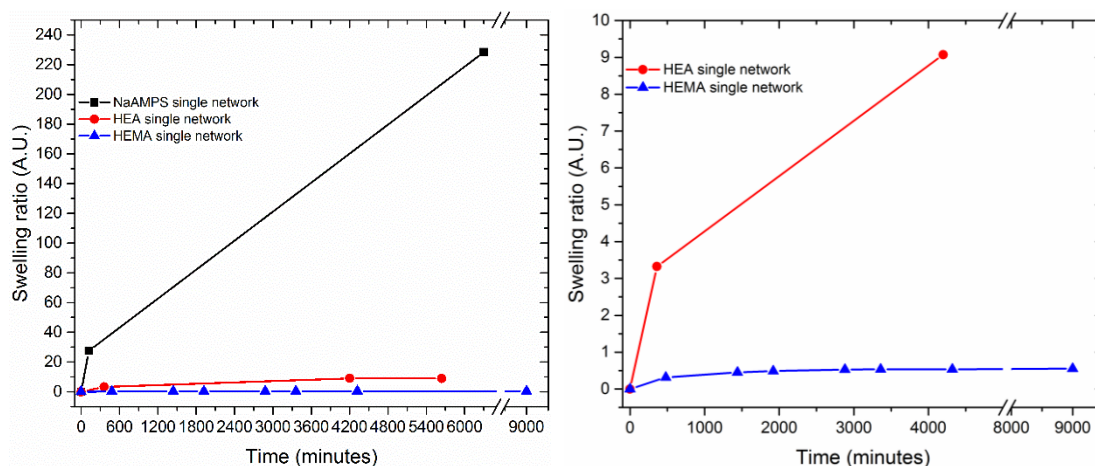


**Figure 3-26:** Comparison of swelling kinetics for p(NaAMPS), p(HEA) and p(HEMA) (left) and focusing on p(HEA) and p(HEMA) (right).

### 3.7 Double Networks

As discussed in Chapter 1, there can be great advantages to using a combination of networks as a double network in order to create a material that has mechanical and physical properties better than the sum of its parts. Therefore, double networks were synthesised in an attempt to increase the resilience of the hydrogel under more rigorous extraction procedures such as SFE (see Chapter 4). Given the complex nature of the  $^1\text{H}$  NMR procedure utilised for the analysis of single networks (Section 3.1), plus the difficulties of the dehydrating and swelling necessary in the synthesis of double networks especially with such a small surface area available in an NMR tube, attempts to apply this method to the *in situ* NMR tube procedure proved unsuccessful therefore only physical properties of the respective homo-networks alongside these double networks will be compared.

### 3.7.1 Physical-Covalent DNs

Combining a physically crosslinked network with a covalently crosslinked network can result in a DN material with significantly improved properties. Double networks consisting of sodium alginate plus either NaAMPS, AMPS or acrylamide (AAm) were investigated where sodium alginate is the physically crosslinked hydrogel through a divalent metal ion, Figure 3-27.

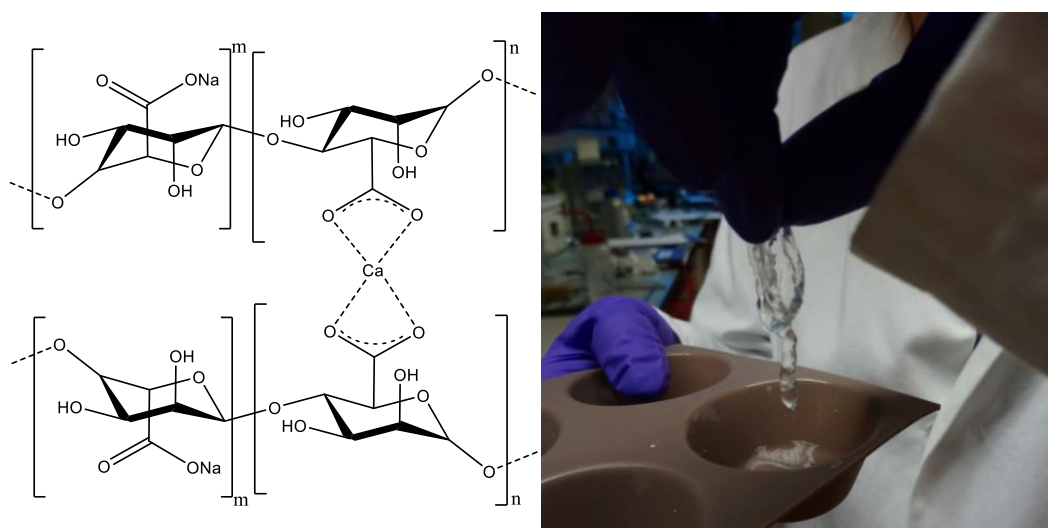


**Figure 3-27:** Sodium alginate gel physically crosslinked using Ca<sup>2+</sup> as the divalent metal ion.

#### 3.7.1.1 NaAMPS

The standard monomer concentration in the p(NaAMPS) hydrogels is ~30 wt%, however, this was found to not be compatible with the addition of sodium alginate. On the other hand, it was observed that a concentration of ~2.5 wt% was compatible.<sup>17</sup> In view of this the monomer concentration was reduced to ~2.5 wt% (initiator and crosslinker concentration also reduced accordingly), however, this did not produce a 'solid' gel when UV cured as is seen at 30 wt%. Thus, the challenge was to find a monomer concentration that was both compatible and produced a solid network.

The pre-polymerisation solution is a transparent solution when preparing the single network, however, the 15 and 20 wt% pre-mix solutions that contained sodium alginate were cloudy. It is suggested that this is the sodium alginate in suspension rather than dissolving into a fully homogenous transparent solution. These cloudy solutions were still polymerised as standard procedure with a degree of success. The 15 wt% solution produced a highly viscous polymer that remained a liquid rather than

solid gel matrix, Figure 3-28. The 20 wt% appeared to produce a solid hydrogel within seconds of UV exposure as standard, however, on closer inspection (touch) the gel was much more sticky and much more stretchy than the standard single network p(NaAMPS).



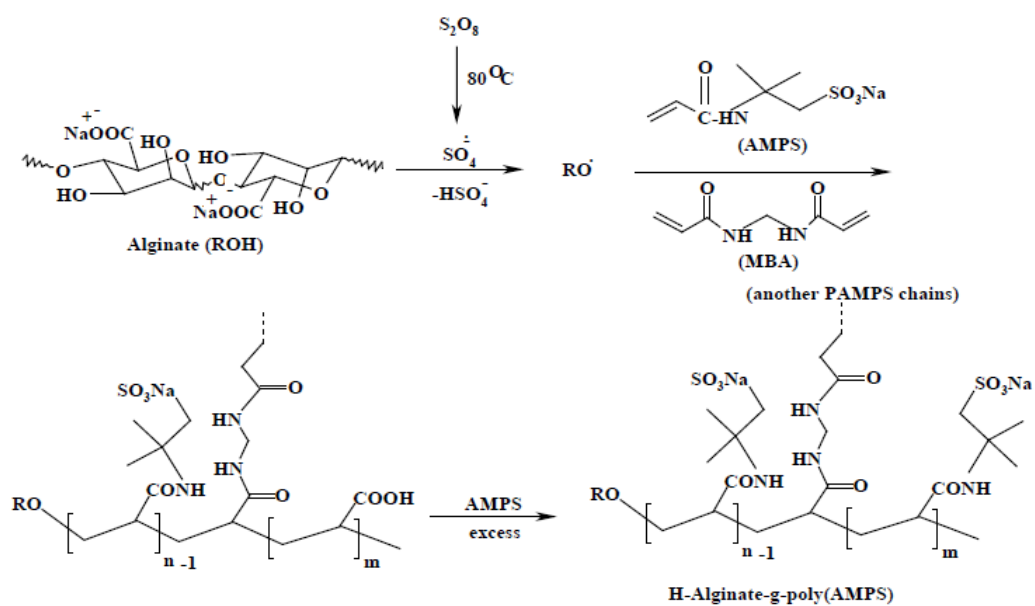
**Figure 3-28:** Viscous polymer formed at 15 wt% monomer.

Both the 15 and 20 wt% gels were then swollen in a  $\text{Ca}^{2+}$  solution in order to form the second physical network in the double network system.

Furthermore, attempts to adapt the acrylamide/alginate literature procedures by switching the acrylamide for NaAMPS also appeared unsuccessful. For example Yuk *et al.* use methylene bisacrylamide as crosslinker and ammonium persulfate with TEMED as initiator. It is hypothesised in this case that the lack of gelation could be because of an acid/base reaction between the TEMED used to catalyse these reactions with the sulfonate groups available on the NaAMPS monomer that are the key difference between the two monomers. However, this was not rectified by increasing the concentration of TEMED to above stoichiometric equivalents.

Sadeghi *et al.* suggest that a thermal polymerisation containing AMPS and alginate would result in grafting of the AMPS onto the alginate backbone, Scheme 3-1.<sup>17</sup>





**Scheme 3-1:** Sadeghi *et al* proposed mechanistic pathway for synthesis of alginate-AMPS hydrogel.<sup>17</sup> However, as this method involves stirring, the product was gel particulate rather than a single molded solid, Figure 3-29, therefore it is deemed not useful for the application. Further, the addition of a solution of  $\text{Ca}^{2+}$  showed no observable changes to the granules.



**Figure 3-29:** Proposed AMPS-graft-alginate reaction product.

### 3.7.1.2 Acrylamide

Acrylamide – sodium alginate hydrogels were synthesised as various literature protocols, such as that of Liu *et al.*<sup>18</sup>, Yang *et al.*<sup>19</sup> and Yuk *et al.*,<sup>20</sup> can be found that use this combination.

One procedure investigated was that of Yang *et al.*<sup>19</sup> This thermal polymerisation of acrylamide (with sodium alginate also in the solution) synthesised a solid gel, Figure 3-30, which did not visibly change upon the addition of calcium chloride solution (source of divalent ions for crosslinking of sodium alginate).



**Figure 3-30:** Acrylamide gel containing sodium alginate (left) and with added  $\text{Ca}^{2+}$  solution (right).

Cyclic compression testing to 5N indicated that both these materials have good recovery properties from this load, with the first cycle only marginally tougher in both cases, Figure 3-31. Although there was no observable change on addition of  $\text{CaCl}_2$  to the gel, a difference is evidenced during compression of the two materials. The IPN is significantly tougher, with a decrease in compression required to reach the 5N load set compared to pre second network crosslinking, as theory suggests. Whilst the maximum stress for the two materials is similar ( $0.0126 \text{ N mm}^{-2}$ , standard deviation  $0.00009 \text{ N mm}^{-2}$ , before  $\text{Ca}^{2+}$  addition and  $0.01029 \text{ N mm}^{-2}$ , standard deviation  $0.0001 \text{ N mm}^{-2}$ , after IPN formation), the maximum compression strain is very different. Before full IPN formation the average maximum strain of the material is 78.1 % (standard deviation 1.66 %) whereas once the physical-covalent IPN is fully formed maximum strain is 42.2 % (standard deviation 1.03 %).

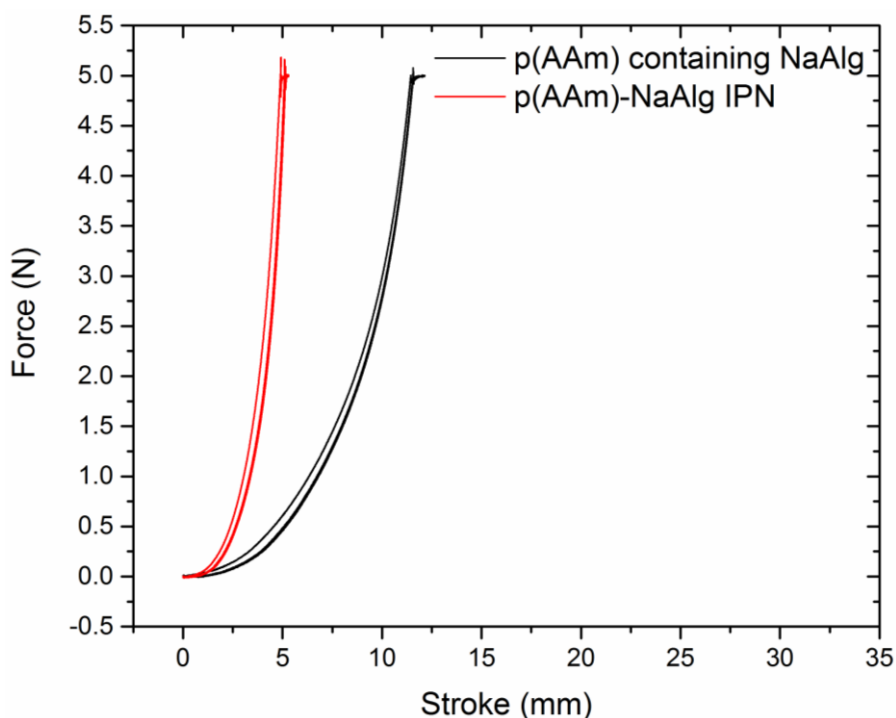


**Figure 3-31:** Overlaid compression cycles for the p(NaAlg) hydrogel before and after the second (physical) network was crosslinked.

## 3.7.2 Covalent-Covalent DNs

### 3.7.2.1 NaAMPS-HEA

Initially, a single network p(NaAMPS) hydrogel was synthesised *via* standard procedure before being dried in the 70 °C oven until a xerogel was formed. This was subsequently swollen in 3 ml of 30 wt% pre-polymerisation HEA solution for 24 hours in the absence of light before being UV cured as standard procedure. However, on exposure to the UV light, it became obvious that there was not enough monomer / volume of solution and that 24 hours may not have been long enough for complete diffusion throughout the network, Figure 3-32. However, this did highlight a strange result in that the double network is white and opaque whereas both individual single networks are colourless and transparent. This was attributed to clashing refractive indices.

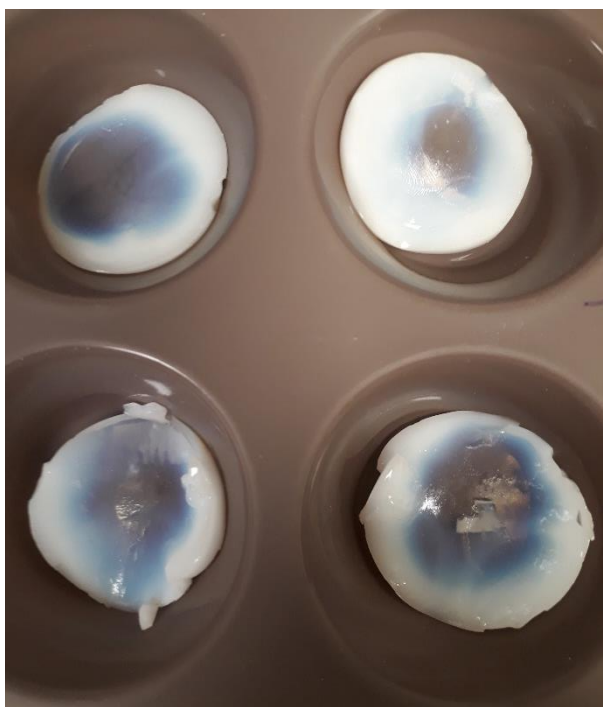


**Figure 3-32:** Initially synthesised double networks.

#### 3.7.2.2 NaAMPS-HEMA

The same IPN procedure was tested to combine p(NaAMPS) and p(HEMA) networks. Here 10 ml of a 10 wt% HEMA solution was absorbed by a pre-made p(NaAMPS) xerogel then thermally polymerised *via* standard procedure to create an evenly distributed 1:1 (by mass) sequential IPN. This was then dried in the vacuum oven to give an indication of second network content by gravimetry. Here a 1.2682 g p(NaAMPS) xerogel absorbed all of the 10 ml of 10 wt% HEMA solution (HEMA content: 1 ml, 1.073 g). After thermal polymerisation and dehydration (as described in Chapter 7) the total mass was 2.4594 g indicating the mass of the second network was 1.1908 g suggesting quantitative retention of the second monomer, which is an indication that it has polymerised as it is was not volatile enough to be removed in the vacuum oven.

The swelling kinetics of this double network xerogel were then investigated, Figure 3-33. Interestingly, this showed that the swelling ratio of the double network was in between those of the component single networks. The EWC for this double network was calculated = 98.8 %.

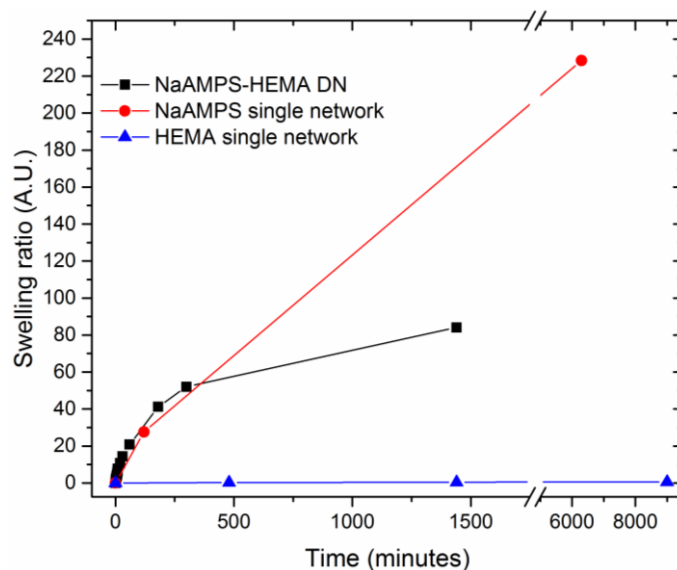
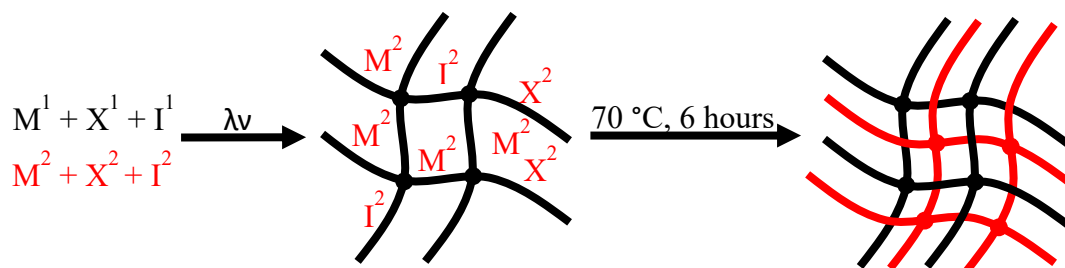


**Figure 3-33:** Overlaid swelling kinetics of NaAMPS and HEMA single networks as well as the combined double network.

Initially, the standard sequential synthetic procedure of IPN formation was tested. However, when HEMA was used as the first network, the swelling kinetics illustrate that it is incredibly difficult to achieve the absorption of the second network components. Conversely, while the NaAMPS hydrogel is highly absorbent, the challenge here was to find a suitable, water-soluble thermal initiator / attempting to absorb HEMA for a bulk polymerisation.

It was determined that a synthetic procedure somewhere between the sequential and simultaneous synthetic pathways may overcome these issues. All the components for the two networks would be included in the initial solution (as with the simultaneous method) but then there would be two sequential reactions carried out. The first would be the photopolymerisation to form the NaAMPS network followed by the thermal-polymerisation to form the p(HEMA) network. This would take advantage of the difficulties experienced when attempting to synthesise the p(HEMA) homo-network *via* photopolymerisation, discussed previously, Scheme 3-2.



**Scheme 3-2:** pseudo-simultaneous IPN synthesis; both reaction mixtures are present prior to first network polymerisation but the reactions are carried out in sequence. Where M denotes monomer, I = initiator, X = Crosslinker. Black is the first network and red is the second. Filled circles are crosslinking points.

It was attempted as a 30 wt% NaAMPS and 30 wt% HEMA starting solution; Figure 3-34 displays the product of the first (UV-induced) polymerisation where it can be seen that a solid hydrogel has not formed as is the case for the p(NaAMPS) single network but that a highly viscous 'gel' is observed.

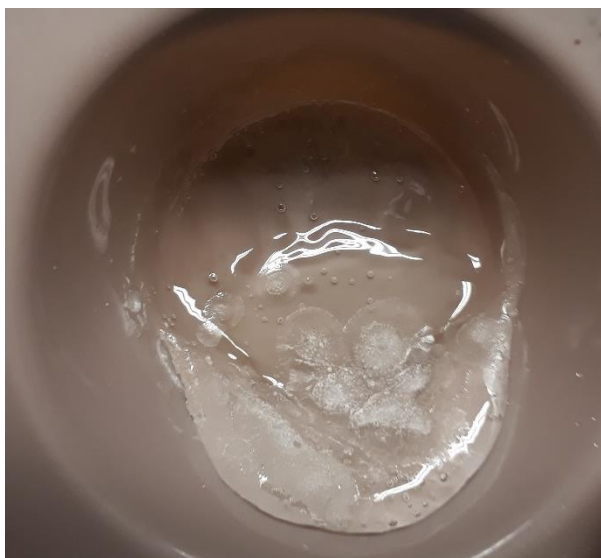


**Figure 3-34:** p(NaAMPS)-HEMA after first UV-induced polymerisation but before thermal (HEMA) polymerisation.

The swelling kinetics of this DN were then recorded, Figure 3-35. Where it is observed that, once again, the DN expresses swelling behaviour in between that of the equivalent single networks. This can again be treated as evidence that both monomers underwent their respective polymerisations, though further analysis would be needed in order to establish, how much, if any, co-polymerisation has taken place during this process.

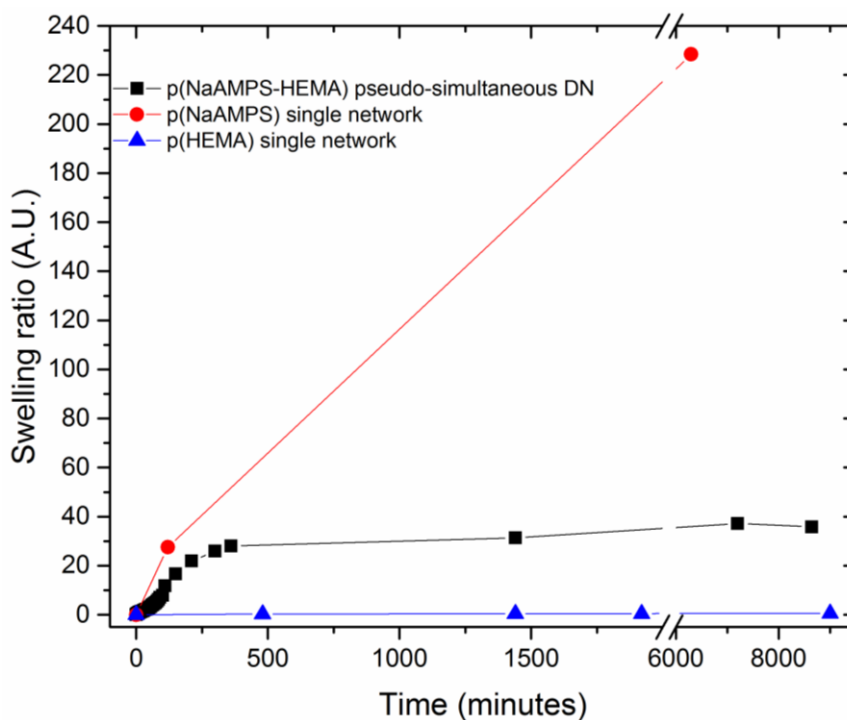


**Figure 3-35:** Swelling kinetics of the p(NaAMPS-HEMA) pseudo-simultaneous DN compared to the equivalent single networks.

Comparing the swelling kinetics of the sequential DN with the pseudo-simultaneous DN gives an insight into the effect of the polymerisation process on the physical properties, Figure 3-36. As illustrated, the sequential DN demonstrates faster swelling kinetics, achieving a greater swelling ratio. Future work would include the synthesis of a single network copolymer of AMPS-HEMA to compare the effect of the method of monomer combination in the materials.

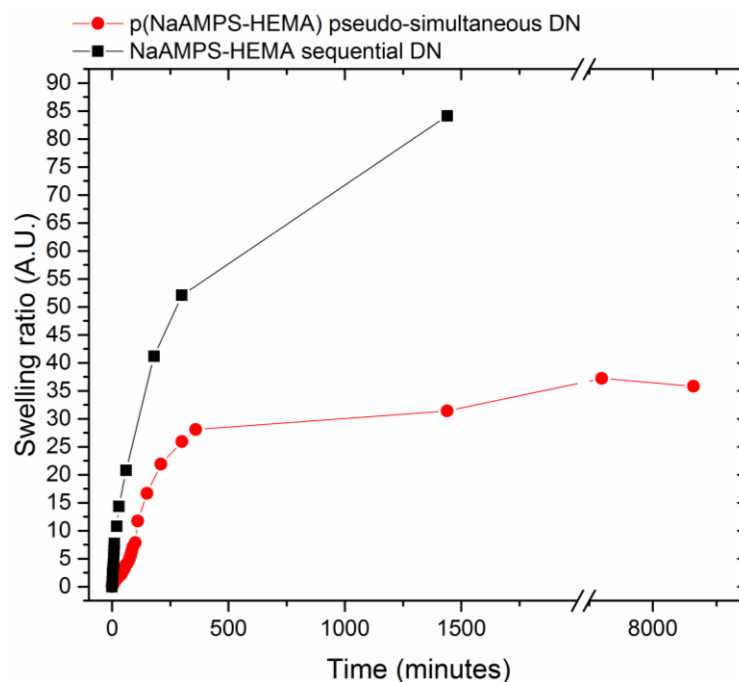


**Figure 3-36:** Comparison of the swelling kinetics of two NaAMPS-HEMA DN hydrogels synthesised via two different routes.

### 3.8 Conclusions

A standard synthetic procedure for the synthesis of p(NaAMPS) hydrogels was initially adopted. In order to improve the process for industrial scale up and processing, various characteristics of the hydrogel were investigated including the polymerisation time, light source, initiator concentration and crosslinker concentration. It was found that the initiator concentration was already optimised but that varying the concentration of crosslinker significantly altered the physical properties. It was also suggested that using a double network could significantly improve the physical properties of the hydrogel. To this end, a physical-covalent IPN and a covalent-covalent IPN have been investigated where monomer compatibility issues made the physical-covalent system unusable but the covalent-covalent system has shown positive initial results.

For simplicity and proof of concept the device investigated in subsequent chapters is a standard single network p(NaAMPS) hydrogel, unless otherwise stated.



### 3.9 References

- 1 S. Lowe, PhDthesis, University of Warwick, 2017.
- 2 S. J. Beckers, S. Parkinson, E. Wheeldon and D. K. Smith, *Chem. Commun.*, 2019, **55**, 1947–1950.
- 3 C. Zhang and A. J. Easteal, *J. Appl. Polym. Sci.*, 2007, **104**, 1723–1731.
- 4 S. Çavuş, *J. Polym. Sci. Part B Polym. Phys.*, 2010, **48**, 2497–2508.
- 5 O. Hazer, C. Soykan and S. Kartal, *J. Macromol. Sci. Part A*, 2008, **45**, 45–51.
- 6 Y. A. Aggour, *Polym. Degrad. Stab.*, 1994, **45**, 273–276.
- 7 A. Anastasaki, V. Nikolaou, Q. Zhang, J. Burns, S. R. Samanta, C. Waldron, A. J. Haddleton, R. Mchale, D. J. Fox, V. Percec, P. Wilson and D. M. Haddleton, *J. Am. Chem. Soc.*, 2014, **136**, 1141–1149.
- 8 UVP Ultraviolet Crosslinkers, <https://www.uvp.com/crosslinker.html>, (accessed October 2016).
- 9 S. M. Paterson, Y. S. Casadio, D. H. Brown, J. A. Shaw, T. V. Chirila and M. V. Baker, *J. Appl. Polym. Sci.*, 2013, **127**, 4296–4304.
- 10 G. W. Scherer, in *Encyclopedia of Materials: Science and Technology*, eds. K. H. Jürgen Buschow, R. W. Cahn, M. C. Flemings, B. Ilshner, E. J. Kramer, S. Mahajan and P. Veyssi re, Elsevier, 2001, pp. 9797–9799.
- 11 K. Nalampang, R. Panjakha, R. Molloy and B. J. Tighe, *J. Biomater. Sci. Polym. Ed.*, 2013, **24**, 1291–1304.
- 12 D. L. Holmes and N. C. Stellwagen, *Electrophoresis*, 1991, **12**, 612–619.
- 13 N. Efron and N. Brennan, *Optician*, 1987, **194**, 29–41.
- 14 O. Okay and S. Durmaz, *Polymer (Guildf.)*, 2002, **43**, 1215–1221.
- 15 J. Rault, A. Lucas, R. Neffati and M. Monleon Pradas, *Macromolecules*, 1997, **30**, 7866–7873.
- 16 A. D. H. Al-shohani, PhD thesis, University College London, 2016.
- 17 M. Sadeghi, F. Shafiei, E. Mohammadinasab, L. Mansouri and H. Shasavar, *Biosci. Biotechnol. Res. Asia*, 2014, **11**, 111–114.
- 18 J. Liu, Y. Pang, S. Zhang, C. Cleveland, X. Yin, L. Booth, J. Lin, Y. L. Lee, H. Mazdiyasi, S. Saxton, A. R. Kirtane, T. Von Erlach, J. Rogner, R. Langer and G. Traverso, *Nat. Commun.*, 2017, **8**, 1–9.
- 19 C. H. Yang, M. X. Wang, H. Haider, J. H. Yang, J. Y. Sun, Y. M. Chen, J. Zhou and Z. Suo, *ACS Appl. Mater. Interfaces*, 2013, **5**, 10418–10422.
- 20 H. Yuk, T. Zhang, S. Lin, G. A. Parada and X. Zhao, *Nat. Mater.*, 2016, **15**, 190–196.

## 4. Optimising Swelling, Storage and Recovery

Hydrogels are materials that can be used as devices that will absorb sweat and the malodorous compounds within. This chapter details investigations into optimising all the stages of this process, leading to the most efficient device possible. This will also allow for comparison between the proposed new device and current Unilever methods.

### 4.1 Current Unilever Methods

The current industrial standard test method for antiperspirant / deodorant products involves test subjects wearing the test product under controlled conditions (regulations around eating and drinking, underarms pre-washed and product applied for them). Depending on the specific test, they are either then sent to go about their day as normal or are subjected to forced conditions of increased temperature / humidity in the 'hot room' to mimic climates from around the world. These subjects then have their armpits sniffed by 'experts' and marked out of five based on the strength of the malodour present, Figure 4-1. This is very subjective although the 'experts' are chosen for their sensitivity to smell and there is always a panel of testers with an average value taken. However, it is only a semi-quantitative method, which is very subjective, that gives little insight into the efficacy of a product nor to the identity of the problem compounds that may be present.

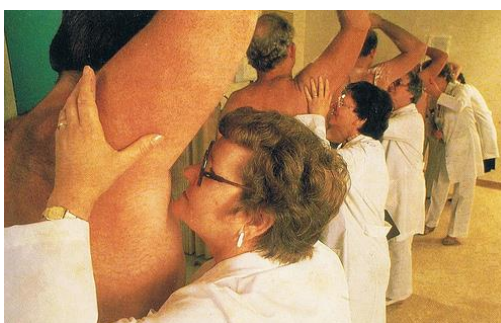


**Figure 4-1:** An insight into current, industrial olfactory assessment.

### 4.1.1 Gravimetry

The only other option currently available is for removable textile patches to be fixed into the armpits of t-shirts which are then worn by the test subjects before they are removed and weighed for the mass of perspiration produced. These studies can vary depending on the advertising claim being evaluated, but typically this would be for a 'normal' 24 hours, or after a period of exercise / in the 'hot room' (temperature and humidity controlled, usually both at elevated conditions, to mimic international environments). This gives limited information which may be of use when testing an antiperspirant product but does not help with malodour information as there is not necessarily a correlation between high volume of sweat and a high level of malodour.

Neither of these methods give information about which chemical compounds need focusing on to tackle a particular malodour.

## 4.2 Model Sweat Uptake Kinetics

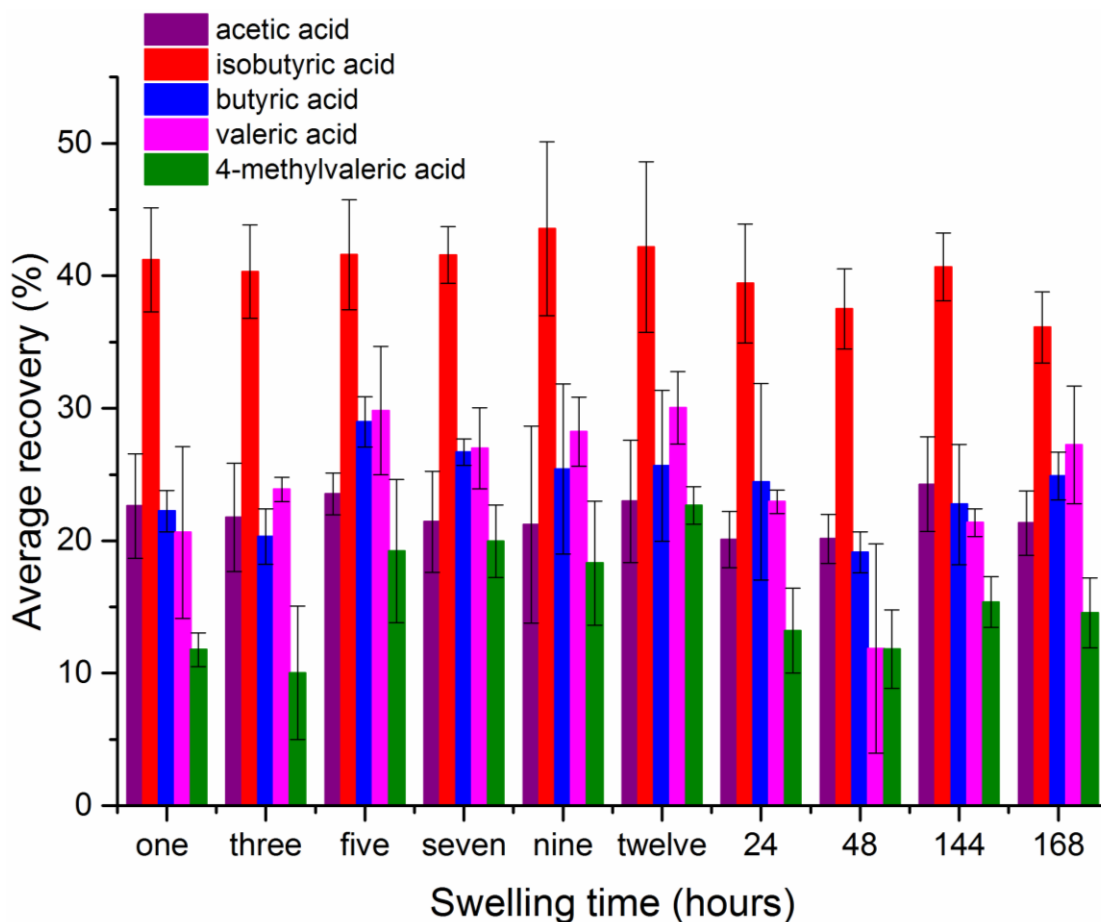
The uptake kinetics study was carried out to determine the optimum time a dosed hydrogel should be left to absorb 'sweat' before recovery is attempted, in order to optimise recovery (this would also determine appropriate time periods it should be worn in 'real' studies). Each hydrogel was placed in a jar with 0.5 ml of model sweat and sealed for the appropriate length of time. The mass of model sweat (0.55 g) was chosen based on the mass of sweat observed in studies previously. It is suggested that a 'heavy sweater' can produce 2 g of sweat per axilla per time period. For simplicity, extraction was carried out *via* a basic solvent extraction process (24 hours in 3 ml of solvent) in order to determine uptake of malodorous compounds *via* GC. This process is optimised in Section 4.4.

Table 4-1 shows the average percentage uptake, and associated standard deviation across all time points measured by gravimetry. The data indicate that uptake was quantitative at all time points, with the majority being absorbed in less than an hour and all time points thereafter being within a standard deviation of each other.

**Table 4-1:** Average uptake percentage and associated standard deviation ( $\sigma$ ) over absorption time where  $n = 3$ .

Absorption time (hours)	Uptake (%)	$\sigma$
1	97.3	2.03
3	98.0	1.35
5	97.8	1.67
7	99.3	1.70
9	99.7	1.42
12	98.7	4.65
24	97.7	0.808
48	98.3	1.70
144	97.8	1.67
168	>99.9	3.27

Figure 4-2 illustrates VFA recovery percentage from these model sweat absorption hydrogel kinetics. It demonstrates that there is no significant difference in the percentage recovery across all the time points for all five VFAs studied. Considering all the VFAs are in the stock solution at approximately the same concentration, the variability in the recovery requires investigation.



**Figure 4-2:** Comparison of the average recovery of VFAs from dosed hydrogels using different swelling lengths of swelling time.

The outcome of this investigation is that the standard absorption procedure of 0.5 ml model sweat solution added to a hydrogel in a 60 ml (4 cm diameter) jar and left sealed for 24 hours prior to further experimentation will be adopted for all further studies, unless stated otherwise.

### 4.3 Swelling monitored by Contact angle

Contact angle measurements were used as a measure of the speed of absorption – the faster the contact angle decreased, the quicker the drop of water is absorbed.<sup>1</sup>

Tecophilic™ is a range of polyurethanes, commercially available, produced by Lubrizol.<sup>2</sup> It reportedly absorbs water, like a hydrogel, and therefore was deemed to be an interesting comparison product to the hydrogels synthesised in this work.

The data in Table 4-2 suggests that, initially, the Tecophilic™ product is the most hydrophilic as it has the lowest contact angle. These data are converted to

percentage of the initial contact angle for each material tested, which is displayed in Figure 4-3, as there is a difference in the initial contact angle due to the relative hydrophilicity of the surfaces. From both these representations of the data, the favourability of the p(NaAMPS) hydrogel for this application is obvious in the sharp decrease in the contact angle between the first two time points recorded, suggesting absorption within minutes. The initial steep drop may be due to wetting of the surface before the more shallow decrease indicating absorption as suggested by Modaressi and Garnier.<sup>1</sup> Note, the difficulty in collecting data every minute for p(NaAMPS) as the contact angle continually changed a noticeable amount hence, data was recorded every two minutes. As Figure 4-4 illuminates, the initial water droplet is clearly defined but after ~10 minutes the software fails to make a distinction between the droplet itself and the hydrogel surface and therefore cannot calculate a contact angle.

**Table 4-2:** Average contact angles of a water droplet, on the three materials tested, over time.

Time (minutes)	Average Contact Angle (°)		
	Tecophilic™	P(AMPS) hydrogel	Polyester Patch
0	71.4		124.2
1		105.2	150.2
2	67.3		142.1
3	66.4	37.1	123.4
4	65.5		121.0
5	63.5	33.7	120.6
6	64.0		124.0
7	62.3	29.3	115.9
8	62.6		112.9
9	62.4		116.1
10	60.5	24.6	113.3

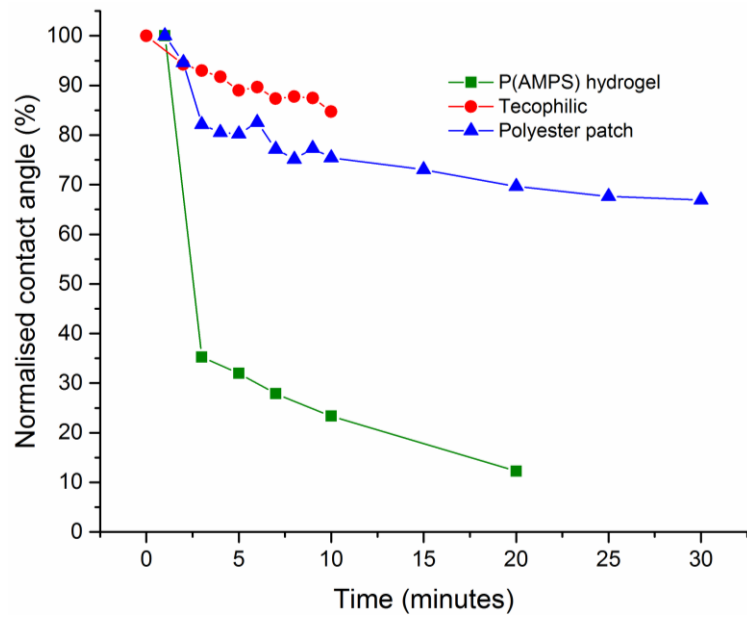


**Figure 4-3:** Average contact angle of the three materials, normalised to their own starting contact angle.

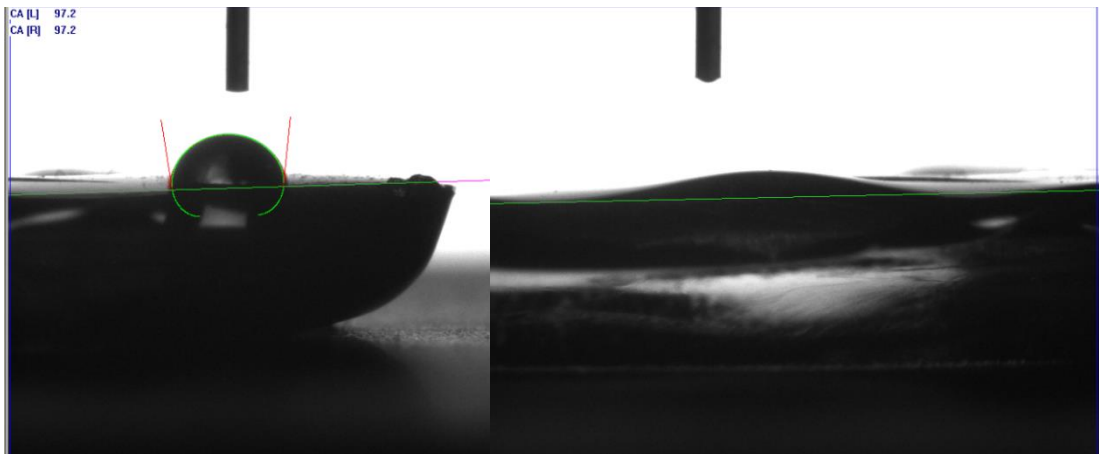


**Figure 4-4:** Contact angle of p(NaAMPS) at two different time points; 2 minutes (left) and 10 minutes (right).

## 4.4 Solvent Extraction

Solvent extractions have long been a traditional procedure employed in small molecule analysis for a variety of applications.<sup>3</sup> This includes everything from a simple, minimal solvent extraction to a Soxhlet extraction and as such these will all be examined.

### 4.4.1 Recovery Optimisation – simple solvent extraction

Standard solvent recovery uses ethyl acetate as solvent, it was chosen based on the fact that it is a volatile solvent convenient for GC analysis, immiscible with water and is not absorbed by the hydrogel. Garcia-Villalba *et al.* also found ethyl acetate to be the best solvent in a similar application; the extraction of VFAs from aqueous supernatants of faecal samples, when comparing it to diethyl ether and dichloromethane.<sup>4</sup>

In order to optimise the recovery method, different surface areas of hydrogels were investigated alongside different extraction time lengths and methods within a basic minimal solvent extraction procedure. No difference in recovery was observed between the whole and cut up hydrogels over 24 hours, however, when compared to the shorter time period of one hour, both with and without sonication, the cut up hydrogel showed a significantly better recovery. This is most likely due to the increased surface area. Furthermore, it suggests that the 24 hour samples showed no difference as this was long enough for the recovery from the whole hydrogel to reach the same concentration as the more efficient cut up hydrogel. It can also be seen in Figure 4-5 that sonication improves recovery when comparing the 1 hour samples for both the whole and cut up hydrogels. Notably, in Figure 4-5 it is clearly illustrated that significantly less acetic acid is recovered compared to the other VFAs regardless of recovery method employed although there is less variability in its recovery across the different methods. This is thought to be because acetic acid is the shortest chain VFA used here and therefore the most volatile, although it has not been proven that it is not because it is more difficult to remove from the hydrogel due to it having the highest charge density / polarity as the smallest acid.



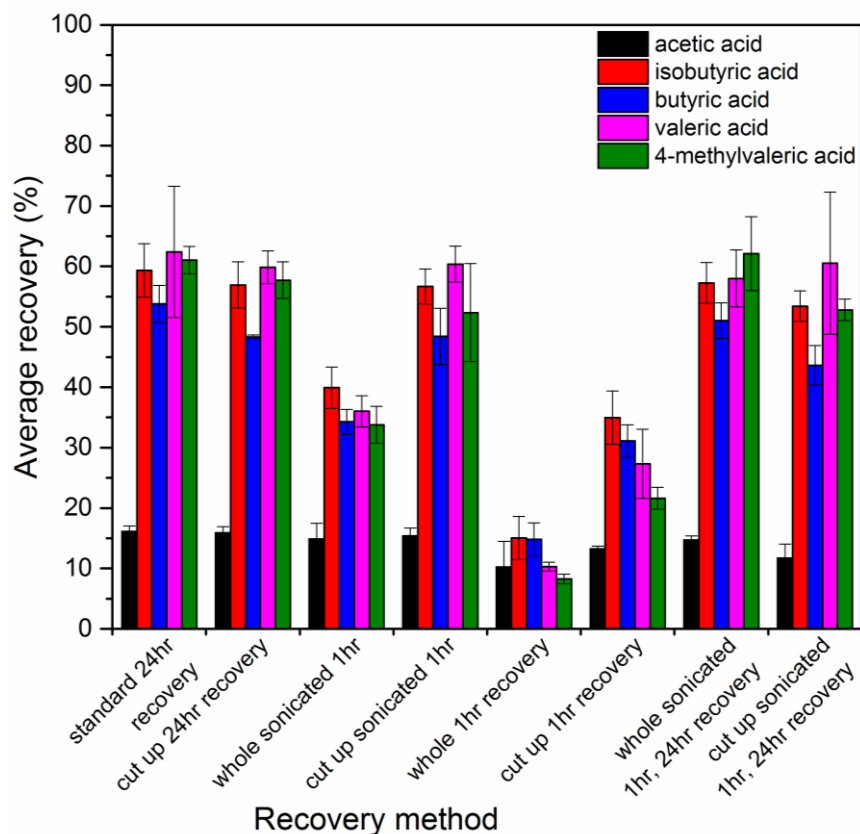


**Figure 4-5:** Analytical recovery data from the different solvent extractions for comparison.

The data are also in agreement with literature which suggests that most solvent extraction methods are 30 – 80 % efficient.<sup>5</sup> This was further investigated by determining the partition coefficient of the utilised volatile compounds between water and ethyl acetate, Table 4-3. This illustrated that there is a 65-77 % extraction efficiency for all 12 compounds tested, from the aqueous formulation into the chosen extraction solvent, ethyl acetate. With the exception of the acetic acid recovery, the partition recovery data indicates that the hydrogel matrix does not inhibit recovery from the aqueous solvent within.

**Table 4-3:** Percentage recovery from liquid-liquid extraction based on GC peak areas.

<b>Volatile Compound</b>	<b>Recovery (%)</b>
solvent (Ethyl Acetate)	105
Acetic acid	73.1
Propionic acid	71.3
Trans-2-nonenal	66.2
Isobutyric acid	72.2
Butyric acid	73
2-methylbutyric acid	74.2
Isovaleric acid	76
Valeric acid	76.7
4-methylvaleric acid	72.5
Hexanoic acid	69.7
3-mercapto-1-hexanol	70.5
4-ethyloctanoic acid	76.5

In addition, Figure 4-6 illustrates the recovery rates when comparing increased recovery time. When comparing the 24 hour and 7 day (168 hours), it can be seen that there is a slight increase in the recovery percentage of all five acids tested, with the increased duration although it is not a significant one when accounting for the error bars. This is also an increase on the middle data set on the graph which is the same total time but split the opposite way; *i.e.* the week one, 24 hour samples has been left absorbing for 168 hours (7 days) then extracted for 24 hours (a total of 192 hours) whereas the week zero, 7 day recovery samples have been left absorbing for only 24 hours but extracting for 168 hours (also a total of 92 hours) to determine whether it is the length of time or the stage in the process that this time is utilised that is the most important factor. As anticipated, Figure 4-6 clearly evidences that it is the extended time being part of the extraction procedure that is beneficial rather than just the length of time itself as the longer absorption with shorter extraction combination gave the worst recovery of the three.

Furthermore, the 24 + 24 is more reproducible than the other two experiments as indicated by the shorter error bars in Figure 4-6.

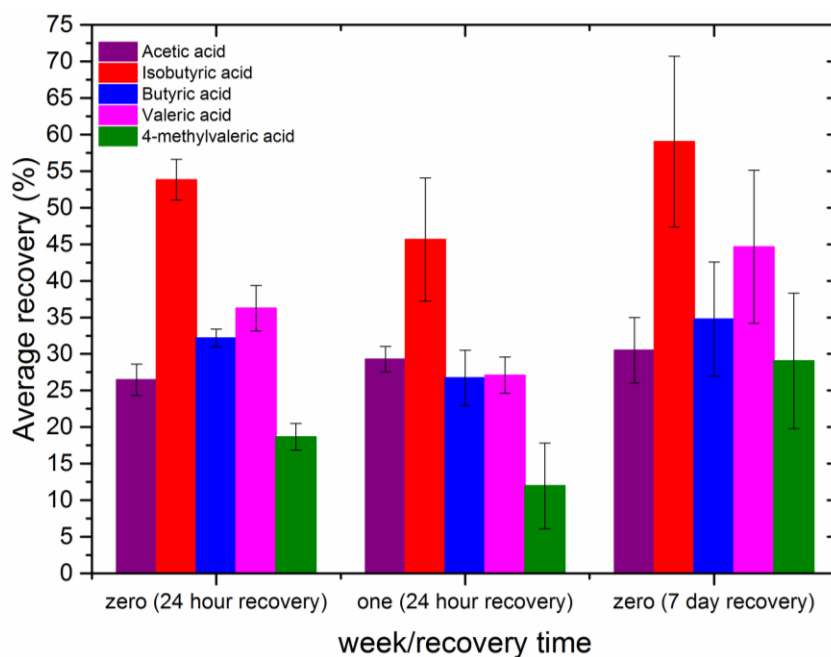


Figure 4-6: Analytical recovery data from different length of extractions.

## 4.5 Soxhlet

This is a standard chemistry technique with respect to solvent extractions. A Soxhlet extraction was carried out so that a recovery comparison between the polyester patches, currently employed for scent olfactory analysis, and a hydrogel could be made. This is because a polyester patch will absorb the extraction solvent added if a simple solvent extraction with minimal solvent (standard procedure with a hydrogel) is attempted.

After reviewing the literature, several different extractions using various solvents were reported as part of the process of analysing VFAs. Examples include diethyl ether<sup>6-9</sup> and binary solvent systems,<sup>10</sup> most notably chloroform/ethanol mix as developed by Folch *et al.*<sup>11</sup> and Bligh & Dyer.<sup>12</sup> The hydrocarbon solvents are the traditional choice with the mixed solvent procedure developed later as a preference. Notably, these extractions are from fabrics such as gauze<sup>13</sup> or socks<sup>6,9</sup> or more directly from biological samples.<sup>7,8,10-12,14,15</sup> Literature for extraction of hydrogels focuses on removal of any possible monomer using aqueous/polar solvents.<sup>16</sup> However, as discussed previously, the interaction between the hydrogel and chosen solvent system had to be considered, hence the traditional, non-polar diethyl ether was investigated.

As can be seen in Figure 4-7, a mixture of volatiles was recovered *via* this method, after rotary evaporation to concentrate the extracts, from both the hydrogel and the polyester patch. The overlaid spectra, and more obviously, the calculated results in Figure 4-8, indicate a very similar level of extraction from both the hydrogel and the textile.

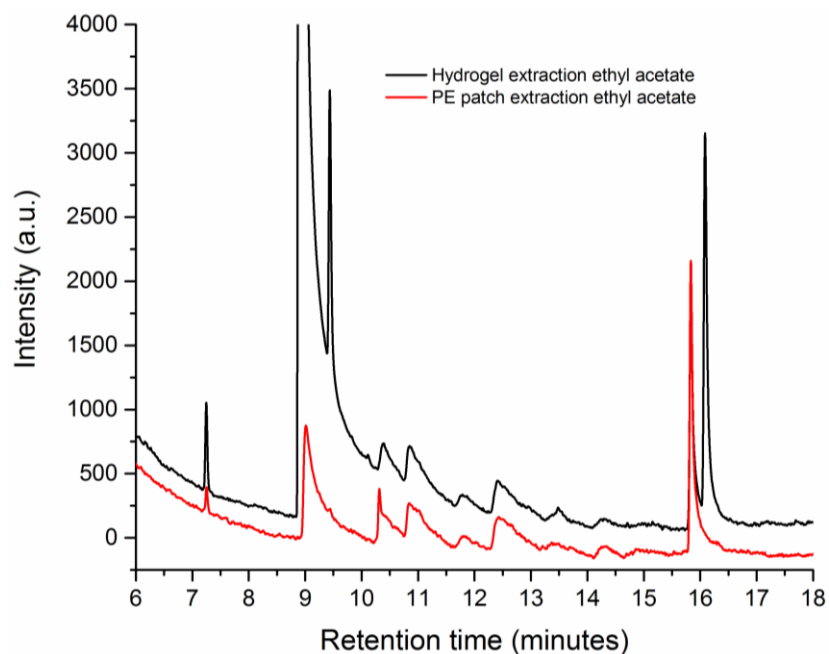


**Figure 4-7:** Overlaid GC chromatograms from the Soxhlet extraction of a hydrogel and a polyester patch.

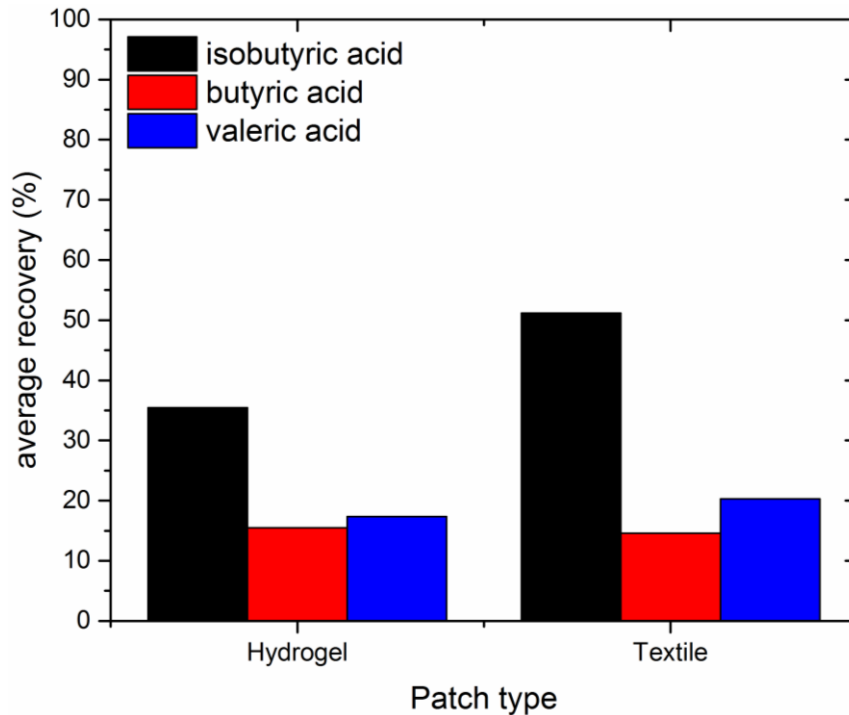


**Figure 4-8:** Concentration of three of the malodour acids as percentage of the dosed concentration.

A larger study of this method would need to be carried out to validate the reproducibility and reliability of this more complex process. Although Soxhlet extraction is a relatively short extraction method compared to simple solvent extraction (~5 hours compared to 24 hours), it is more labour intensive and, due to it being a more complicated process involving heat and rotary evaporation, there is a much greater risk of losing analytes throughout. It also uses an increased volume of solvent, therefore is a less environmentally friendly and cost effective technique.

Interestingly, Figure 4-9 illustrates the stark difference in the extraction efficiency of the two different solvent extractions of interest for the hydrogel. In the case of all five acids calculated, the Soxhlet performs significantly worse than the 24 hours, no input, minimal solvent extraction procedure. This is theorised to be due to the challenges suggested above.

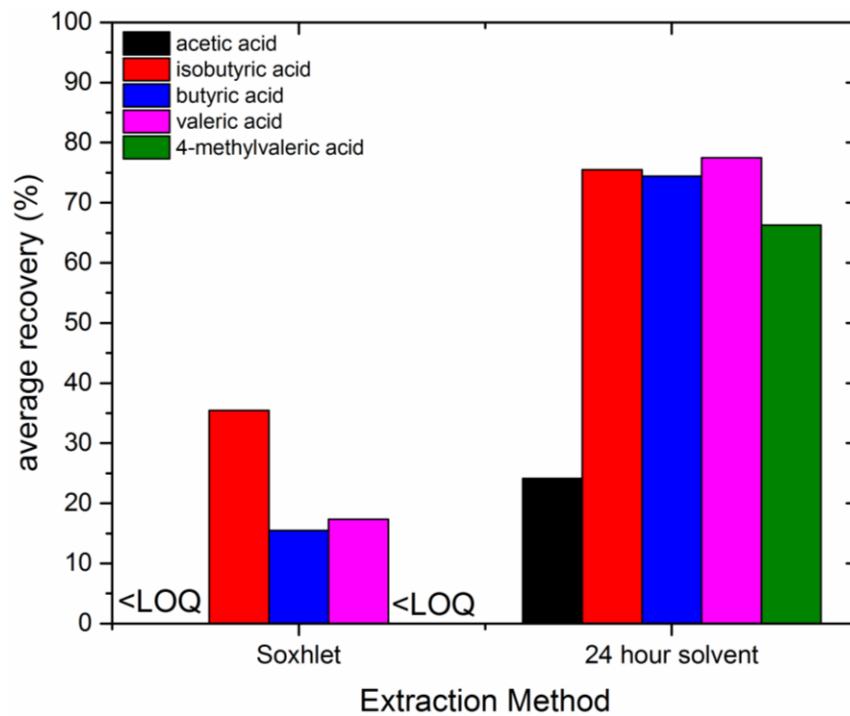


**Figure 4-9:** Comparison of simple solvent recovery and soxhlet extraction of a hydrogel.

Schafer suggested quantitative lipid extractions are often not possible *via* Soxhlet extraction due to solvents' poor ability to displace polar analytes from stable matrices.<sup>7</sup> The combination of all these negative factors mean that this is not a favourable extraction method for this application.

## 4.6 Supercritical Fluid Extraction

Supercritical fluid extraction (SFE) is a greener technique than the normal solvent-based techniques already discussed due to its minimisation of solvent used. Although this has potential as an extraction method that would allow for comparison between collection matrices, the hydrogel extraction *via* this method is still in its infancy and undergoing method development and optimisation / validation at Suprex (a spin-out company of Prof. Marriot at Bangor University). Investigations into using this technique are still ongoing with Figure 4-10 illustrating some initial chromatograms from preliminary extractions; top is a 20 minute supercritical fluid extraction using acetonitrile and CO<sub>2</sub>, of a dosed hydrogel and bottom a dosed hydrogel extracted at 90 bar and 35 °C where the volatile fatty acid peaks are between 0 and 7.5 minutes and a benzoic acid internal standard at 12 minutes. This indicates there is potential in this method.

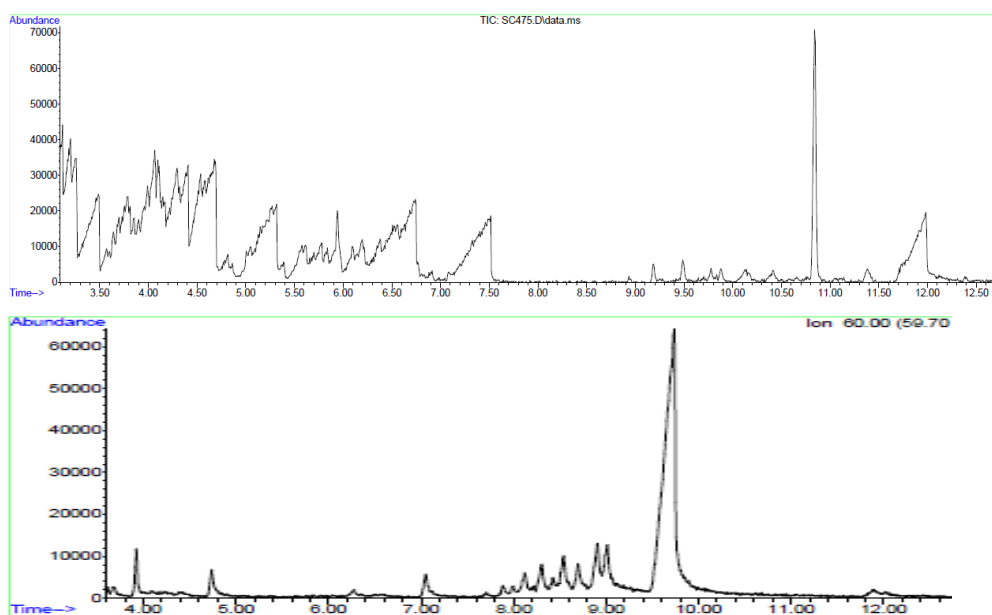


**Figure 4-10:** Example total ion count (TIC) chromatograms, supplied by Suprex, from the method development of SFE of hydrogels.

#### 4.6.1 Optimisation of conditions

The temperature, pressure and solvent systems were experimented with in order to improve extraction. As shown in Figure 4-11, the main observation is the damage caused to the hydrogel by SFE not seen in previous extraction methods. It was noted that the worst SFE method was when acetonitrile was used as a co-solvent with  $\text{sCO}_2$  so it was deemed that this would be added after the extraction chamber, before analysis.

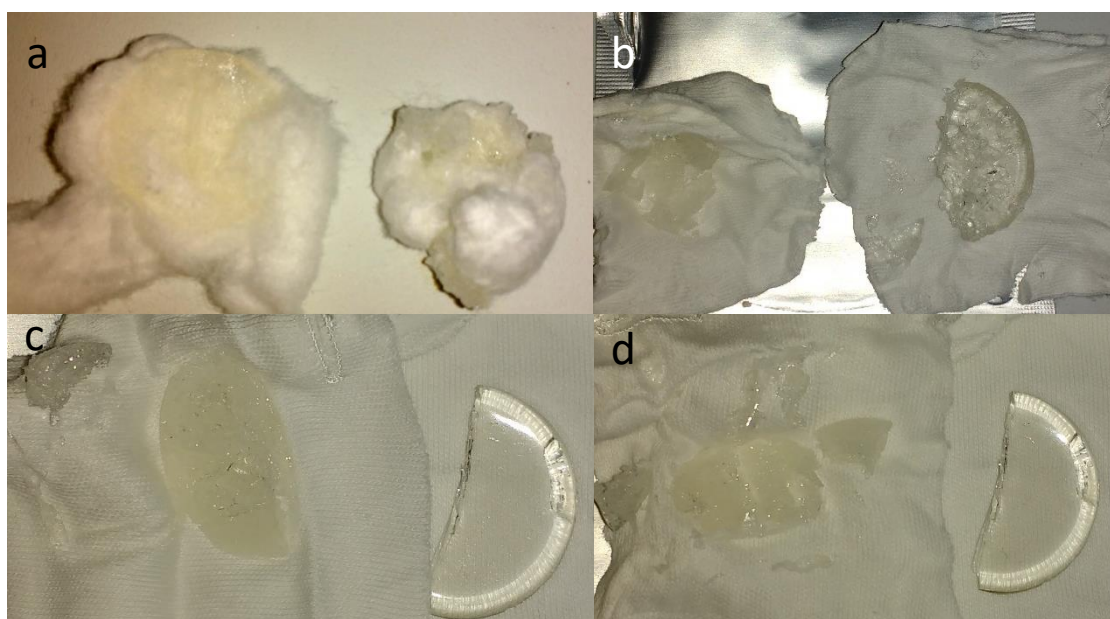


**Figure 4-11:** Hydrogels after various SFE procedures; 0.2 mol% Hydrogel after 20 min at 90 bar/35 °C (left) And after 20 min at 300 bar/50 °C (right) (a), 1.0 mol% X-linker Hydrogel  $\text{CO}_2$  only, 300 bar (b), 2.0 mol% X-linker Hydrogel  $\text{CO}_2$  only, 300 bar (c), and 2.0 mol% X-linker Hydrogel  $\text{CO}_2$  and acetonitrile, 300 bar (d). All hydrogels are p(NaAMPS) where the mol% refers to the concentration of crosslinker (PEGDA).

Other non-solvent extraction methods for GC analysis exist, for example thermal desorption and gas analysis. These are discussed in Chapter 2, but not examined here, as we did not have the technology available.



## 4.7 Stability Studies

The end goal of this project is to create a device that not only can absorb sweat then release it with a stimuli / extraction technique but also that may be stored, with minimal effort until a suitable time for analysis. Testing is often carried out in UK / EU, but ideally, sampling would take place all over the world to assess efficacy under different environmental conditions. Currently, collected samples are vacuum packed and store at -80 °C making it difficult for testing / sampling to be carried out anywhere apart from at the testing facility as shipping under such conditions is impractical and expensive. This means that limited data are collected for product use in extreme climates.

### 4.7.1 One month Room Temperature Incubation

Preliminary data illustrated an increase in recovery between week zero and week one for all five VFAs which highlighted the need for the swelling equilibrium study. Furthermore, week four (the final week) had a percentage concentration recovered that was at least the same as week zero indicating a stable capture device over time (Figure 4-12). Although notably, for three of the VFAs, there was a decrease week-on-week from week one to week four, however, for butyric acid and acetic acid there was an increase in recovery in the final week. Furthermore, valeric acid shows an oscillating pattern across the weeks. Moreover, Table 4-4 indicates that the mass loss percentage was insignificantly different across all four weeks tested.

**Table 4-4:** Mass data for preliminary stability test.

Time (weeks)	Hydrogel Mass (g)			Change in Mass over storage time (%)
	Before absorption	After uptake	After time	
0	3.279	3.667	N/A	N/A
1	3.340	3.860	3.850	-0.257
2	3.329	3.852	3.842	-0.262
3	3.337	3.840	3.831	-0.237
4	3.253	3.752	3.743	-0.235

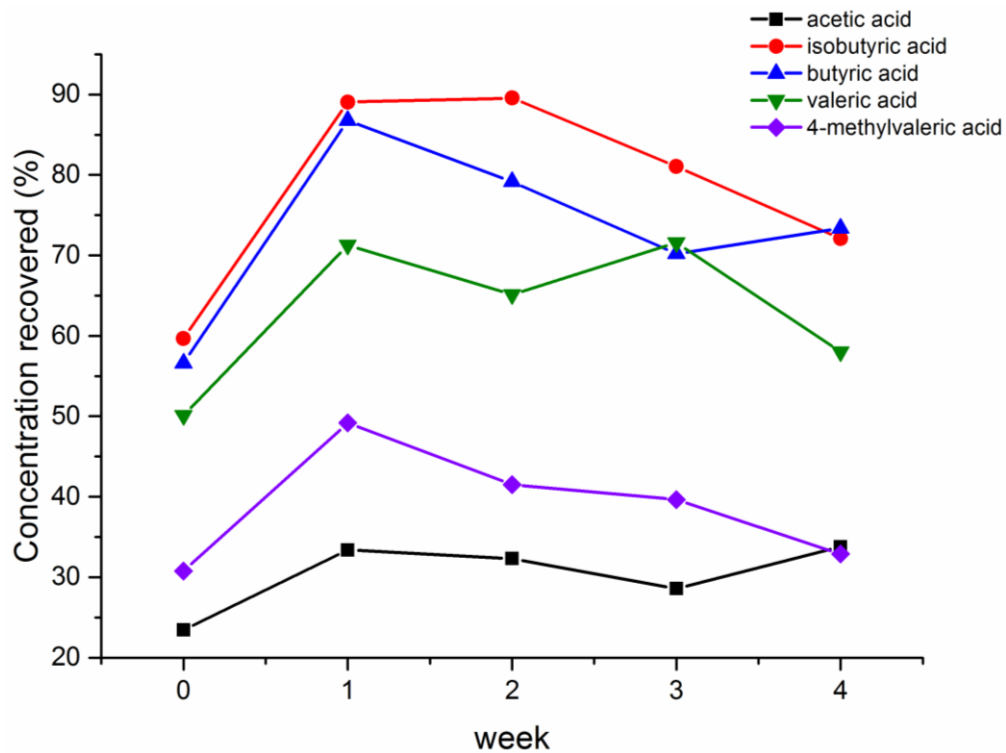


**Figure 4-12:** Calculated percentage concentration recovered of the five VFAs with calibration curves over a four week stability study at 25 °C.

The week zero sample should be comparable to the standard 24 hour recovery and the 24 hour swelling time samples from the previous studies. For three of the analysed VFAs (isobutyric acid, butyric acid and valeric acid), the measured recovery amounts were comparable to those obtained during the standard 24 hour recovery. For the remaining two VFAs (acetic acid and 4-methyl valeric acid) the measured recovery amounts were comparable to those obtained by the 24 hour swelling sample. The inconsistency of these measurements (between all three studies) highlights the need for optimisation of the swelling and recovery method.

## **4.8 Conclusion**

In conclusion, the research in this chapter has demonstrated that a hydrogel can absorb a relevant volume of 'sweat' in less than one hour and this can also be maintained over 24 hours, therefore hydrogels would work for any study length to be tested (including 24 hour efficacy claims). It was then illustrated that a simple 24 hour solvent extraction in a minimum amount of non-polar solvent (3 ml of ethyl acetate or acetonitrile) was the most efficient solvent extraction when compared to shorter extraction times or increased surface area methods. The results within this chapter could go towards a factor which real data would be multiplied by to determine 'true' concentrations of malodours. Finally, it was established that the hydrogels with 'sweat' could be stored, at room temperature, a major goal of this project.

## 4.9 References

- 1 H. Modaressi and G. Garnier, *Langmuir*, 2002, **18**, 642–649.
- 2 The Lubrizol Corporation, Tecophilic™ TPU, <https://www.lubrizol.com/Life-Sciences/Products/Tecophilic-TPU>, (accessed January 2019).
- 3 S. Moldoveanu and V. David, in *Modern Sample Preparation for Chromatography*, 2015, pp. 131–189.
- 4 R. Garcia-Villalba, J. A. Gimenez-Bastida, M. T. Garcia-Conesa, F. A. Tomas-Barberan, J. C. Espin and M. Larrosa, *J. Sep. Sci.*, 35AD, **15**, 1906–1913.
- 5 Agilent and Markes, THERMAL DESORPTION Introduction and Principles, <http://www.chem.agilent.com/cag/country/principles.pdf>, (accessed July 2016).
- 6 A. M. Curran, S. I. Rabin, P. A. Prada and K. G. Furton, *J. Chem. Ecol.*, 2005, **31**, 1607–1619.
- 7 K. Schafer, *Anal. Chim. Acta*, 1998, **358**, 69–77.
- 8 T. Seppanen-Laakso, I. Laakso and R. Hiltunen, *Anal. Chim. Acta*, 2002, **465**, 39–62.
- 9 F. Kanda, E. Yagi, M. Fukuda, K. Nakajima, T. Ohta and O. Nakata, *Br. J. Dermatol.*, 1990, **122**, 771–776.
- 10 A. J. Sheppard, W. D. Hubbard and A. R. Prosser, *J. Am. Oil Chem. Soc.*, 1974, **51**, 416–418.
- 11 J. Folch, M. Lees and G. H. Sloane Stanley, *J. Biol. Chem.*, 1957, **226**, 497–509.
- 12 E. Bligh and W. Dyer, *Can. J. Biochem.*, 1959, **37**.
- 13 P. Prada, A. Curran and K. Furton, *Anal. Methods*, 2010, **2**, 470–478.
- 14 E. D. Dodds, M. R. McCoy, L. D. Rea and J. M. Kennish, *Lipids*, 2005, **40**, 419–428.
- 15 M. R. Sahasrabudhe and B. W. Smallbone, *J. Am. Oil Chem. Soc.*, 1983, **60**, 801–805.
- 16 S. Durmaz and O. Okay, *Polymer*, 2000, **41**, 3693–3704.

## 5. Real Sampling, bacteria and qualitative screening

In previous chapters, the work has been carried out using a 'model sweat' mixture; an aqueous solution of 10 volatile free fatty acids, one unsaturated aldehyde and one thioalcohol, known to be involved in axilla malodour. This chapter explores the use of the hydrogel devices in 'real life' settings *in vivo* as well as dealing with key, living elements of the axillary biome *in vitro* by looking at cell cultures as further evidence of the passive nature of the presence of the hydrogel when *in situ*. Finally, the addition of indicators examines an immediate qualitative handle for pre-screening.

### 5.1 Bacterial Assay

These data are provided in collaboration with Diane Cox of Unilever Colworth, where, to show that the hydrogel does not affect the natural bacterial microbiome on the axillary skin, a staphylococcus epidermis assay on pig skin was carried out that compared the culture in open air and covered with a hydrogel.<sup>1</sup> Where T0 and T4 indicate time incubated at 37 °C prior to buffer scrub analysis (0 and 4 hours respectively). It should also be noted that  $<\log_{10}3$  is the limit of sensitivity when using the plating protocol and therefore this should be treated as no countable cells were recovered from the control.

**Table 5-1:** Summary of the results of the bacterial assay on pig skin test. N.B. T4 uninoculated (with and without hydrogel) account for failure to achieve total sterility of the pig skin, *via* radiation, prior to testing.

Treatment	Cells recovered, log <sub>10</sub> CFU/cm <sup>2</sup>
T0 uninoculated	<3.00
T0 inoculated	5.86
T4 uninoculated	<4.00
T4 inoculated	8.77
T4 uninoculated + hydrogel 1	<4.00
T4 inoculated + hydrogel 1	7.16
T4 uninoculated + hydrogel 2	<4.00
T4 inoculated + hydrogel 2	6.78

The cell count data in Table 5-1 and illustrated in Figure 5-1 demonstrate that similar results were obtained from the hydrogel-covered and standard pigskin experiments. Although the cell count from the hydrogel experiments appears lower, this is due to some cells being removed on the hydrogel and is therefore treated as an underestimate. It is also useful to note that the hydrogel patches were shown, by contact print, to be sterile prior to use. This is seen as a positive as it is evidence that no external bacteria or other contaminants are being added into the axilla when the hydrogel is introduced therefore it can be assumed that all malodour comes from the armpit itself. This all indicates that data regarding sweat obtained by using the hydrogel devices will be representative of 'real-life' data.

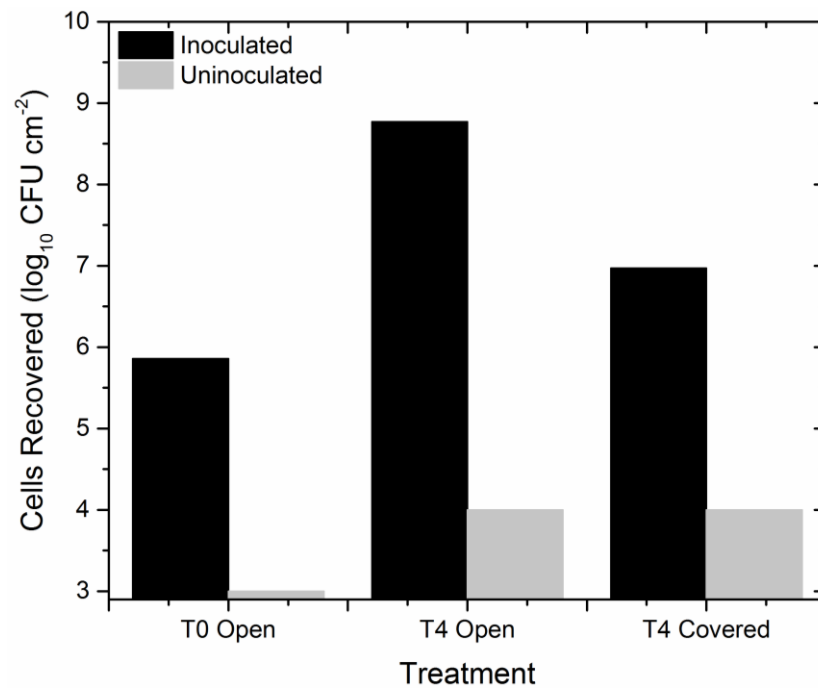


**Figure 5-1:** Illustration of the bacterial assay results.

## 5.2 Unilever Study

Using hydrogels synthesised at Warwick, an *in situ* study was carried out at Unilever's R&D facility in Port Sunlight, near Liverpool by myself. Standard p(NaAMPS) hydrogels (synthesised at University of Warwick by myself), were tested against textile patches. Figure 5-2 illustrates the olfactometry data recorded from unbiased assessment of the underarms after 24 hour wear cycle of the hydrogels / textile patches as described in Chapter 7. The data presented are the average of six sensory assessments by six different people on each armpit. It shows that, within error, there is no difference between the ratings recorded when a textile patch is worn compared to when a hydrogel patch is worn. Especially when considering that the textile and the hydrogel were worn in the same underarm on different (consecutive) days which would lead to variation in results even under otherwise identical conditions. Similarly differences between left and right axilla, within the same time period, are expected.<sup>2-4</sup> This is a good indication that the hydrogels do not affect the axilla microbiome, complimentary to the bacterial studies, above. Note there is expected to be a noticeable difference in sensory assessment, across the participants, as the panel of assessed volunteers are known to emit different levels of odour.

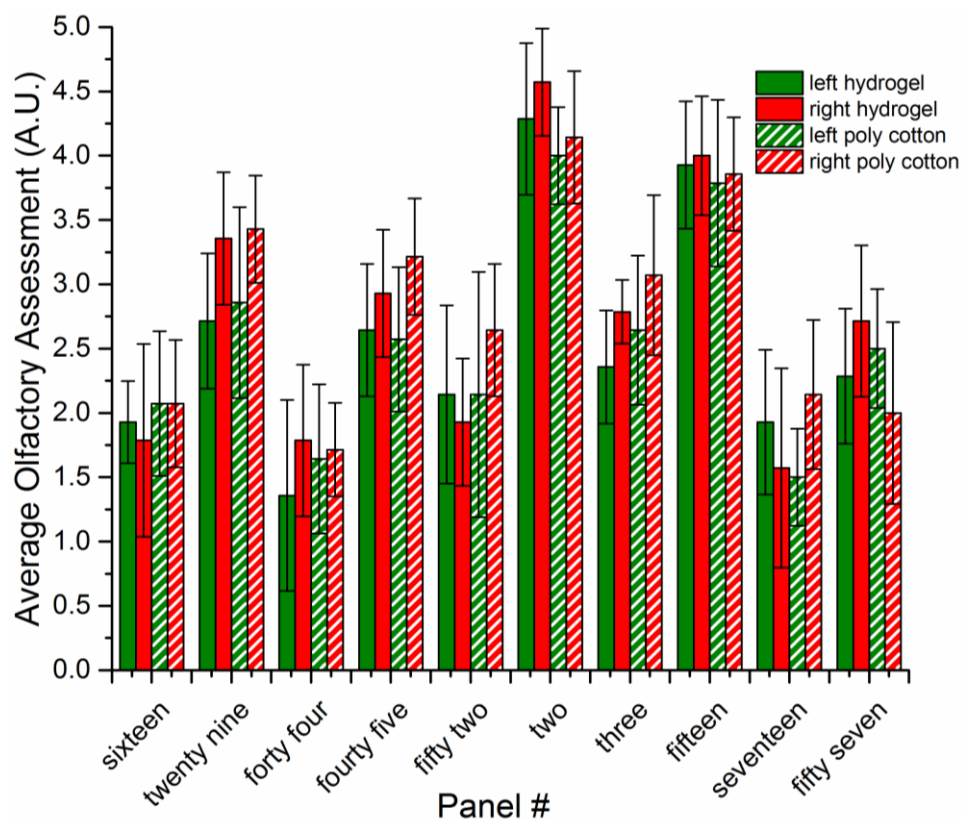


**Figure 5-2:** Anonymised data from the olfactory assessment of the hydrogel and textile patch comparison study.

In collaboration with Steph Blissett (Unilever Port Sunlight), the hydrogels worn as part of this study were then extracted *via* standard solvent extraction procedure and analysed by GC-MS. This illustrated that 21 different compounds were identified in the samples (that were not found in an unworn hydrogel extraction, the 'blank'). Of these 21, de Costello *et al.* list 11 of these as being previously reportedly emanating from the skin. However, the authors recognise that their list is not necessarily exhaustive (as is compiled from a review of the literature) but that it is a useful database from which further research, such as this work, will be stimulated and add to.<sup>5</sup> The mean number of different compounds identified per sample was 13.75 (n = 20, SD ± 2.4) with the greatest number of different compounds identified in a single sample = 18, Figure 5-3.



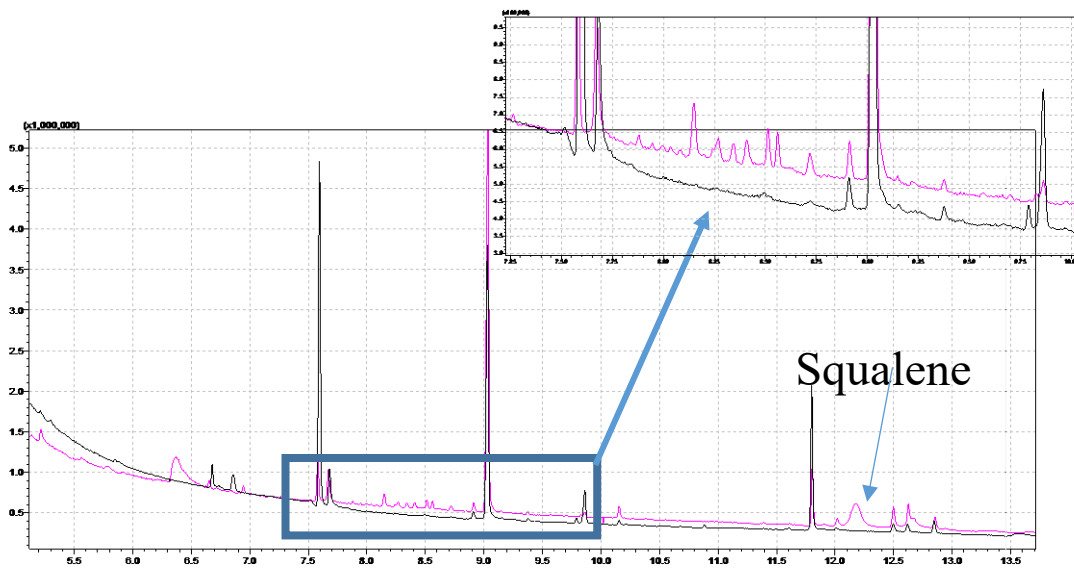


**Figure 5-3:** Chromatogram of sample containing 18 different identified compounds (pink line) compared to the 'blank' extract (black line) (supplied by Steph Blissett, Unilever Port Sunlight).

The greatest difference in number of different compounds identified between a participant's two samples was 5. Most of the participants had a greater number of compounds identified in their first sample (mean = 14.20, S.D. =  $\pm 1.8$ ,  $n = 10$ ) compared to their second (mean = 13.30, S.D. =  $\pm 2.9$ ,  $n = 10$ ), regardless of which underarm was sampled on which day although this was not statistically significant. Similarly, there was no significant trend when comparing left to right; the mean number of compounds identified from left samples was 14.10 (S.D. =  $\pm 2.5$ ) compared to 13.40 in the right (S.D. =  $\pm 2.4$ ). Notably, three compounds used in the model sweat were identified in some of the samples; propanoic acid (13), butyric acid (8), and 2-methylbutanoic acid (11). All three were observed more often in the first day than the second, this is consistent with the general trend observed. Of the two participants with the highest olfactometry scores (2 and 15, Figure 5-2) both of participant 2's samples and participant 15's left sample contained all three of these known malodour compounds, Figure 5-4. The pattern of first vs. second sample continues in this comparison as 15's second sample (right sample) contained only propionic acid of these three compounds of interest.

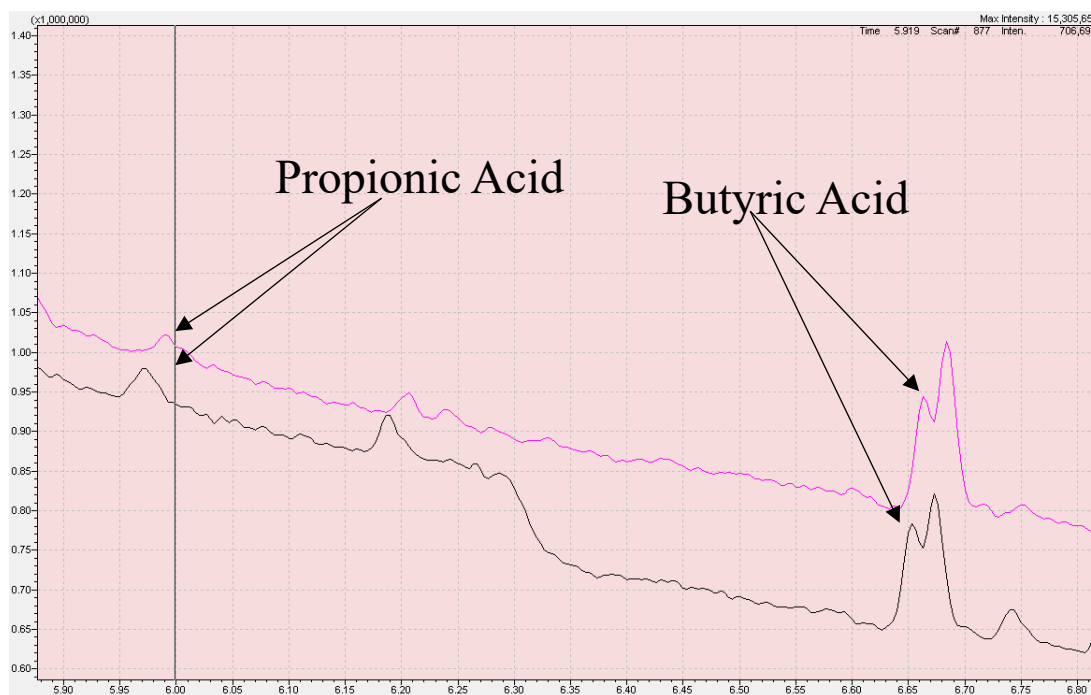


**Figure 5-4:** Overlaid GC-MS chromatograms for participant 2's samples, highlighting the presence of propionic acid and butyric acid (supplied by Steph Blissett, Unilever Port Sunlight).

This analysis only includes compounds that are present in concentrations above the limit of detection of the method applied.

### 5.3 Real Sampling

As the end goal of the project is to create a device suitable for use *in vivo*, hydrogels have been worn by anonymous volunteers as a preliminary test to determine the viability of the device. These volunteers would affix a hydrogel under one or both underarms for the duration of their exercise, *e.g.* a one hour gym session. These samples were then stored in sealable pouches until recovery, or immediately recovered as discussed in Chapter 4, and analysed by the methods described in Chapter 2. Figure 5-5 illustrates that the GC of these samples reveals peaks in the chromatograms, as predicted with the model sweat solution in Chapter 4. As illustrated, there are fewer peaks than anticipated from these worn hydrogels which could be for a number of reasons. This could be due to these particular volunteers not being particularly sweaty / smelly volunteers as, unlike in industry standard tests, no pre-screening was carried out on the volunteers to determine this. It is also likely that they were wearing antiperspirant / deodorant products as there were no conditions on participants. Further, there may not have been enough time between

sweating and removal of the hydrogel for bacterial metabolism to occur and therefore a lack of the expected compounds. Conversely, it may be that there are other compounds present but they are at concentrations lower than the current analytical limit of detection (LOD, see Chapter 2).

There are similarities and differences between the peaks in all four volunteer chromatograms, Figure 5-5. This suggests that there are some common compounds within the malodour profile of some of the volunteers but also some differences especially in quantity and therefore potential strength of malodour.

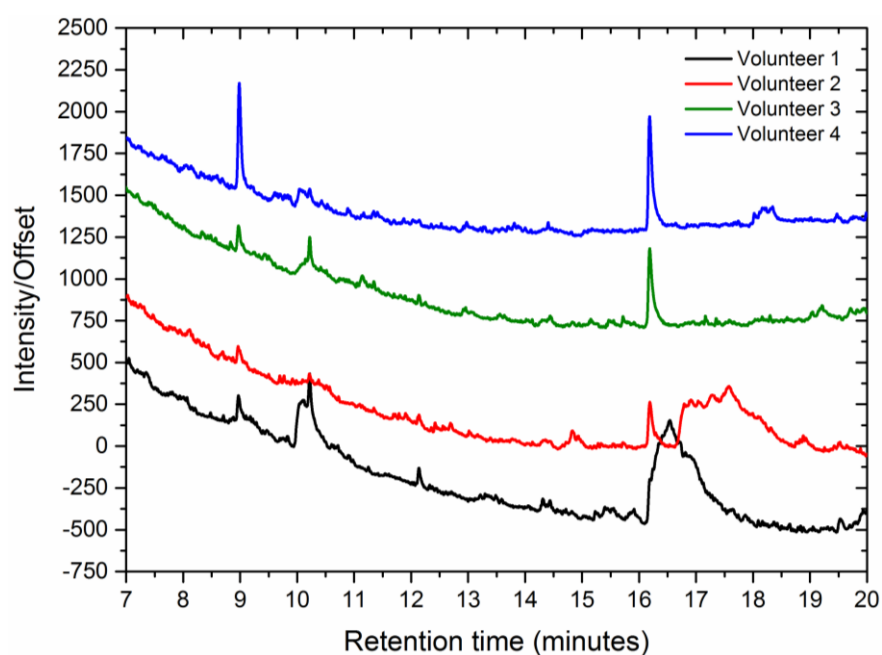


**Figure 5-5:** Stacked example chromatograms of real sweat collected using hydrogels.

One of these real samples is then stacked with two of the VFAs in Figure 5-6. This illustrates that two of the peaks in that sample occur at the same elution times as those for acetic and propionic acids respectively, which suggests that this is their identity. This is where the importance of the combined techniques such as GC-MS, become apparent as further information is required for conclusions on the identity of components in the real samples to be made. For further studies, a more comprehensive library of retention times of sweat components would need to be created.

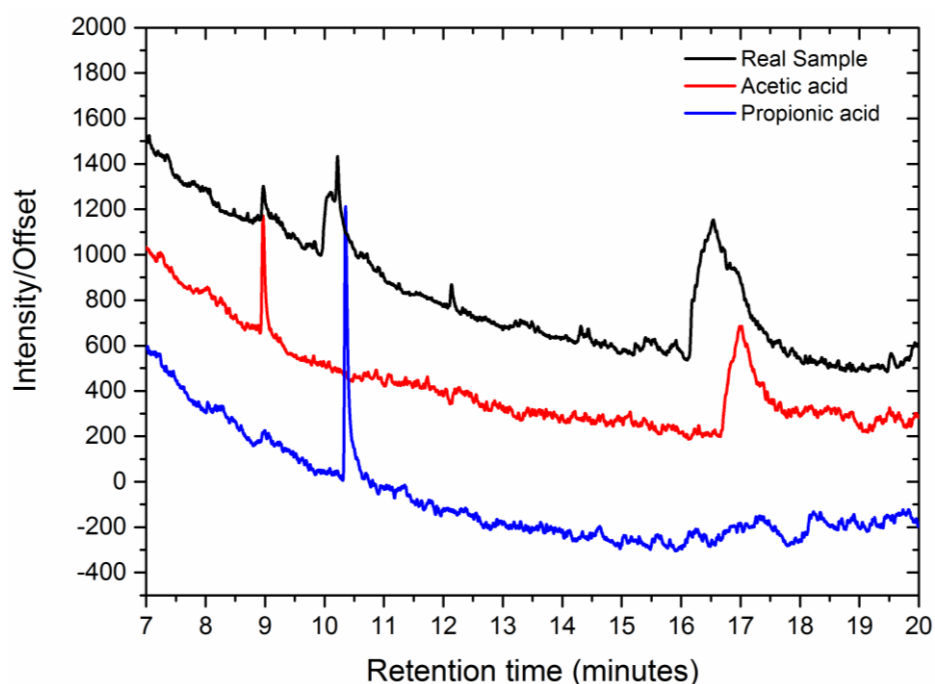


**Figure 5-6:** Stacked chromatograms comparing a real sweat sample and two VFAs.

## 5.4 Additives

Hydrogels are widely used as delivery vehicles, *e.g.* in the medical industry for drug delivery, therefore it is known that hydrogels can incorporate far more than just water. The following work investigates the addition of pH indicators as an immediate tool for qualitatively pre-screening samples or possible additional methods of quantitative analysis. Finally, the incorporation of fragrance is investigated with the potential for a future product or more complex device.

### 5.4.1 Indicators

As discussed in Chapter 1, indicators were to be used to allow for a more immediate indication of volatiles present in human sweat. Thus far, two indicators have been used, quinine and bromophenol blue. These pH indicators work on accepting and donating protons and the changes this causes to the  $\pi$ -interactions in the molecules leading to the visible colour / fluorescence changes we rely on as indicators.

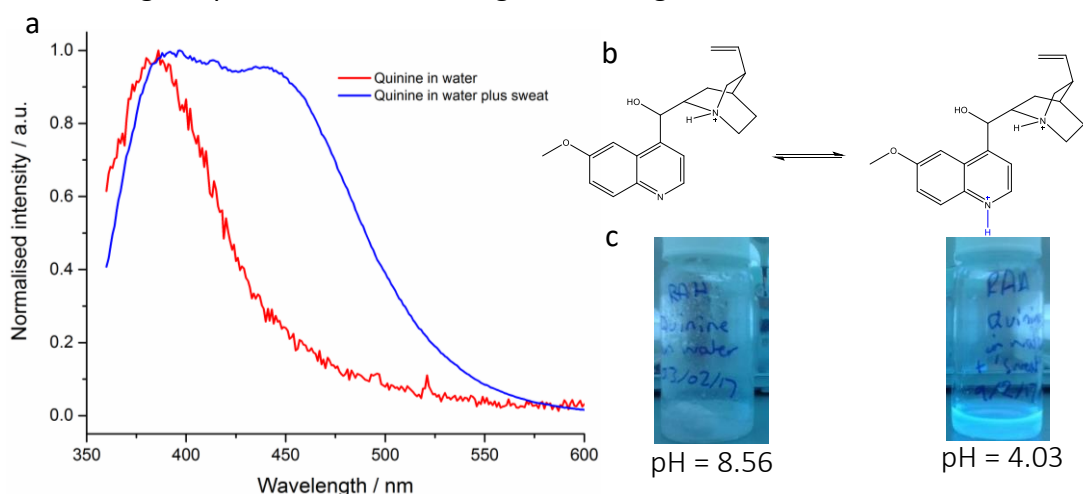
Furthermore, as well as an immediate colour response, quantification could be achieved *via* spectroscopy, for example concentration could be calculated *via* UV-Vis. The Beer-Lambert equation would allow for the calculation of an unknown concentration based on the UV absorption by creating a calibration curve of

absorption vs. concentration. However, this would only give a total acid concentration rather than individual data. UV-Vis data are presented for the bromophenol blue experiments but this quantification was not carried out.

#### 5.4.1.1 Quinine and Quinine Sulfate

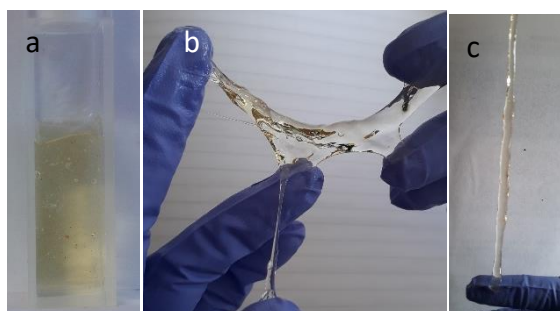
Quinine is a common, pH-dependent fluorophore; under acidic conditions, the addition of the proton to the lone pair on the nitrogen disrupts the conjugation that was otherwise quenching the fluorescence. Following the work of Liu *et al.*,<sup>6</sup> attempts were made to introduce quinine to the p(NaAMPS) hydrogels as an indicator of the presence of sweat, as quinine has pH-sensitive fluorescence and sweat is acidic.<sup>7</sup> As quinine has very limited solubility in water, which is a large part of both the hydrogel and sweat, quinine sulfate was also investigated as this salt form has increased aqueous solubility.

Figure 5-7 illustrates the pH-dependent fluorescence of quinine in water using model sweat to decrease the pH. This can be seen in the fluorescence spectra and the photographs taken, when using the UV nail lamp (broad band with  $\lambda \sim 360$  nm) as the UV source. Quinine has a fluorescence at  $\sim 400$  nm in general conditions, on decreasing the pH, this shifts to a longer wavelength, *ca.* 460 nm.



**Figure 5-7:** a) Overlaid fluorescence spectra of quinine at the two different pH. b) the corresponding structures of quinine. c) the corresponding photos of the solutions under the UV lamp with the recorded pH of the solutions.

Figure 5-8a shows the products of the initial polymerisation attempt. As can be seen, the quinine 'gel' is more yellow than the standard hydrogel and required more passes under the Light Hammer (10 instead of the standard 5) to form a gel disc. When using quinine sulfate the polymerisation was disrupted further, (Figure 5-8b and c) which is theorised to be due to quinine sulfate's increased solubility, compared to quinine, in water.



**Figure 5-8:** a) The quinine 'gel' that is yellow in colour. b and c) Photos of the quinine-AMPS polymers that did not form a stable gel network as standard p(AMPS) hydrogels do.

There are currently two possible explanations as to why quinine disrupts the polymerisation; firstly, although quinine has a vinyl bond where polymerisation can take place, once it adds to the chain it could terminate the chain due to a lack of a neighbouring electron withdrawing group, therefore preventing the normal highly-cross linked network forming. Kobayashi and Iwai reported the copolymerisation of cinchona alkaloids in the 1980s,<sup>8,9</sup> however, they also reported a decrease in yield and inherent viscosity with the increase in quinine content. The second possibility is that photo-polymerisation is inhibited due to absorbance of the UV by the quinine.

These same quinine concentration gels were synthesised in NMR tubes for 'gel' <sup>1</sup>H NMR analysis. These give evidence for the lack of polymer gel network formation when 10 mg of indicator was added to the reaction mixture, as the vinyl groups are observable with both quinine and quinine sulfate (Figure 5-9).

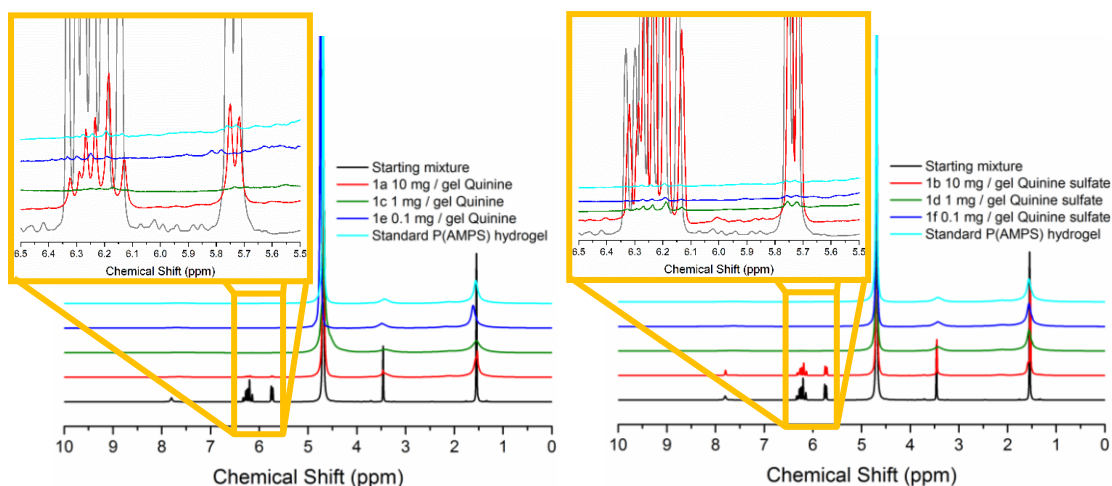


**Figure 5-9:** Left: Stacked  $^1\text{H}$  NMR spectra of the hydrogels synthesised containing different concentrations of quinine. Right: the same spectra for the gels containing quinine sulfate.

Even though the polymerisation was not as desired, pH-fluorescence of the ‘gels’ was still tested. As can be seen in Figure 5-10, the fluorescence maxima shifts from  $\sim 380$  nm to  $\sim 470$  nm with the addition of the model sweat, this is in agreement with the aqueous solution (Figure 5-7).

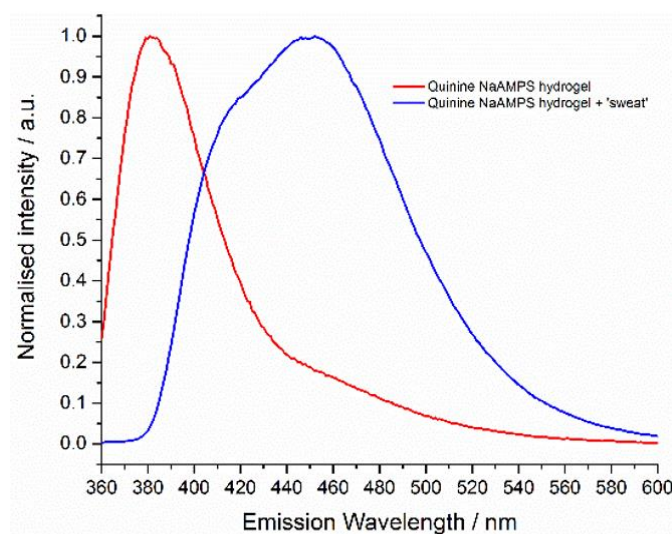


**Figure 5-10:** 10 mg /gel quinine fluorescence spectra overlaid.

In order to ensure gelation of the hydrogels during synthesis, the concentration of quinine used was decreased. Reducing the concentration to 1 mg or 0.1 mg per hydrogel (compared to the previous 10 mg) ensured that hydrogel networks, with a structure more akin to the standard hydrogels, were synthesised. As can be observed in Figure 5-11, for both quinine and quinine sulfate, there is still a high enough concentration in the hydrogel to elicit the pH-dependent fluorescence when the

same volume of sweat is added to the gels, as observed when using 10 mg of active ingredient.

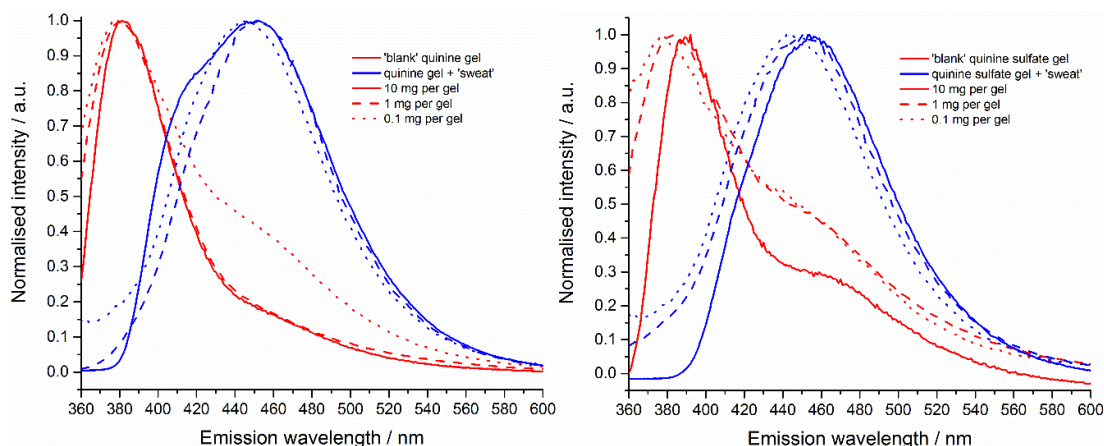


**Figure 5-11:** Left: Normalised overlaid fluorescence spectra of the three different concentrations of quinine tested to-date. Right is the same spectra using quinine sulfate.

As one of the key properties of the hydrogel is its ability to absorb aqueous solutions, this property was then exploited to synthesise an indicator-containing hydrogel post-polymerisation, Figure 5-12. Figure 5-13 illustrates that the fluorescence response is the same from a hydrogel whether the quinine is added pre- or post-polymerisation. This appears to be a viable solution to the polymerisation problems described above.

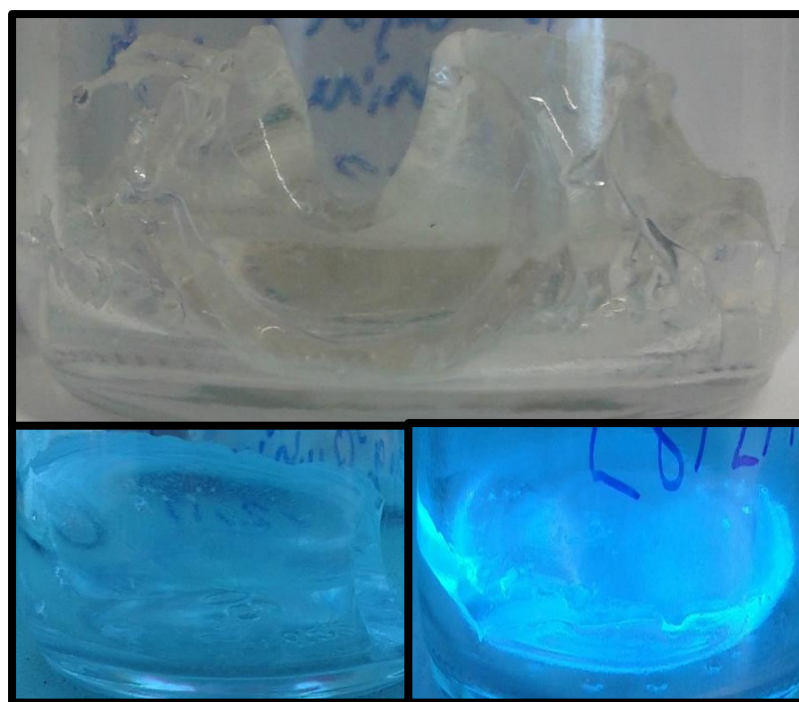


**Figure 5-12:** Quinine rehydrated hydrogel (top), under the UV light (bottom left), under the UV light with absorbed model sweat (bottom right).



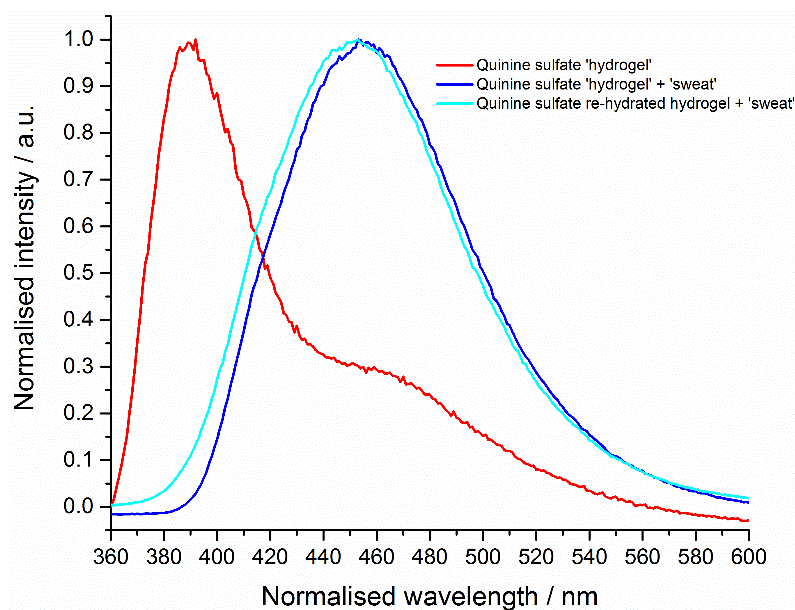


**Figure 5-13:** Normalised fluorescence spectra illustrating that the quinine can be added pre- or post-polymerisation for the same detection result.

These hydrogels were further tested on real, axillary-produced sweat. A challenge with using quinine as a visual indicator is that, whilst  $\lambda_{\text{max, em}}$  shifts to a longer wavelength, under a UV lamp, the quinine hydrogel alone will fluoresce also (Figure 5-14b), necessitating the use of a fluorescence spectrophotometer.

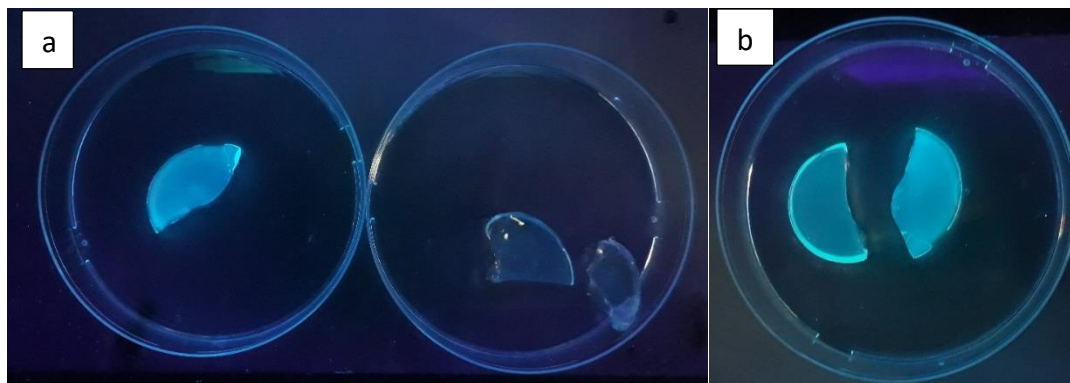


**Figure 5-14:** a) Worn hydrogels that contain quinine sulfate (left) and no indicators (right) under UV lamp. b) Comparison of worn and unworn halves of a quinine sulfate – containing hydrogel under a UV lamp.

Figure 5-15 illustrates the fluorescence data of the ‘blank’ quinine hydrogels with the worn (dark blue trace) and dosed (turquoise trace) versions, where a difference can be observed between the worn (or dosed) and unworn samples (red and pink traces).

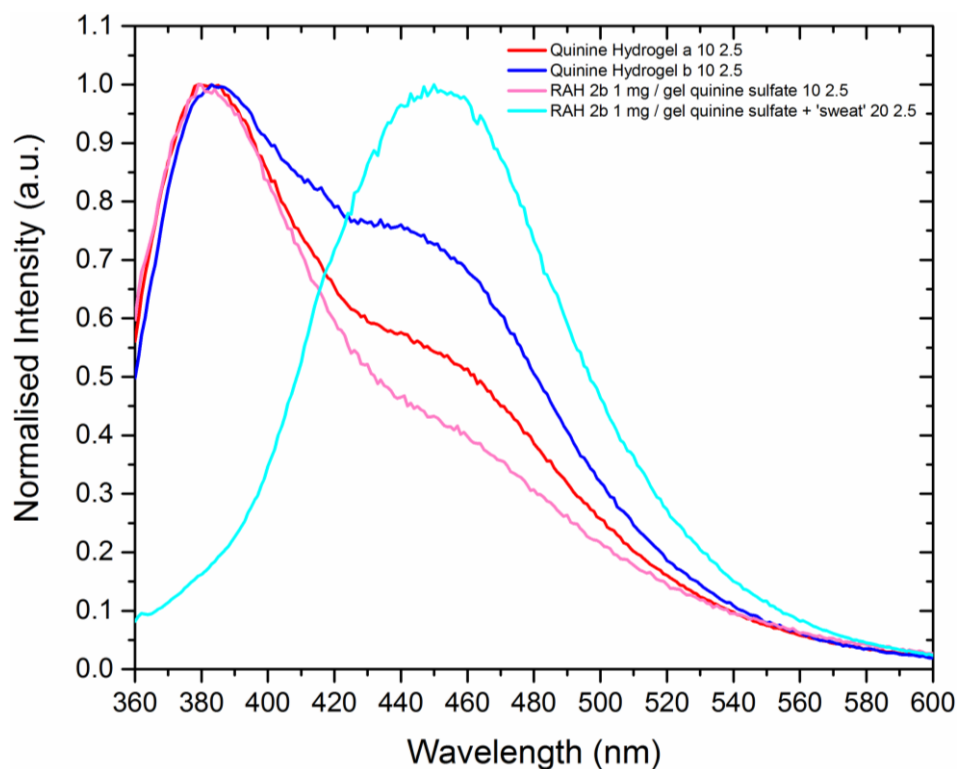


**Figure 5-15:** Normalised overlaid data of the worn quinine sulfate hydrogel and the equivalent model sweat spectra.

Quinine and quinine sulfate are found in tonic water and most commonly used as an antimalarial.<sup>10-12</sup> This means they have already been approved for human consumption, however, they are both classed as skin irritants and therefore leaching studies would need to be carried out to determine if they are safe to be worn for a period of time.

While this could be a useful analytical technique allowing for quantification of total acids *via* pH-induced fluorescence, it is not practical as a qualitative screening tool.

#### 5.4.1.2 Bromophenol Blue

Bromophenol blue (BPB) is a common pH indicator, where it is the protonation / deprotonation of the phenol oxygen that is responsible for the colour that is visible. Bromophenol blue is a pH indicator which is yellow at pH = 3 and blue at pH = 4.6. When the oxygen is protonated (under strongly acidic conditions) the hydroxyl group is not involved in the conjugated  $\pi$ -bonding of the aromatic ring, however, when the phenolate anion is present (basic conditions) the lone pair will conjugate into the aromatic ring and the blue colour is observed.

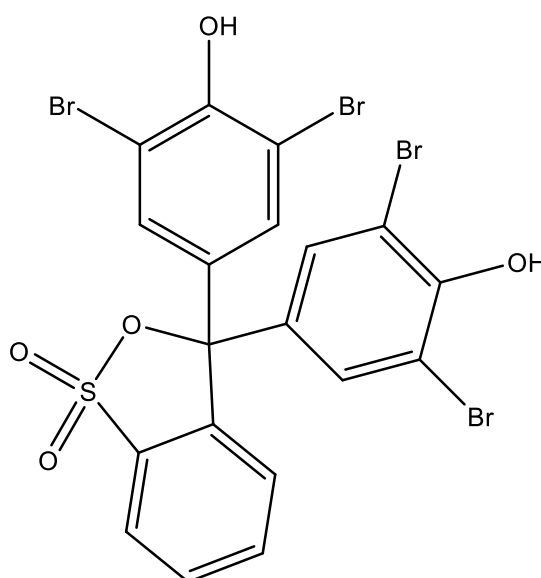


**Figure 5-16:** Structure of bromophenol blue.

This indicator was used as it was readily available and has previously been shown to work for sweat related sensors.<sup>13,14</sup> As an aqueous solution of NaAMPS has a basic pH (measured with probe as pH = 6.0), the standard hydrogels, with bromophenol blue added pre-polymerisation, are purple, Figure 5-17a. When 0.5 ml of model sweat is added and left to absorb (as standard procedure) a colour change takes place but only around the edge of the hydrogel, Figure 5-17b. To overcome this, the concentration of bromophenol blue in the hydrogel was reduced and the indicator experiment was repeated (Figure 5-17c and d respectively). Visible colour change of the hydrogels was monitored by UV-Vis spectroscopy (Figure 5-18). Although the

peak at  $\sim 600$  nm is visible in all three samples (purple region), there is a clear appearance of a peak at  $\sim 450$  nm (yellow region) when the model sweat is added.

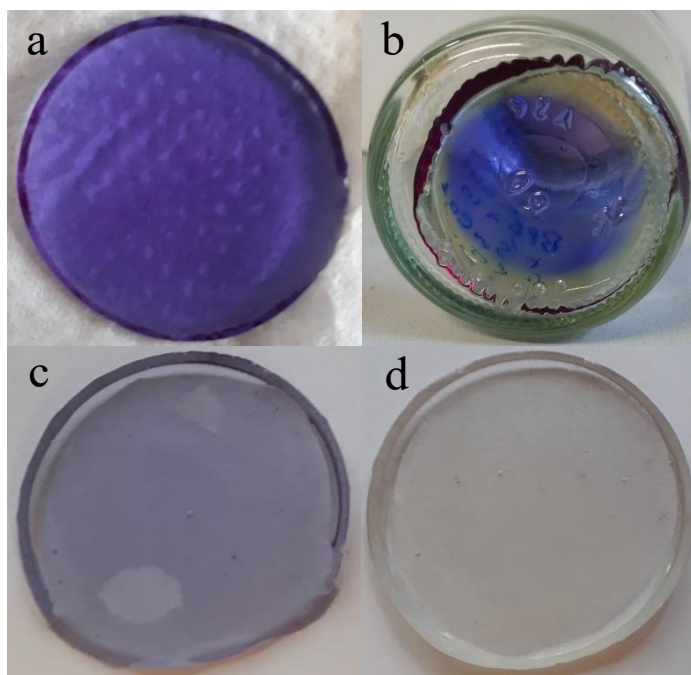


**Figure 5-17:** Original standard hydrogel containing BPB (a), with 0.5 ml added model sweat (b), decreased concentration of BPB (c), with 0.5 ml added model sweat (d).

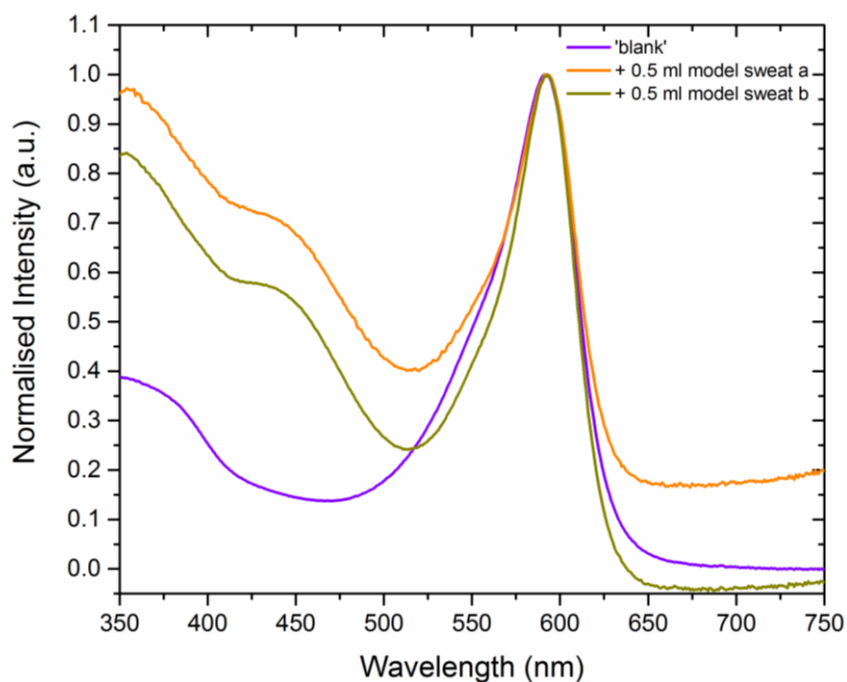


**Figure 5-18:** UV-Vis spectra of a BPB containing hydrogel, before and after the addition of model sweat.

## Worn Bromophenol Blue Hydrogels

These were also tested by being worn in the axilla by volunteers as described previously. Figure 5-19 illustrates the before and after of bromophenol blue containing hydrogels when worn by a volunteer during exercise. This illustrates that the blue to yellow transition is achieved *in vivo* as well as during the model studies.

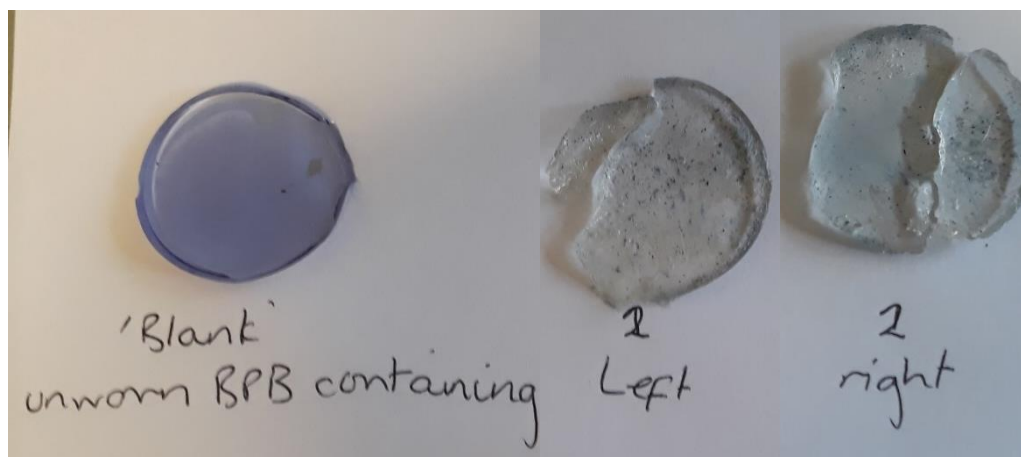


**Figure 5-19:** Unworn (left) and worn (right) hydrogels all containing bromophenol blue.

Where the colour change is clearly visible to the eye in this case, it is less obvious in the UV-Vis spectra (Figure 5-20). The peak in the yellow region is only visible as a change in gradient between 420 and 450 nm in the worn samples in combination with a decrease in the height of the peak in the blue region (normalised data).

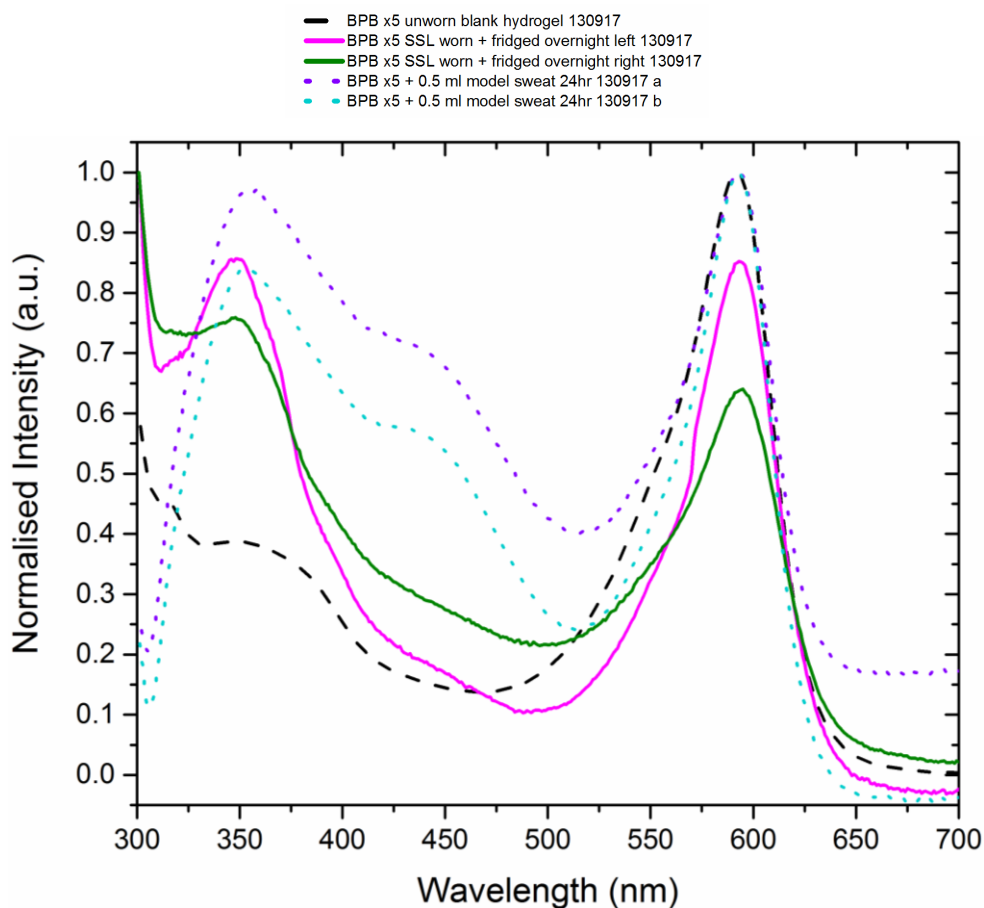


**Figure 5-20:** Overlaid UV-vis spectra of a ‘blank’ BPB hydrogel (---), when model sweat is added (---) and the volunteer worn hydrogels (solid line).

Although the bromophenol blue will be freely solvated in the hydrogel, one of the reasons it was chosen is that it has no known associated hazards.<sup>15</sup> Furthermore, there is a “500 Dalton rule” associated with transcutaneous delivery. Bos and Meinardi illustrated that there is a rapid decline in skin absorption of small molecules at approximately 500 Da.<sup>16</sup> Bromophenol blue has an RMM = 669.96 Da and therefore would be above this limit. Further work is required to examine whether the bromophenol blue leaches from the patch to the skin.

#### 5.4.1.3 *p*(HEMA)

Using an indicator and collecting UV-Vis data in this manner has added complications when using HEMA containing hydrogels. As discussed in Chapter 3, *p*(HEMA) hydrogels are opaque white with even a small amount of water within (the xerogels are transparent and colourless). With the addition of BPB, the colour change is still visible to the eye as, initially, opaque pale blue hydrogels are formed which, on addition of acid, become yellow as is illustrated by the addition of acetic acid to the hydrogel in Figure 5-21. This means using it for qualitative screening is still possible, however, UV-Vis data was not possible using the available equipment due to the high opacity of these materials. Future work could involve investigating the use of diffuse reflectance measurements instead.

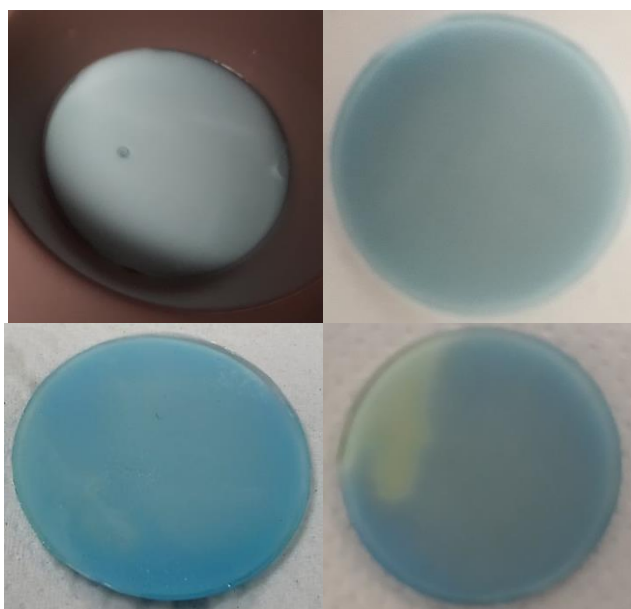


**Figure 5-21:** *p*(HEMA) hydrogels containing bromophenol blue.

## 5.4.2 Fragrance

The incorporation of fragrance into an otherwise standard p(NaAMPS) hydrogel was investigated as a potential future product or possibly a more advanced collection device.<sup>17</sup> The oily fragrance ('New Day') is immiscible in the aqueous NaAMPS solution therefore it is incorporated into the hydrogels as dispersed droplets, Figure 5-22. Two concentrations of fragrance were incorporated, where, as expected, the lower concentration displayed smaller fragrance droplets. Both hydrogels smelled strongly of the fragrance after polymerisation and continued to do so for several weeks and months after initial synthesis. It was also observed that the addition of fragrance increased the curing time required to form a solid hydrogel akin to the standard.



**Figure 5-22:** p(NaAMPS) hydrogels containing 'New Day' fragrance at 1 % (v/v) fragrance (a), 0.5 % (v/v) fragrance (b) and no fragrance incorporated (c).

This was then repeated using a more aqueous soluble fragrance known as 'White Willow', Figure 5-23, however, this still exhibited the same fragrance droplet formation as with the 'New Day' fragrance.

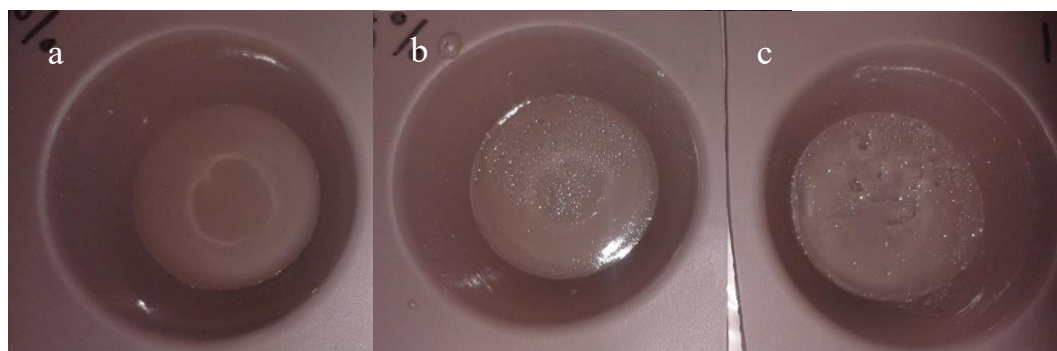


**Figure 5-23:** p(NaAMPS) hydrogels containing 'White Willow' fragrance at 0.1 % (v/v) fragrance (a), 0.5 % (v/v) fragrance (b) and 1 % (v/v) fragrance (c).



Further optimisation would be required to examine further decreasing the concentration of fragrance to eliminate the biphasic appearance whilst maintaining fragrance release. Studies would also be required into the rate of the fragrance release, for example by headspace GC-MS.

## **5.5 Conclusion**

It has been evidenced, through *in vitro* bacterial assay and *in situ* olfactory assessment, that the hydrogels do not alter the bacterial microbiome as they neither introduce bacteria nor restrict the growth of the natural bacteria, as they are not an occlusive material. This suggests they are a suitable device for collecting realistic, quantifiable data. *In situ* collection of real sweat also evidenced the viability of the device *in vivo*. Furthermore, the addition of pH indicators provides the potential for non-extraction based quantification of total acid concentration or the ability to qualitatively pre-screen samples. This was further evidenced by *in situ* testing. Finally, the addition of fragrance to the hydrogel, as a potential product additive, appeared possible, though further work would be required if this was to become part of the sensory device.

## 5.6 References

- 1 D. Cox, *Testing hydrogel patches in an inoculated pigskin model*, 2016.
- 2 C. Ferdenzi, B. Schaal and S. C. Roberts, *Chem. Senses*, 2009, **34**, 565–571.
- 3 S. Bird and D. B. Gower, *J. Steroid Biochem.*, 1982, **17**, 517–522.
- 4 M. Egert, I. Schmidt, H. Hohne, T. Lachnit, R. A. Schmitz and R. Breves, *FEMS Microbiol. Ecol.*, 2011, **77**, 146–153.
- 5 B. D. L. Costello, A. Amann, H. Al-Kateb, C. Flynn, W. Filipiak, T. Khalid, D. Osborne and N. M. Ratcliffe, *J. Breath Res.*, 2014, **8**, 014001.
- 6 C. Liu, Y. Furusawa and K. Hayashi, *Sensors Actuators, B Chem.*, 2013, **183**, 117–123.
- 7 J. L. Matousek and K. L. Campbell, *Vet. Dermatol.*, 2002, **13**, 293–300.
- 8 N. Kobayashi and K. Iwai, *J. Am. Chem. Soc.*, 1978, **100**, 7071–7072.
- 9 N. Kobayashi and K. Iwai, *J. Polym. Sci. Polym. Chem. Ed.*, 1980, **18**, 223–233.
- 10 NICE, Quinine, <https://bnf.nice.org.uk/drug/quinine.html>, (accessed March 2019).
- 11 Datapharm, Quinine Sulfate Tablets BP 200mg, <https://www.medicines.org.uk/emc/product/5866/smpc>, (accessed March 2019).
- 12 S. O’Keefe, Tonic Water Contains Quinine, <https://www.bestfoodfacts.org/tonic-water-contains-malaria-medicine/>, (accessed March 2019).
- 13 R. Peng, Z. Sonner, A. Hauke, E. Wilder, J. Kasting, T. Gaillard, D. Swaille, F. Sherman, X. Mao, J. Hagen, R. Murdock and J. Heikenfeld, *Lab Chip*, 2016, **16**, 4415–4423.
- 14 G. Tashiro, M. Wada and M. Sakurai, *J. Invest. Dermatol.*, 1961, **36**, 3–4.
- 15 Sigma-Aldrich, Bromophenol Blue SDS.
- 16 J. D. Bos and M. M. H. M. Meinardi, *Exp. Dermatol.*, 2000, **9**, 165–169.
- 17 B. Buchs, W. Fieber, F. Vigouroux-Elie, N. Sreenivasachary, J.-M. Lehn and A. Herrmann, *Org. Biomol. Chem.*, 2011, **9**, 2906–2919.

## 6. Conclusions & Future Work

Current industrial standard methods for the analysis of the efficacy of antiperspirant / deodorant products are somewhat archaic and provide minimal quantitative information; the mass of sweat produced and the general level of perceived malodour through weighing sweat collected in textile patches and olfactory assessment (marked out of five) respectively. The goal of this research was to create a sampling device and analytical method that would update the efficacy testing of future products and provide more detailed quantitative information on specific malodorous compounds.

Chapter 2 demonstrated the development of a successful GC-FID method for the separation and quantification of malodorous compounds involved in body odour. This followed the work of Fleming *et al.* in both the method and the column choice (30 m polar PEG column, internal diameter 0.32 mm, film thickness 0.25  $\mu\text{m}$ ).<sup>1</sup> HPLC and GC-MS were also investigated, however, GC-FID was the preferred analytical technique for quantification purposes. GC-MS was found to be useful for identification of the unknown compounds found in the real samples from the study carried out at Port Sunlight (Chapter 5). Future development would include the use of thermal desorption and solid phase microextraction as possible extraction / injection techniques into a GC. A further chromatography technique to be investigated is supercritical fluid chromatography, a complimentary technique to GC and LC.

Chapter 3 initially detailed the investigation of the synthesis of p(NaAMPS) hydrogels as devices for absorption of sweat. In this investigation the optimum synthetic procedure for these materials was determined, the optimum photoinitiator concentration was found to be 0.065 mol% with 1 pass (7 seconds) under the Light Hammer. As part of this investigation a method for analysis of these materials by solution state NMR was developed. The crosslinker concentration of these hydrogels was then further optimised with a focus on the swelling kinetics and mechanical properties.

Alternative monomers, such as HEMA and HEA, were also compared, however, these were found to be more challenging to synthesise compared to p(NaAMPS) and also did not swell to the same degree (a necessity of this application).

More complex architectures, such as double network IPNs, were then investigated to determine if they could add mechanical strength to the device. Initially, alginate was used as a physical network in combination with the p(NaAMPS) network before attention turned to combining two covalent networks; NaAMPS with HEA or HEMA. The NaAMPS and HEMA combination was focussed on whereby it became apparent that the swelling kinetics were between the individual networks' behaviours. This has led to an MChem project investigating the effect of which network is synthesised first in the sequential IPN synthesis and the effect of the ratio of the two networks on the swelling and mechanical properties. Future work would include imaging these different materials as well as determining the effect of supercritical fluid on the IPNs in order to be able to use supercritical fluid extraction. As well as further work on the physical-covalent combination as alternative materials plus the synthesis of a p(NaAMPS-co-HEMA) single network for comparison.

Chapter 4 applied the p(NaAMPS) hydrogels from Chapter 3 in an investigation of absorption and extraction of a model sweat mixture of 10 VFAs, one unsaturated aldehyde and one thiol in aqueous solution. Several extraction methods were tested such as simple solvent (including sample pre-treatment), Soxhlet and supercritical fluid extraction. It was found that simple solvent extraction (minimum solvent, sealed for 24 hours) without any sample pre-treatment (cutting up / sonication of samples) was the most effective. SFE proved promising, however, further method development is required to optimise device stability during this process whilst retrieving all analytes. Although Soxhlet extraction allowed for the comparison between a hydrogel and a textile patch, it was found to be time and resource consuming, which is non-ideal with industrial application in mind. The results did indicate that the absorption and extraction from the novel hydrogel devices are comparable to the textile patches already in use by Unilever.

Furthermore, it was found that dosed p(NaAMPS) hydrogel devices could be stored for up to 4 weeks at room temperature prior to extraction and analysis. This gave

promising initial results, an improvement on the current vacuum packing and storage at -80 °C, a key element for future global testing. A future study using the hydrogel devices *in vivo* would be required to compare to storage of the textiles.

In Chapter 5 it was demonstrated (in collaboration with Unilever Colworth) that the p(NaAMPS) hydrogels do not disrupt the natural bacterial microbiome. This was further evidenced when these hydrogel devices were then tested *in situ* at Unilever Port Sunlight in a typical sweating study (tested against current textile patches), where it was found that the hydrogel devices did not affect the olfactory assessment.

Chapter 5 also illustrated that the absorption and recovery investigated using model sweat in Chapter 4, could be successfully applied to samples collected *in situ*. The p(NaAMPS) hydrogel devices were tested on volunteers at Warwick, where it was found that they do absorb over the course of exercise activities and can be extracted to determine malodorous compounds. This is excellent proof of concept and even showed, by GC-FID, some differences between volunteers. The hydrogel devices worn for 24 hour periods as part of the Port Sunlight study were also extracted and analysed by GC-MS which successfully identified some of the known malodour samples as well as giving insight into other unknown compounds found in axillary sweat. Further studies involving hydrogel devices being worn and extracted, eventually using the SFE technique would be required to gain more data. Studies would also be required which included antiperspirant / deodorant products being worn to determine if their efficacy can be determined using the devices; the ultimate goal of this device.

Further, the addition of pH indicators to the hydrogels was investigated for use as a qualitative pre-screening method. Both quinine (sulfate) and bromophenol blue (pH sensitive fluorophore and chromophore respectively) were shown to be successful indicators of the acid content of sweat with both the model sweat and real samples. Quinine was found to be less useful as a screening tool as it fluoresces with and without sweat (it is the emission wavelength that shifts) but could be used as an alternative quantitation tool. Bromophenol blue could be used as a colour indicator visible for pre-screening or for quantitation *via* UV-Vis where a total acid concentration could be calculated using the Beer-Lambert law. If this were to be

pursued, further optimisation would be required for the p(HEMA)-containing hydrogels as they are opaque.

This investigation into the use of indicators led to a PhD project investigating the use of (PEG) dibromomaleimide as a colorimetric / fluorescence indicator of the presence of thiol compounds and the possibility of decreasing their volatility using long chain polymer analogues so as to obtain better analytical data for this type of compound. This would then also be incorporated into a hydrogel device and as an end goal would be part of a multicomponent device that can give insights into the various different functional groups involved in malodour, preferably quantifiably, perhaps in a compartmentalised device similar to some of the smart devices investigated recently such as that reported by Koh *et al.*<sup>2</sup>

Future work would also include further development of the full device, including the sticky, breathable backing, which would involve carrying out peel testing on the Universal Tester.

Even though development is required before these hydrogel devices can be regularly used in industrial applications, extensive progress has been made in producing and testing a material that will bring antiperspirant / deodorant testing into the 21<sup>st</sup> century.

- 1 S. E. Fleming, H. Traitler and B. Koellreuter, *Lipids*, 1987, **22**, 195–200.
- 2 A. Koh, D. Kang, Y. Xue, S. Lee, R. M. Pielak, J. Kim, T. Hwang, S. Min, A. Banks, P. Bastien, M. C. Manco, L. Wang, K. R. Ammann, K.-I. Jang, P. Won, S. Han, R. Ghaffari, U. Paik, M. J. Slepian, G. Balooch, Y. Huang and J. A. Rogers, *Sci. Transl. Med*, 2016, **8**, 366–165.

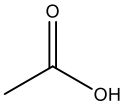
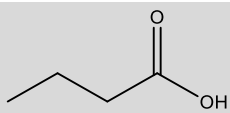
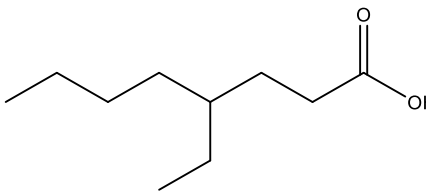
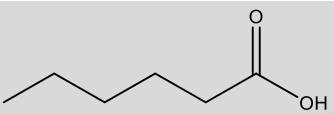
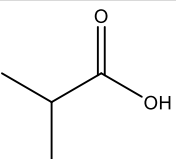
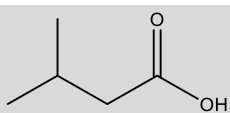
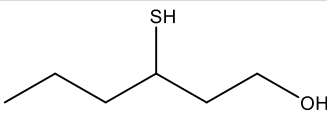
## 7. Experimental Techniques

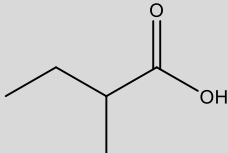
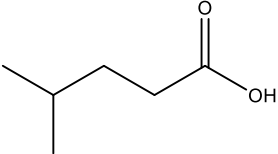
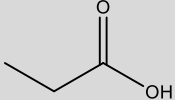
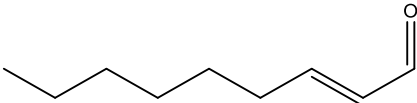
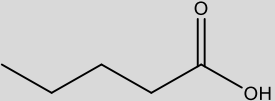
### 7.1 Materials

#### 7.1.1 Model Sweat Solution

Table 7-1 presents the compounds used to prepare the model sweat solution; all materials were used as supplied. Bromobenzene was purchased from Sigma-Aldrich and used as supplied.

Table 7-1: Volatile compounds used.

Name	Description	Purity (%)	Supplier
Acetic acid		>99	Fisher Scientific
Butyric acid		99+	Acros Organics
4-Ethyl-octanoic acid		97	Alfa Aesar
Hexanoic acid			Merck
Isobutyric acid		99	Alfa Aesar
Isovaleric acid			Merck
3-Mercapto-1-hexanol		96	Alfa Aesar

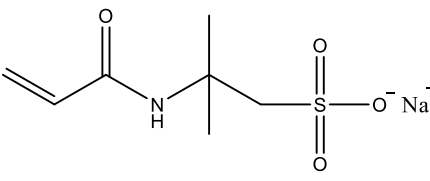
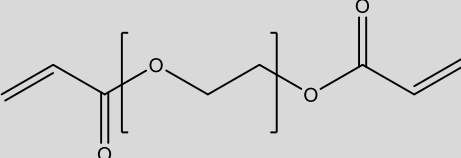
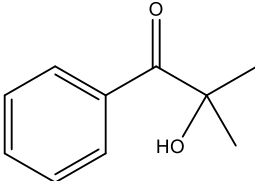
2-Methylbutyric acid		98	Sigma Aldrich
4-Methylvaleric acid		99	Alfa Aesar
Propionic acid			Merck
Trans-2-nonenal		97	Sigma Aldrich
Valeric acid		99	Alfa Aesar



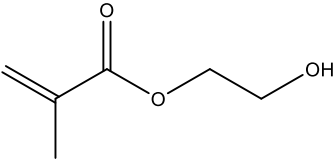
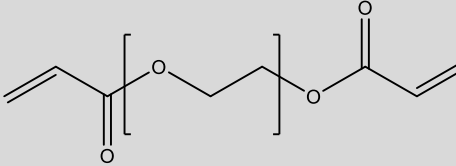
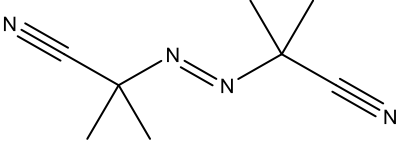
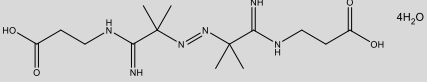
## 7.1.2 Polymerisation

Table 7-2 and Table 7-3 present the materials used to prepare p(NaAMPS) and p(HEMA) hydrogels respectively; all materials were used as supplied.

**Table 7-2:** Starting materials for synthesis of p(NaAMPS) hydrogels.

Name	Description	Purity (%)	Supplier
2-Acrylamido-2-methylpropane sulfonic acid sodium salt (NaAMPS)		50 (in water)	Sigma Aldrich
Poly(ethylene glycol) diacrylate			Sigma Aldrich
2-Hydroxy-2-methylpropiophenone (Irgacure 1173)		97	Sigma Aldrich (BASF)

**Table 7-3:** p(HEMA) thermal polymerisation materials.

Name	Description	Purity (%)	Supplier
2-Hydroxyethyl methacrylate (HEMA)			Sigma Aldrich
poly(ethylene glycol) diacrylate			Sigma Aldrich
2,2-azobis(2-methylpropionitrile) (AIBN)		98	Sigma Aldrich
2,2'-Azobis[N-(2-carboxyethyl)-2-methylpropionamide] tetrahydrate			Wako Chemicals

Hydroxyethyl acrylate (HEA) was purchased from Sigma Aldrich and used as supplied.

Acrylamide (>99 %), *N,N'*-methylenebisacrylamide (99 %), ammonium persulfate (98+ %) and tetramethylethylenediamine (99 %) were purchased from Sigma-Aldrich and used as supplied.

Sodium alginate was purchased from Vickers Labs and used as supplied.

Calcium chloride was purchased from Fisher and used as supplied.

### 7.1.3 Indicators

Quinine and quinine sulfate were purchased from Acros Organics and used as supplied.

Bromophenol blue was purchased from Sigma-Aldrich and used as supplied.

Fluorescein isothiocyanate (FITC) was purchased from Thermo Fisher and used as supplied.

#### 7.1.4 Fragrances

White Willow and New Day were kindly supplied by Unilever and used as supplied.

#### 7.1.5 Solvents

Ethyl acetate and acetonitrile (both HPLC grade) were purchased from Fisher and used as supplied.

Diethyl ether was purchased from Fisher and used as supplied.

Deuterium oxide and chloroform-d (99.8 % with TMS) were purchased from Sigma Aldrich and used as supplied.

### 7.2 Model Sweat Solution

Acetic acid, propionic acid, isobutyric acid, butyric acid, isovaleric acid, 2-methylbutyric acid, valeric acid, 4-methylvaleric acid, hexanoic acid, 3-mercapto-1-hexanol, trans-2-nonenal and 4-ethyl octanoic acid were used in a mixed solution to mimic sweat (concentration of the stock mix in water was 1 % (v/v) which equates to  $\sim 1\text{-}3\text{ mmol dm}^{-3}$  of each individual volatile in water), Table 7-1.

### 7.3 Hydrogel Synthesis

#### 7.3.1 Standard Procedure

To prepare standard p(NaAMPS) hydrogels, a batch aqueous solution was prepared from 46.4 g 2-acrylamido-2-methylpropane sulfonic acid sodium salt (NaAMPS, 50% in water, 0.10 mol), 0.1077 g poly(ethylene glycol) diacrylate (PEGDA,  $M_n \sim 575\text{ g mol}^{-1}$ , 0.2 mmol), 0.01 ml of the photoinitiator Irgacure 1173 (2-hydroxy-2-methylpropiophenone, 0.07 mmol) and 30.5 ml water in the absence of light, Table 7-2. This was allowed to stir before 3 ml aliquots were transferred to each individual mould (30 mm diameter) *via* syringe, then photo cured. The UV source used for the synthesis was a Light Hammer®, Figure 7-1, where standard procedure is 5 passes (at  $5\text{ m min}^{-1}$ , each pass  $\sim 7$  seconds UV exposure).



**Figure 7-1:** The Light Hammer®.

For equivalent HEA hydrogels, a large batch aqueous solution was prepared from 11.6 g hydroxyethyl acrylate (HEA, 0.10 mol), 0.05385 g poly(ethylene glycol) diacrylate (PEGDA,  $M_n \sim 575 \text{ g mol}^{-1}$ , 0.1 mmol), 0.005385 ml of the photoinitiator Irgacure 1173 (2-Hydroxy-2-methylpropiophenone, 0.03 mmol) and 29.1 ml water in the absence of light. This was allowed to stir before 3 ml aliquots were transferred to each individual mould *via* syringe, then photo cured. The UV source used for the synthesis was a Light Hammer®, Figure 7-1, where standard procedure is 5 passes (at  $5 \text{ m min}^{-1}$ , each pass  $\sim 7$  seconds UV exposure).

### 7.3.2 Initiator Concentration

#### 7.3.2.1 *p*(NaAMPS)

Standard preparation of *p*(NaAMPS) hydrogels was followed with the exception of the initiator concentration was decreased from 0.065 mol% to 0.013 mol% and 0.0013 mol% respectively.

#### 7.3.2.2 *p*(HEA)

This followed the equivalent *p*(HEA) procedure for photo-induced polymerisation except the initiator concentration was increased. These were mixed in a smaller batch (total volume approximately 10 ml) as they were for NMR studies. 2.85 g HEA (0.025 mol), 0.0132 g PEGDA (0.023 mmol), 0.0013 or 0.013 ml Irgacure 1173 (0.008 and 0.08 mmol, respectively) and 7.14 ml water were combined in the absence of light. This was allowed to stir before 1 ml aliquots were transferred to 5 mm NMR tubes *via* syringe, then photo cured. The UV source used for the synthesis is a Light

Hammer<sup>®</sup>, Figure 7-1, where standard procedure is 5 passes (at 5 m min<sup>-1</sup>, each pass ~ 7 seconds UV exposure).

### 7.3.3 Crosslinker Concentration

Standard p(NaAMPS) hydrogels were synthesised containing 0.2 (standard), 0.5, 1.0 and 2.0 mol% PEG diacrylate as crosslinker.

### 7.3.4 Use of indicators

#### 7.3.4.1 *Quinine and quinine sulfate*

Initially, quinine was tested in aqueous solution; 10 mg of quinine was added to 10 ml of water and the pH recorded. 0.25 ml of the model sweat solution was then added and the pH recorded. Fluorescence spectroscopy was carried out on both samples.

p(NaAMPS) hydrogels containing quinine were synthesised *via* standard procedure with the addition of 10, 1 or 0.1 mg quinine per hydrogel added to the monomer solution pre-polymerisation. This was carried out using both quinine and quinine sulfate.

Alternatively, a standard p(NaAMPS) hydrogel was dehydrated as standard, then rehydrated with 3 ml of an aqueous solution containing 10 mg quinine sulfate overnight.

#### 7.3.4.2 *Bromophenol Blue*

Bromophenol blue, 3 mg, was added to the standard p(NaAMPS) solution prior to polymerisation as standard procedure. 0.5 ml of model sweat was added and left to absorb as per standard procedure before UV-Vis analysis of the bromophenol blue-containing hydrogels was carried out before and after model sweat addition.

The concentration of bromophenol blue was then reduced to 1.5 mg in the batch and the process repeated. This concentration was also used in the materials tested with real sweat.

Bromophenol blue, 0.2 mg, was added to a standard aqueous HEMA solution (for thermal solution polymerisation, subsection 7.3.7.2). 3 ml aliquots of this were

transferred to the silicon moulds for polymerisation in the oven as standard procedure.

### 7.3.5 Addition of Fragrances

A standard batch of p(NaAMPS) pre-polymerisation solution was prepared then 3 aliquots of 12 ml each were transferred to separate 20 ml vials. 12, 60 and 120  $\mu\text{l}$  of 'New Day' were added to each of these vials to create 0.1, 0.5 and 1.0 v/v% materials respectively. These were then shaken before being transferred to moulds and polymerised as standard procedure. This was repeated using 'White Willow'.

### 7.3.6 UV source

The standard UV light source was a Light Hammer<sup>®</sup> (Figure 7-1) equipped with a 'H bulb' which supplies UV light over a wide range of wavelengths, Figure 7-2.<sup>1</sup> A conveyor belt underneath (speed  $\sim 5 \text{ m min}^{-1}$ ) controls the exposure of the sample to the UV light for a few seconds per pass.

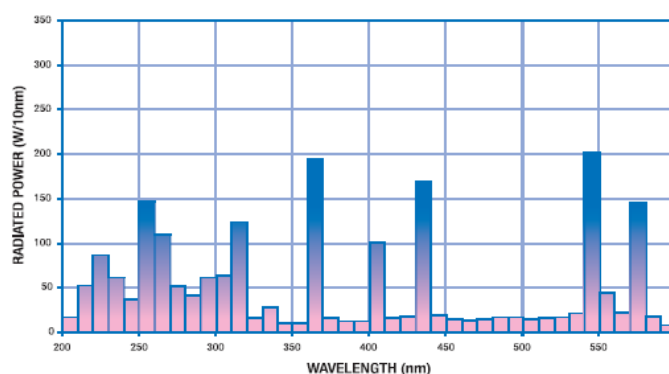


**Figure 7-2:** Output spectrum of 10'' Fusion UV Electrodeless Bulb; H bulb (13 mm).

In comparison, the UV "nail lamp" supplies light  $\sim 360 \text{ nm}$  (Figure 7-3),<sup>2</sup> however, this requires more than an hour of exposure which leads to over exposure to increased temperatures.



**Figure 7-3:** UV nail lamp that was used as an alternative UV light source.

A UVP CL-1000 Ultraviolet Crosslinker was also tested as a UV curing source, with varying intensities and exposure times investigated. The bulb in this unit emits UV light at 254 nm.<sup>3</sup>

### 7.3.7 Thermal Polymerisations

#### 7.3.7.1 Bulk Polymerisation

To 9.87 g of 2-hydroxyethyl methacrylate (HEMA, 75.84 mmol) was added 44 mg of poly(ethylene glycol) diacrylate (PEGDA, 0.076 mmol) and 74 mg 2,2-azobis(2-methylpropionitrile) (AIBN, 0.45 mmol). Once homogenous, this was transferred to an aluminium pan or a 3 ml aliquot was transferred to a silicon mould and sealed in a plastic bag. This was then placed in the oven at 70 °C for 6 hours. Once cool, this was sealed in a jar containing 50 ml of deionised water to swell and release any residual monomer. The water was changed twice daily by decanting the water, weighing the hydrogel and recording the mass (see 7.4.1 Swelling Kinetics) and resealed in the jar with a fresh 50 ml of deionised water. The collected water was then analysed by UV-vis for residual monomer.

#### 7.3.7.2 Solution Polymerisation

To 20 ml of deionised water, 9.87 g of 2-hydroxyethyl methacrylate (HEMA, 75.84 mmol), 44 mg of poly(ethylene glycol) diacrylate (PEGDA,  $\sim 575 \text{ g mol}^{-1}$ , 0.076 mmol) and 0.19 g VA-057 (2,2'-azobis[N-(2-carboxyethyl)-2-methylpropionamide]tetrahydrate, 0.45 mmol) was added. 3 ml aliquots of this were transferred to individual silicon moulds as standard procedure. These were sealed in a plastic bag then placed in the oven at 70 °C for 6 hours.

### 7.3.8 Double Network Synthesis

Physical networks were synthesised by dissolving sodium alginate in water, to create a 1 wt% solution, before adding a 0.1 M aqueous solution of calcium chloride.<sup>4</sup>

#### 7.3.8.1 P(AAm)-alginate Double Network

Sodium alginate, 0.47 g, and 3.7 g acrylamide (AAm) were added to 25.8 g deionised water (total monomer concentration = 14 wt%, mass ratio 1 : 8 alginate : acrylamide) in a jar. To this was added 2.3 mg N,N'-methylenebisacrylamide (MBA, 0.028 mol%), 3.7 mg ammonium persulfate (APS, 0.031 mol%) and 3.2 mg

tetramethylethylenediamine (TEMED, 0.152 mol%). Once homogenous this was heated at 50 °C overnight. After polymerisation, approximately 3 g of the gel was transferred to a scintillation vial and 3 ml of a 0.3 M aqueous solution of calcium chloride was added to crosslink the alginate and complete DN formation.<sup>5</sup>

#### *7.3.8.2 Sequential Double Network Synthesis.*

For a NaAMPS-first DN the standard single p(NaAMPS) network synthetic procedure was initially followed. These hydrogels were then dehydrated in a 70 °C oven before being rehydrated with an aqueous solution of HEMA, crosslinker and thermal initiator. Once absorbed (minimum 24 hours) these were then placed in an aluminium pan, sealed in a plastic bag and put in an oven at 70 °C for the thermal polymerisation to take place. Alternatively, an initial p(HEMA) xerogel was synthesised (see 7.3.7.1 Bulk Polymerisation), then this was allowed to swell in the standard aqueous NaAMPS pre-polymerisation solution for 1 week. This was then polymerised by passing under the UV lamp conveyor belt system.

#### *7.3.8.3 One-pot sequential DN synthesis.*

To reduce the time required in the 2-step synthesis, the swelling step was removed by mixing all components required for both networks in the pot prior to the first reaction. To a scintillation vial, 18 g of 50 % aqueous solution NaAMPS, 1.5698 g deionised water, 0.042 g PEGDA and 0.0042 g of Irgacure 1173 were added and stirred until homogenous. Simultaneously, to a separate vial, 9.87 g HEMA 0.044 g PEGDA and 0.074 g AIBN were mixed until homogenous. The two solutions were then combined, stirred briefly, then 3 ml aliquots were syringed into silicon moulds prior to exposure to UV light (10 -15 passes under the UV conveyor belt system). The moulds were then immediately transferred to a sealed plastic bag and placed in the oven at 70 °C for 6 hours as per the HEMA bulk thermal polymerisation.

## **7.4 Hydrogel Absorption**

Hydrogel absorption and recovery was tested by first putting the hydrogel in a 60 ml jar (diameter 4 cm) with 0.5 ml of the previously described stock aqueous mixture of volatile compounds. This was sealed with Parafilm and left for 24 hours to allow the hydrogel to absorb the solution.



### 7.4.1 Swelling Kinetics

Hydrogels were synthesised *via* standard procedure (unless otherwise stated) and then dried in the oven at 70 °C for a minimum of six hours. They were then sealed in individual jars containing deionised water and placed in an incubator at 22 °C. At pre-determined time points the hydrogels were removed from the water, the surfaces dried using a Kim wipe, then the mass recorded before being returned to continue swelling. In the case of the thermally-induced bulk polymerisation, the hydrogel did not need to be dried prior to swelling.

## 7.5 Recovery Procedure

### 7.5.1 Standard Process

The standard recovery procedure was to weigh the dosed hydrogel then place in a clean jar with 3 ml of ethyl acetate and leave for 24 hours. 1 ml of this solution was removed and placed in a 1.5 ml Chromacol vial with 0.1 ml PhBr stock solution (stock concentration  $\sim 40 \text{ mmol dm}^{-3}$ ) and immediately analysed by GC as described below.

#### 7.5.1.1 Partition

1 ml of model sweat (section 7.2) was freshly prepared in a 7 ml vial. To this was added 1 ml of ethyl acetate and sealed. This was manually shaken for 30 seconds then left to settle ( $\sim 1$  minute). The ethyl acetate was then pipetted from the top into a Chromacol vial before immediate analysis *via* GC-FID. This was then compared to an equivalent concentration of VFA mix run in ethyl acetate as a fresh, concurrent sample using the equation:

$$\%recovery = \frac{A_{part}}{A_{100}} \times 100 \quad (7-1)$$

Where  $A_{part}$  is the area in the chromatogram from the partition experiment and  $A_{100}$  is the area in the chromatogram of the equivalent '100 %' concentration sample.

### 7.5.2 Solvent extraction optimisation

The standard procedure was modified by either leaving for only 1 hour, sonicating, cutting up (manually with a scalpel) or a combination of the above.

### 7.5.3 Soxhlet Extraction

A standard p(NaAMPS) hydrogel (synthesised in-house, as standard) and a textile patch (supplied by Unilever) were tested side-by-side. To each, 0.5 ml of the aqueous model sweat solution was added and left in separate sealed jars for 24 hours for absorption. After this period, each were placed in separate glass-wool Soxhlet thimbles within a standard Soxhlet set-up (Figure 7-4) containing approximately 150 ml of diethyl ether. These were left to reflux at 40 °C for 5 hours.<sup>6</sup> The solvent was then removed *via* rotary evaporation before being refilled with ~1.5 ml of ethyl acetate for analysis by gas chromatography.



**Figure 7-4:** Side-by-side Soxhlet extraction set-up.

### 7.5.4 Supercritical Fluid Extraction

Supercritical fluid extraction (SFE) was carried out in collaboration with Steven Cenci at Suprex. Extractions were carried out using a Waters MV-10 ASFE. Hydrogels were dosed with 100  $\mu$ l of a 100 ppm volatile solution, wrapped in pre-cleaned cotton wool and placed into a 5 ml Waters stainless steel extractor. Runs were performed in the presence of either only CO<sub>2</sub> at a flow rate of 5 g min<sup>-1</sup> or CO<sub>2</sub>/acetonitrile at a total flow rate of 5 g min<sup>-1</sup>. Pressure and temperature were varied between 90 – 300 bar and 35 – 50 °C, respectively, as was the inclusion of a co-solvent, acetonitrile (4 ml) and whether it was included pre- or post-extraction chamber. The run times tested were 5-20 minutes. Extracts were analysed by GC-MS.

### 7.5.5 One month storage stability study.

Hydrogels were dosed with 0.5 ml of the model sweat solution and left to absorb for 24 hours as per standard procedure. The 0 time point was then also recovered as standard, whilst the rest were transferred to heat-sealable aluminium pouches and stored in an incubator at 25 °C for up to 4 weeks prior to standard extraction and analysis at the predetermined time points.

## 7.6 Analytical Techniques

### 7.6.1 Gas Chromatography

All GC-FID analysis was performed on a Shimadzu GC2014 equipped with a Shimadzu A020i autosampler, the injection temperature was 200 °C. The GC was fitted with a polar Stabilwax-DA column from (30 m length, 0.32 mm ID and 0.25 µm film thickness). The carrier gas was hydrogen, supplied by an external hydrogen generator. The injection volume was 1 µl with a 39 split ratio. The detector was a flame ionisation detector (FID) with a flame temperature of 300 °C, and a sampling rate of 40 ms. The heating profile was 60 °C for 2 minutes and then heated to 220 °C at 8 °C min<sup>-1</sup> where it remained for a further 5 minutes.

Samples were analysed by preparing an analyte sample of a known concentration and serial diluting until the analyte peak could no longer be observed in the chromatogram. This gave a calibration curve for each individual volatile compound along with an assumed lower detection limit, which is a concentration between the last serial dilution where the analyte was observed and the first where it could no longer be observed. The calibration curve can then be used to determine the concentration of volatile(s) in a sample of unknown concentration.

All samples were originally solubilised in ethyl acetate containing bromobenzene as an internal standard. The concentration of bromobenzene was kept constant in all samples (~5 mmol dm<sup>-3</sup>). This was then used to determine the concentration ratio and subsequently the peak area ratios of the analytes. Results are reported in this manner to account for any changes in GC performance over time.

#### 7.6.1.1 Gas Chromatography – Mass Spectrometry

GC-MS was carried out on a single quadrupole Shimadzu GCMS QP2010s. Fitted with an AOC20 autosampler and a Restek Rxi-1ms column (15 m length, 0.25 mm internal diameter and 0.25  $\mu\text{m}$  film thickness). The carrier gas was helium (supplied from a cylinder). The column oven temperature program was; 35 °C for 2 minutes, increased to 100 °C at 2 °C  $\text{min}^{-1}$  (5 minute hold). Injection temperature was 35 °C and detector and transfer line temperatures were both 200 °C.

Selected ion monitoring mode (SIM mode) monitored 43, 45, 60 and 74 as per Wu *et al.*<sup>7</sup>

#### **SFE Extracts**

GC-MS of these extracts was carried out on an Agilent GC-MS 6890 fitted with a Phenomemex Zebron column. Injections were 2  $\mu\text{l}$  with a 2:1 split mode. The column oven temperature program was; 60 °C for 3 minutes, increased to 150 °C at 6 °C  $\text{min}^{-1}$  (5 minute hold). Injection temperature was 250 °C.

#### **Real Sampling**

GC-MS was carried out on a single quadrupole Shimadzu GCMS QP2010s fitted with a DB-WAX column (20 m length, 0.18 mm internal diameter and 0.18  $\mu\text{m}$  film thickness). The column oven temperature program was; 60 °C for 1.33 minutes, increased to 220 °C at 15 °C  $\text{min}^{-1}$  (2 minute hold). Injection temperature was 250 °C and detector and transfer line temperatures were both 200 °C.

MS scan mode was 33-550  $m/z$  every 0.2 seconds from 3 minutes until the end of the heating method (13.99 minutes).

#### 7.6.1.2 Esterification

Butyric acid, 0.25 ml, was added to a vial with 0.6 ml chlorotrimethylsilane, this was sealed and placed in the oven at 70 °C.

To synthesise an example FAME; to a scintillation vial, 0.1 ml butyric acid was added to 1 ml 0.5 % *p*-toluenesulfonic acid monohydrate (*p*-TSA) in methanol and this was put in the oven at 100 °C for 1 hour.

## 7.6.2 High Performance Liquid Chromatography

Reverse-phase HPLC was carried out on an Agilent 1260 Infinity stack fitted with a C-18 column and a UV detector set to 205 nm. Samples were dissolved in 15 : 85 % acetonitrile : water solvent system and the sample was run with a gradient from 15 % acetonitrile to 40 % over 30 minutes then up to 100 % in the remaining 5 minutes.<sup>8</sup>

## 7.6.3 Absorption monitoring by contact angle.

Drop shape analysis (DSA) of water droplets was carried out on three different materials using a Krüss DSA100 drop shape analyser system with a tilting table. 5  $\mu$ l droplets of deionised water were suspended from a flat-tipped needle before contact with the material surface. The Laplace-Young equation was used to determine contact angle using Krüss software.

## 7.6.4 Proton NMR Studies

### 7.6.4.1 Gel NMR

The hydrogel pre-mix was prepared in a batch as standard procedure with the exception that the H<sub>2</sub>O was replaced with D<sub>2</sub>O to enable NMR analysis. 1 ml was transferred to an NMR tube and passed under the Light Hammer for the specified number of passes (1, 5, 10 or 50). These NMR tubes were then wrapped in aluminium foil until immediately prior to analysis.

For the post-polymerisation monomer doping, 0.1 ml of a 50 % NaAMPS solution (containing 10 % red food colouring) was added to the NMR tube containing the '50 passes' gel.

<sup>1</sup>H NMR analysis was carried out on a Bruker NMR av300 MHz instrument with D<sub>2</sub>O used as the locking solvent, unless otherwise stated, including in the gel. Residual water in D<sub>2</sub>O  $\delta$ H: 4.79(H, b s, OH).

For NaAMPS monomer  $\delta$ H(300MHz; D<sub>2</sub>O; Me<sub>4</sub>Si) 1.5 (6 H, s, Me), 3.5 (2 H, s, CH<sub>2</sub>), 5.7 (1 H, d, J = 9 Hz, C=CH), 6.2 (1 H, dd, J = 18 Hz, C=CH), 6.6 (1H, dd, J = 18 Hz, 9 Hz, C=CH), 7.9 (1 H, s, NH). For spectra, see Chapter 3. For p(NaAMPS): 1.5 (6H, br, Me), 3.5 (2H, br, CH<sub>2</sub>).

HEA monomer:  $\delta\text{H}$ (300MHz;  $\text{D}_2\text{O}$ ;  $\text{Me}_4\text{Si}$ ): 3.8 (2H, t,  $J = 4.5$  Hz,  $\text{CH}_2$ ), 4.3 (2H, t,  $J = 4.5$  Hz,  $\text{CH}_2$ ), 6.0 (1H, d,  $J = 9$  Hz,  $\text{C}=\text{CH}$ ), 6.2 (1H, dd,  $J = 15$  Hz, 9 Hz,  $\text{C}=\text{CH}$ ), 6.4 (1H, d,  $J = 15$  Hz,  $\text{C}=\text{CH}$ ).

p(HEA) hydrogels:  $\delta\text{H}$ (300MHz;  $\text{D}_2\text{O}$ ;  $\text{Me}_4\text{Si}$ ) 1.8 (2H, br,  $\text{CH}_2$ ), 2.45 (1H, br, CH), 3.8 (2H, br,  $\text{CH}_2$ ), 4.3 (2H, br,  $\text{CH}_2$ ).

Quinine and quinine sulfate containing hydrogels are the same broad peaks as the standard p(NaAMPS) plus the vinyl peaks of the monomer.

#### 7.6.4.2 Ester NMR

Butyric acid 1.0 (3H, t,  $J = 7.5$  Hz,  $\text{CH}_3$ ), 1.7 (2H, dt,  $J = 7.5$  Hz,  $\text{CH}_2$ ), 2.3 (2H, t,  $J = 7.5$  Hz,  $\text{CH}_2$ ), 11.5 (1H, s, OH).

The analysis of the trimethyl silane esters was also carried out on a Bruker 300 MHz instrument but using deuterated chloroform as the solvent;  $\text{CDCl}_3$   $\delta\text{H}$  7.26 (1H, s, CH)

Butyric acid, trimethylsilyl ester:  $\delta\text{H}$ (300MHz;  $\text{CDCl}_3$ ;  $\text{Me}_4\text{Si}$ ) 0.07 (9H, s,  $\text{CH}_3$ ), 1.0 (3H, t,  $J = 7.5$  Hz,  $\text{CH}_3$ ), 1.7 (2H, m,  $\text{CH}_2$ ), 2.35 (2H, t,  $J = 7.5$  Hz,  $\text{CH}_2$ ).

For methyl esterification product:  $\delta\text{H}$ (300MHz;  $\text{D}_2\text{O}$ ;  $\text{Me}_4\text{Si}$ ) 0.86 (3H, t,  $J = 7.5$  Hz,  $\text{CH}_3$ ), 1.58 (2H, m,  $\text{CH}_2$ ), 2.3 (2H, t,  $J = 7.5$  Hz,  $\text{CH}_2$ ), 3.65 (3H, s,  $\text{CH}_3$ )

#### 7.6.5 UV-Vis Spectroscopy

UV-Vis spectroscopy was carried out on an Agilent Technologies Cary 60 UV-Vis instrument using a quartz cuvette for all liquid measurements.

Hydrogel-based measurements were carried out by sticking the hydrogel to the outside of the cuvette holder as demonstrated in Figure 7-5.

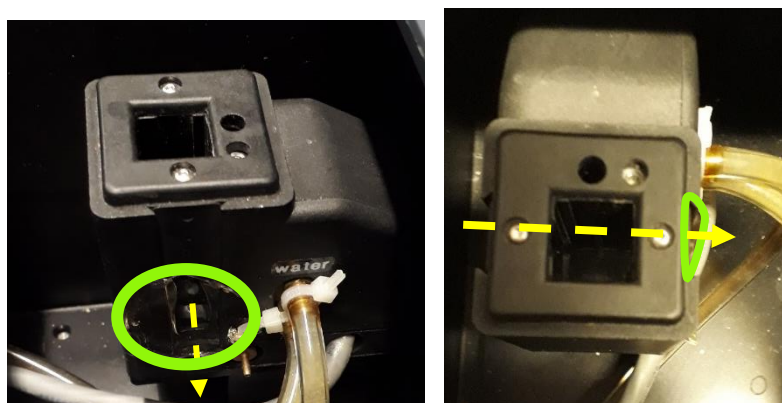


Figure 7-5: Demonstration of hydrogel *in situ* in the UV-vis spectrometer.

### 7.6.6 Fluorescence Spectroscopy

Emission Spectra were recorded on an Agilent Technologies Cary Eclipse Fluorescence Spectrophotometer using a quartz cuvette. For the quinine investigations, the excitation wavelength ( $\lambda_{\text{ex}}$ ) was set to 336 nm.

### 7.6.7 pH readings

pH readings of the indicator solutions were recorded using a Mettler Toledo pH probe with a 3-point calibration.

### 7.6.8 Fourier-Transform Infrared Spectroscopy (FTIR)

FTIR was carried out on a Bruker Vector 22 FTIR machine equipped with a Golden Gate ATR accessory.

### 7.6.9 Thermogravimetric Analysis (TGA)

TGA was carried out on a Mettler Toledo Star<sup>e</sup> TGA/DSC1 instrument under nitrogen. 40  $\mu\text{l}$  alumina pans were used and the method was heating from 25 °C to 1000 °C at a heating rate of 10 °C  $\text{min}^{-1}$ .<sup>9</sup>

### 7.6.10 Dynamic Mechanical Analysis (DMA)

DMA was carried out on a Perkin Elmer DMA8000 with tension clamp geometry. Frequency sweeps were performed between 1 and 25 Hz at approximately 25 °C.

### 7.6.11 Mechanical Testing

#### *7.6.11.1 Tensile Testing*

Tensile testing was carried out on a Shimadzu EZ-LX, fitted with a 500 N load cell, using the tensile jig set with serrated grips. Elongation was from a 0.1 N pre-load before measurements were carried out at 30  $\text{m min}^{-1}$ .

#### *7.6.11.2 Compression Testing*

Compression testing was carried out on a Shimadzu EZ-LX, fitted with a 500 N load cell, using compression plates. Materials were compressed to 5 N, which was then maintained for 30 seconds then released to no force. This was cycled three times per material tested.

### 7.6.12 Laser Scanning Confocal Microscopy

2 ml of a 0.05 % (w/v) solution of Fluorescein isothiocyanate in water was added to the hydrogel and left to absorb for 24 hours at 37 °C (in the absence of light). Imaging by LCSM was carried out at room temperature using a Leica TCS SP5-X confocal microscope with a 458 nm Ar laser for excitation at 561 nm.

## 7.7 Bacterial assay

In collaboration with Diana Cox at Unilever Colworth, an inoculated pigskin assay was carried out as follows. Pigskin was obtained from a local butcher, cleaned, cut into 4 cm x 4 cm pieces, sterilised by  $\gamma$ -irradiation, and stored at -20 °C until required. Pigskin pieces were allowed to thaw overnight in a fridge, then transferred to individual sterile Petri dishes containing moistened tissues. The pieces were gently swabbed with 96 % ethanol and the petri dishes were warmed in an incubator at 35 °C and held until ready for use. Each pigskin piece was inoculated with a suspension of *S. epidermidis* (200  $\mu$ l) and the cells were evenly distributed using a sterile spreader. *S. epidermidis* ATCC 12228 was grown in Tryptone soy broth with Tween (TSBT), harvested by centrifugation, and re-suspended in sterile phosphate-buffered saline (PBS). Using a spectrophotometer, the turbidity was adjusted to an optical density (OD) of  $\sim$ 0.3 with PBS (equivalent to  $\sim$ 108 colony-forming units (cfu) per ml). Petri dishes containing the inoculated pigskin pieces were placed in an incubator for 1 hour at 35 °C to allow the bacterial cells to settle.

Sampling to determine recovered cell counts was performed using sterile scrub cups (2 cm diameter) consisting of a Teflon cylinder and Teflon rod. The cylinder was held tightly against the skin surface and aliquots (0.75 ml) of quench fluid pipetted within. The skin surface was agitated by means of the Teflon rod and this procedure was carried out twice for 30 seconds each, and the retained fluids pooled. Serial dilutions of the buffer scrubs were made in sterile diluent and plated on Tryptone soy agar with Tween (TSAT) for colony counting.<sup>10</sup>



## **7.8 *In Situ* Sampling**

An *in situ* sampling study was carried out on an anonymised panel at Unilever R&D facility in Port Sunlight UK in May 2017. The panel contained 10 women. On day 1 of the study each woman's underarms were washed and dried then a hydrogel (pre-synthesised at University of Warwick, by R Hand, following standard procedure) with a breathable, adhesive backing was fixed in one underarm (random assignment), whilst a poly(cotton) patch was fixed in the other underarm of a cotton t-shirt. These were then worn for 24 hours. After 24 hours, both patches were removed and immediately placed in sealable pouches. The women then faced the standard olfactory panel before repeating this process with the underarm switched. The third day was for collection of samples and assessment only. In future studies these patches will then be analysed by several characterisation techniques.

Other real samples were collected by volunteers wearing a hydrogel, attached with a sports tape of their choice, for a period of approximately 30-60 minutes whilst at the gym or doing other sporting activity.

## 7.9 References

- 1 Heraeus Noblelight Fusion UV Inc., UV Curing from Heraeus Noblelight Fusion UV, [http://www.fusionuv.com/uploadedFiles/PDF\\_Library/SB661\\_Fusion\\_Difference.pdf](http://www.fusionuv.com/uploadedFiles/PDF_Library/SB661_Fusion_Difference.pdf), (accessed August 2016).
- 2 A. Anastasaki, V. Nikolaou, Q. Zhang, J. Burns, S. R. Samanta, C. Waldron, A. J. Haddleton, R. Mchale, D. J. Fox, V. Percec, P. Wilson and D. M. Haddleton, *J. Am. Chem. Soc.*, 2014, **136**, 1141–1149.
- 3 UVP Ultraviolet Crosslinkers, <https://www.uvp.com/crosslinker.html>, (accessed October 2016).
- 4 R. W. Jagers and S. A. F. Bon, *Mater. Horizons*, 2017, **4**, 402–407.
- 5 C. H. Yang, M. X. Wang, H. Haider, J. H. Yang, J. Y. Sun, Y. M. Chen, J. Zhou and Z. Suo, *ACS Appl. Mater. Interfaces*, 2013, **5**, 10418–10422.
- 6 F. Kanda, E. Yagi, M. Fukuda, K. Nakajima, T. Ohta and O. Nakata, *Br. J. Dermatol.*, 1990, **122**, 771–776.
- 7 T. Wu, X. Wang, D. Li, G. Sheng and J. Fu, *Int. J. Environ. Anal. Chem.*, 2008, **88**, 1107–1115.
- 8 A. B. Kroumova and G. J. Wagner, *Anal. Biochem.*, 1995, **225**, 270–276.
- 9 S. Çavuş, *J. Polym. Sci. Part B Polym. Phys.*, 2010, **48**, 2497–2508.
- 10 D. Cox, *Testing hydrogel patches in an inoculated pigskin model*, 2016.

## **Publication of Research in this Thesis**

### **1. Malodour Sampling Method.**

Susan Bates, David M. Haddleton, Rachel A. Hand and Ezat Khoshdel.

WO Pat., WO 2018/082882 A1, 2018.

### **2. Antiperspirant Device and Method.**

Susan Bates, David M. Haddleton, Rachel A. Hand and Ezat Khoshdel.

WO Pat., WO 2018/082881 A1, 2018.